Stony Brook University

Characterization of Hox gene expression during fracture repair and the functional characterization of Mustn1 during development and chondrocyte differentiation

A Dissertation Presented

by

Robert Philip Gersch

To

The Graduate School

In Partial Fulfillment of the

Requirements

For the Degree of

Doctor of Philosophy

In

Genetics

Stony Brook University

December 2008

Stony Brook University

The Graduate School

Robert Philip Gersch

We the dissertation committee for the above candidate for the

Doctor of Philosophy degree hereby recommend

acceptance of this dissertation.

Dr. Michael Hadjiargyrou – Dissertation Advisor
Associate Professor of Biomedical Engineering

Dr. Gerald Thomsen – Chairperson of Defense
Professor of Biochemistry and Cell Biology

Dr. Bernadette Holdener
Associate Professor of Biochemistry and Cell Biology

Dr. James Penna
Assistant Professor of Orthopedics
Stony Brook University

This dissertation is accepted by the Graduate School.

Lawrence Martin
Dean of the Graduate School

Abstract of the Dissertation

Characterization of Hox gene expression during fracture repair and the functional characterization of Mustn1 during development and chondrocyte differentiation

by

Robert Philip Gersch
Doctor in Philosophy

in

Genetics
Stony Brook University
2008

Previously, our laboratory identified several differentially regulated genes during bone fracture repair (BFR). Of these genes, several from the Homeobox family known to be active during development were spatially and temporally localized during BFR. That their activation during BFR is consistent with their roles in development adds support to the idea that development and BFR are analogous processes. Further research was preformed on the musculoskeletal temporally activated novel gene (Mustang a.k.a. Mustn1). This small (9.6kDa) nuclear protein was found to be strongly up-regulated during the early stages of bone fracture repair, especially in the periosteum, osteoblasts, and proliferating chondrocytes. Mustn1 expression was also found to be specific to the musculoskeletal system in adult vertebrates. Further characterization of Mustn1 revealed that this gene is highly expressed in areas of active chondrogenesis, specifically during development of the limb buds, branchial arches, somites and posterior tail. This localization pattern strongly suggests that this

gene plays a role during musculoskeletal development in mouse. To further study the role of Mustn1, we functionally perturbed its expression in the pre-chondrocyte cell line RCJ3.1C5.18 (RCJ) via stable overexpression and RNAi silencing. While overexpressing Mustn1 (at ~2-6 fold levels) in RCJ cells had no effect on chondrocyte proliferation or differentiation, downregulating Mustn1by 52-66% resulted in significant repression of both proliferation rate and matrix/proteoglycan production. These effects were also accompanied by the downregulation of the chondrogenic differentiation markers, Sox9, Collagen II, and Collagen X. Moreover, these inhibitory effects were rescued when Mustn1 was reintroduced into the silenced cell line. To further elucidate its role *in vivo*, we suppressed Mustn1 production in *Xenopus laevis* embryos via antisense morpholino injection. Following Mustn1 suppression, embryos displayed gross craniofacial and musculoskeletal defects, e.g. small, or loss of, eye(s), shortened body axis, as well as kinks within the tail, indicative of disturbances in cartilage and skeletal muscle formation. These defects were reduced in severity or completely ablated upon reintroduction of Mustn1 mRNA into Mustn1 morpholino injected embryos. In addition, the expression of the myogenic differentiation marker MyoD was not altered. However, when Sox9 was assayed in the same manner, its expression was reduced by ~40% in Mustn1 morpholino injected embryos when compared to the control embryos especially within the branchial arches, neural crest cells, and anterior craniofacial regions. Again, reintroduction of Mustn1 RNA rescued the expression pattern of Sox9 in *Xenopus* embryos. These data strongly suggest that Mustn1 is a critical player in chondrogenesis during vertebrate development.

Table of Contents

List of Symbols

AER – Apical Ectodermal Ridge
AP – Activator Protein
BFR – Bone Fracture Repair
BMP – Bone Morphogenic Protein
CBFα/Runx2 – Core Binding Factor α
Co – Control
DKK – Dickkopf
dpc – days past coitum
EGF – Epidermal Growth Factor
FDA – Fluorescein Dextran Amine
FGF – Fibroblast Growth Factor
Gli – Glicentin
HIF-1α – Hypoxia Inducible Factor 1α
Hox – Homeobox
IGF – Insulin-like Growth Factor
IHH – Indian Hedgehog
IL – Interleukin
MABT – Maleic Acid Buffer + 0.1% Tween
MHC – Myosin Heavy Chain
MMP – Matrix Metalloprotease
MO – Morpholino
Mustang (Mustn1) – Musculoskeletal Temporally Activated Novel Gene
NCC's – Neural Crest Cells
OE – Overexpressing
PBST – Phosphate Buffered Saline + 0.1% Tween
PF – Post Fracture Day
PTH – Parathyroid Hormone
PTHrP – Parathyroid Hormone Related Protein
qPCR – Quantitative Reverse Transcriptase Polymerase Chain Reaction
RCJ – Rat Calvaria J3.1C5.18
sFRP – secreted frizzled related protein
SHH – Sonic Hedgehog
TGFß – Transforming Growth Factor – ß
VEGF – Vascular Endothelial Growth Factor
ZPA – Zone of Polarizing Activity

List of Figures & Tables

Acknowledgements

First and foremost, I would like to thank my PI and mentor Michael Hadjiargyrou for all he has done to help me complete my dissertation. His unlimited patience has allowed me to learn according to my own means, namely screwing up each protocol every way conceivable before getting it right. This technique ultimately has given me a greater understanding of every step in each protocol and has molded me into a fine diagnostician and troubleshooter, but it must have been a tremendous irritation to Dr. Hadjiargyrou letting me learn in this way. I am a living testament to his tolerance and forgiveness of my many missteps along the way. In addition I would like to thank the other members of the Hadjiargyrou lab, namely; David Komatsu, Kim Luu, Nan Zhong, Cheng Liu, and Jonathon Chiu, for their guidance over the years. I came into the lab as the younger brother to the laboratory and these elders took me under their wings. They taught me a great deal both in how to perform research and in life.

I would also like to thank the other members of my committee; Dr. Jerry Thomsen, Dr. Bernadette Holdener, Dr. Peter Gergen, and Dr. James Penna, for their advice and motivation during my studies at Stony Brook. Their advice both individually and as a group has help to shape the scientist I have become. They were always there with the kind word or a deserved boot in the butt, whichever I happened to need at the time, and I thank them for both forms of encouragement.

The text of the second chapter of this dissertation is a reprint of material as it appears in The Journal of Orthopaedic Research (2005 Jul;23(4):882-90). The co-authors, F. Lombardo, SC. McGovern, and M. Hadjiargyrou, helped direct and supervise the research that forms the basis for the second chapter of this dissertation. Permission has been granted for use of this copyrighted material by the Wiley-Liss, Inc. a subsidiary of John Wiley & Sons, Inc.

Thanks also to the Biology department at Hartwick College. As much as the faculty of Stony Brook University has shaped my skill in the lab, the faculty at Hartwick College endowed me with the knowledge to not blow up half of Stony Brook University in the endeavor. I would like to especially thank Dr. Mary Allen, my advisor at Hartwick for keeping me on course, and Dr. Stanley Sessions for challenging me and opening my eyes to the world of genetics and all of its possibilities. Your classes changed my life.

I would certainly like to thank those who have helped me complete my research. Particularly I would like to thank Arif Kirmizitas, a kindred spirit without whom I would certainly still be learning to inject frog embryos at this point. Further, Christina Leonhard and Janet Chang helped me with mouse embryo dissection and embedding. Without their guidance, my diligence would be futile. I would also like to thank Drs. Jane Aubin and William Horton for donating the RCJ cells that were so crucial to my work.

As support staff go, Stony Brook University is stacked with the finest. From EH&S and DLAR staff ensuring our safety and humanity, to the maintenance staff and cleaning crew keeping our expensive toys and labs

running smoothly. I would especially like to acknowledge Colleen Michaels, Kate Bell, and Mike Antoszyk who have been saving my butt and making me look good for all these years, your efforts are deeply appreciated.

I would also like to thank all my friends here at Stony Brook. Marc, Jackie, Bobes, Annie, Kate, Amir, Erin, Marlies, Lorenzo, Gina, Mary, Nilsson, Anita, Adam, Andrei, Dan, Doug, Ed, Fred, Hoyan, Lila, Kasey, Liz, Mike, Shawn, Spanner, Suzanne, Sylvia, Tejas, TIMMEH, Vince, Will, and any and all I have missed, you know who you are. Graduate school is a lot like boot camp, except they only break you down. It's up to us to make sure we build each other back up, and I couldn't thank you enough for keeping me sane (or as close as I get anyway) over the last six years.

Finally, I would like to thank my family. I've referred to them as a life-long blessing in the past and that is as true today as ever. Without the support of my parents, sister, grandma, aunts, uncles, and cousins, I truly don't know where I'd be today. Mom and Dad thank you so much, words fail me.

Thank you all.

1. Introduction

Chondrogenesis is the process by which a cartilaginous matrix is formed. This matrix can either serve as an intermediate, as in long bone formation via endochondral ossification during development and regeneration, or as a final product itself, such as the articular cartilage found within joints throughout the body [37]. These divergent forms of cartilage serve vital, but very different, roles during both embryonic development and postnatal growth. However, all cartilage matrix formation can be attributed to the same initial process of formation; chondrogenesis.

The progression of cellular events that occur during development and leads to cartilage formation is well defined [122,123,124,126]. To become cartilage producing specialized cells, a group of mesenchymal progenitors must first migrate together and condense into a tightly packed skeletal blastema. It is then that the master regulator of chondrogenesis, Sox9, becomes up-regulated in the cells located at the center of these condensations. Mesenchymal cells strongly expressing Sox9 differentiate into chondroblasts and pre-chondrocytes within the center of these masses and proliferate while producing immature cartilage matrix identified by the large concentration of the extracellular matrix molecule collagen II [26]. These cells further differentiate into hypertrophic chondrocytes, sometimes forming columnar cells such as in the growth plate of developing long bones [121]. Once these cells become terminally differentiated they begin to

produce mature cartilage matrix marked by the increased presence of collagen X [51].

Following matrix production these cells often undergo apoptosis leaving the cartilage as a largely acellular tissue [125]. This newly formed cartilage is ideal for impact absorption and friction reduction as is required of articular cartilage. Alternatively, this matrix may become mineralized into bone via endochondral ossification. While these major steps have been well documented [51, 125, 126], the events that orchestrate this process remain largely unknown, but recent diligent research has elucidated several key tissues that coordinate chondrogenesis during embryonic development.

1.1 Vertebrate craniofacial development

As this dissertation deals predominately with chondrogenesis, various areas of cartilage formation during embryogenesis are discussed including craniofacial and limb bud development. Unfortunately, craniofacial development in the model system discussed herein, *Xenopus laevis*, has not been extensively studied. However, the tissues directing this process are similar to other vertebrate model systems. In this section, these various systems are discussed.

In vertebrates the craniofacial region is predominately a product of the cranial (cephalic) neural crest cell population (Figure 1). These cells which are initially divided into rhombomeres throughout the fore, mid, and hindbrain migrate ventrally in three different pathways [128]. Neural crest cells (NCC's)

populating rhombomere 2 migrate ventrally to become the first pharyngeal pouch, which becomes the first branchial arch (also known as the mandibular arch). This tissue differentiates to produce Meckel's cartilage which forms the mandible. In addition these cells also form the incus and malleus bones of the middle ear. The NCC's populating rhombomere 4 migrate to form the second pharyngeal pouch which, in turn, forms the stapes bone and styloid process. Finally, the cells of rhombomere 6 migrate to form the third and fourth pharyngeal arches which help form the thyroid and cricoid cartilage as well as the tracheal rings of the neck [129]. In addition to these cells, NCC's localized in the fore and midbrain also undergo chondrogenesis as they migrate to, and help contribute to the nasal process, palate, and mesenchyme of the first pharyngeal pouch [130].

The vertebrate eye is in part formed as these cells migrate from the fore and midbrain, by their contribution to the epidermal thickening of the cranial ectodermal placodes. Eye development involves all three tissue layers as the optic vesicle, which evaginates from the brain, interacts with early paraxial mesoderm and contacts the overlying ectoderm forming the eye cup and vesicle. Further development relies on interactions between the brain and this neural crest cell derived ectoderm throughout embryogenesis [131]. While the timing and duration of these cellular events vary between model systems, overall craniofacial development is very similar between vertebrates.

1.2 Limb bud development

Greater detail is available in regard to limb formation in vertebrates, particularly in mouse and chick. It is well known that limb development is directed by signals originating from the apical ectodermal ridge (AER) which covers the underlying zone of polarizing activity (ZPA). These two regions control the extension of the limb bud via modulating cell division within the progress zone [131]. While these signals and tissues have been well elucidated, what is pertinent to this report is chondrogenic differentiation that occurs to these mesodermal cells after they leave the progress zone. These cells undergo differentiation in a proximal to distal specific manor. Cells that have undergone few divisions become proximal structures such as the femur and humerus while those cells that have undergone many divisions become the distal elements of the limb such as the radius, ulna, tibia and fibia, as well as the carpals and tarsals [132]. However, while these structures develop independently, they are all formed via endochondral ossification whereby mineralized bone replaces a cartilage matrix forerunner. To this end these mesodermally derived cells, as with the ectodermal NCC's in the craniofacial region, must all undergo chondrogenesis. Despite their origin, both the cellular progression and end result of cartilage formation is very similar and much work has been undertaken to elucidate the molecular mechanisms regulating this developmental process.

Chondrogenesis involves the coordination of several complex genetic pathways including the Wingless (Wnt), Bone Morphogenic Protein (BMP), N-

cadherin, Hedgehog and Fibroblast Growth Factor (FGF) signaling pathways [119,122]. Each of these pathways has an impact on cartilage formation at different steps in the process and to different degrees with contrasting results and is discussed in detail below.

1.3 Wnt signaling

Of these signaling pathways related to chondrogenesis, the most closely scrutinized is the Wnt pathway (first identified in *Drosophila* in the wingless mutant) [1]. Several different Wnt molecules have been implicated in cartilage formation by directing many aspects of the chondrogenic process and limb/joint formation. Specific Wnt signaling molecules can act as either enhancers or repressors of chondrogenesis or even regulate musculoskeletal structure formation and patterning. For example, the Wnt-I ligands (most notably Wnt-1 and Wnt-7a) are thought to act as inhibitors of chondrogenesis affecting chondroblast differentiation in the chondrocyte lineage. When ectopically expressed, both molecules display potent inhibition of cartilage formation [1,5,6]. These genes affect the earlier stages of the process allowing mesenchymal condensation to take place but blocking further differentiation of these cells into pre-hypertrophic chondrocytes at the late-blastema/early-chondroblast stage [1,5].

While Wnt-1, Wnt-7a, and others act to inhibit chondrogenesis, there is another group of Wnt molecules, particularly Wnt-3a, Wnt-5a & Wnt 5-b that act as enhancers [2,4,7]. However, while these genes act to enhance

cartilage formation, they work on different steps of the process and actually antagonize each other. For example, Wnt-3a acts early to assist BMP-2 directed chondrogenesis by promoting cell-cell adhesion leading to mesenchymal condensation [2,22]. However, these experiments also suggest that Wnt-3a goes beyond promoting cell-cell adhesion and actually stabilizes cell-cell interactions to the point that the condensed mesenchymal cells cannot differentiate into chondroblasts [22], suggesting that while this gene promotes early stages of chondrogenesis, unless counteracted, it blocks later stages of cartilage formation. Further, the same study also showed that Wnt-3a is also able to dedifferentiate articular chondrocytes.

The blockage of cartilage formation by Wnt-3a requires Wnt-5a and Wnt-5b activation to enable the differentiation of these mesenchyme condensations into chondroblasts and chondrocytes [4,7]. Specifically, Wnt-5a blocks inhibition of maturation by Wnt-3a both via canonical and non-canonical mechanisms [44]. While studies show that Wnt-5a and Wnt-5b both promote chondroblast differentiation, their roles in cell maturation to hypertrophy remains unclear. Some experiments suggest that these factors promote early chondrogenesis but inhibit terminal differentiation [45], while others show that missexpression of either Wnt-5a or Wnt-5b delay or inhibit chondrocyte maturation, although there is support that these highly homologous genes are acting on different steps in the progression of differentiation [7].

While these two groups of Wnt molecules have been heavily investigated their intricate interactions and functions still remain to be clearly elucidated. It comes as no surprise then, that there are several other Wnt proteins implicated in chondrogenesis with roles even less understood. For instance, Wnt-4 missexpression accelerates chondrocyte maturation and bone collar formation [3,7]. Wnt-4 has also been localized to areas of joint initiation although its role during this process remains unclear [7]. In addition, Wnt-6 has been localized to the periphery of the developing limb bud in the chick [24,32], however, this expression pattern may not suggest a role in chondrogenesis. In fact, previous data suggests that Wnt-6 instead functions during myogenesis and may push cells toward a myogenic lineage [46]. Additional experiments have also implicated Wnt-9a (a.k.a. Wnt-14) and Wnt-11 in the Indian Hedgehog (IHH) pathway [7,45], as well as Wnt-16 in cartilage repair and osteoarthritis [48]. However, these three assertions are based solely on expression/localization data and, to date, only the regulation of IHH by Wnt-9a has been supported by functional experimentation [47].

Because of the large number of Wnt signaling molecules with complex interactions causing very different results on chondrogenesis, it may be beneficial to focus on the significantly smaller number of Wnt receptors. The Frizzled family of receptor proteins contains the main binding partners of most Wnt signaling molecules and several of them play roles in chondrogenesis. Frizzled-1 and Frizzled-7 have both been shown as enhancers of chondrogenesis [3,18,19]. While the mechanism by which Frizzled-1 acts is

unclear, it is believed that Frizzled-7 enhances mesenchymal condensations and early chondroblasts differentiation [18,19]. Frizzled-4 also plays a role in chondrogenesis by transducing the signal of Wnt-5a facilitating the blockage of Wnt-3a chondrogenic inhibition [44].

While these frizzled proteins seem to enhance cartilage formation there are several frizzled related proteins that serve to interrupt cartilage development. For example, both sFRP-1 & 2 (secreted frizzled related protein) have been identified as inhibitors of chondrogenesis [16,20]. Both proteins seem to achieve this end by modulating Wnt signaling, perhaps by competition for frizzled receptor sites. However, later work on sFRP-2 knockout mice suggest that loss of this protein causes mild shortening and malformations of the limbs [17], illustrating the confusion surrounding these complex interactions between signaling proteins and receptors. Two final Wnt antagonists worth noting are Frzb-1 and Dickkopf-1 (DKK-1). These proteins are both known to block Wnt Signaling [20,91], although, Frzb-1 has been shown to enhance mesenchymal condensation, suggesting that it only blocks later steps in chondrocyte hypertrophic differentiation [21].

Aside from investigating Wnt secreted molecules, receptors, and related proteins, it is also very important to examine other key downstream signaling molecules that are part of this pathway. For example, three early downstream effectors, Dishevelled proteins (Dvl1, Dvl2, and Dvl3), are all vital for proper Bone Fracture Repair (BFR) as well as chondrocyte proliferation and differentiation, as our laboratory previously showed [127]. These Dvl

proteins are largely important because of their interaction with the key transcriptional mediator of the Wnt pathway, ß-catenin. This gene's activation is the requisite step in the canonical Wnt signaling pathway. Because ß-catenin is necessary for the transcription of target genes activated by several different signaling molecules it is no surprise that it has been linked to several process such as osteogenesis [49], chondrogenesis [50,51], and even the regulation of gap junctions [52].

In chondrogenesis, ß-catenin is required even for BMP-2 stimulation of cartilage formation [50]. ß-catenin also exerts its transcriptional effects by binding to downstream targets such as the transcription factors Lymphoid enhancer factor-1 (Lef-1) and T-cell factor-1 (Tcf-1). While single knockouts of these two genes show little effect on cartilage formation, the double knockout results in limb deficiency suggesting that they play redundant but important roles in limb formation [55]. Further, these two genes also play a role in the dedifferentiation of articular cartilage via Wnt-3a [22]. In addition to Tcf-1, Tcf-4 has also been shown to be necessary for chondrogenesis as a dominant negative form of the protein inhibited cartilage formation [54]. The unique ability to enhance and/or to repress the process of chondrogenesis depending on the availability of extracellular Wnt stimuli illustrates how influential this pathway is to the process of chondrogenesis. The intricacy of the interactions between initial stimuli and their downstream targets also illustrates the complexity and flexibility of this pathway.

1.4 BMP signaling

While the Wnt proteins are some of the most studied regulators of chondrogenesis, the Bone Morphogenic Protein (BMP) family, a subset of the Transforming growth factor beta (TGFβ) signaling superfamily, is the engine that drives this process. Within this family, BMP-2 is the most potent and well characterized chondrogenic stimulators and is routinely used to stimulate chondrogenesis *in vitro* [11, 12, 13]. Specifically, BMP-2 was found to be, by itself, sufficient to induce chondrogenesis [112,113,114]. However, other BMP family members also play vital roles in chondrogenesis. For instance, BMP-6 induces hypertrophy [35] and even shows redundancy with both BMP-2 [41] and TGFβ [36]. BMP-7 is a strong inducer of differentiation, perhaps with even a more robust signal than BMP-2 [37]. However, recent reports show that BMP-7 induces adipogenic differentiation in mesenchymal stem cells but not chondrogenesis in micro-mass culture [111]. Further, BMP-9, BMP-12, and BMP-13 (a.k.a. CDMP-2) have all been shown to induce chondrogenesis *in vitro* [38,39,40]. Other BMP molecules seem to have slightly more involved roles during chondrogenesis; BMP-3 modulates other BMP signals while its overexpression actually delays chondrocyte differentiation [42].

Experiments with BMP-4 show this factor up-regulates collagen II but blocks terminal differentiation and hypertrophy [33,34]. Other studies showed that TGFβ also has the potential to induce chondrocyte proliferation and differentiation [14] and has been spatiotemporally localized to areas of

chondrogenesis in developing rats [118], while TGFβ-3 has been used in surgeries and *in vivo* to ehance cartilage production and repair [115.116]. However, a study in chick limb mesenchymal cells suggests that TGFβ-3 may also work to inhibit chondrogenesis *in vitro* [117]. Even though some members may only act on specific steps in the process; overall, the BMP/TGF signal acts to stimulate chondrogenesis like no other signaling family does.

Because of this vital role triggering cartilage formation, genes acting at several levels of the BMP signaling pathway have been linked to chondrogenic regulation. For example Smads, BMP signaling downstream effectors, have proven to be integral in the transduction of the signal. Smad-1 is the major effector facilitating both BMP stimulation and Epidermal Growth Factor (EGF) repression of chondrogenesis [107] while Smad-5 has been linked to the transactivation of the collagen II promoter in chondroprogenitor cells [109]. Also, the repressor Smad-6 has been shown to block BMP induction of Sox9 [108].

At the transcriptional level, as a result of BMP signal transduction, Sox9 is the critical transcription factor protein. This SRY-related protein is a main transcription factor for Collagen II [25.26] and the master regulator of chondrogenesis [27,28]. Sox9 is also responsible for the regulation of Sox-5 & Sox-6 which both help pattern cartilage formation [76]. In fact, the trio of Sox-5,6, and 9 are sufficient to induce chondrogenesis by stimulating matrix production [77]. The matrix molecule(s) induced by Sox mediated transcription make up the physical structure of cartilage matrix. Collagen II is

the major structural component in cartilage and is produced by proliferating chondrocytes [29]. It was recently found that a synthetic peptide corresponding to residues 195-218 of Collagen II sequence alone can induce hypertrophy in bovine articular cartilage explants [30], suggesting Collagen II may play a role in chondrogenesis even after it has been degraded. Another matrix molecule activated by Sox9 is Collagen IXa1 [59] which is necessary to stabilize Collagen II within the cartilage matrix [60,61]. Collagen XI and the structural proteoglycan Aggrecan can further stabilize the cartilage matrix [62,85]. As hypertrophy is reached chondrocytes begin to produce Collagen X, making it the marker of mature cartilage matrix [30,31].

Although BMP signaling predominately regulates chondrogenesis positively; several signaling proteins that block or repress its activation have been discovered. For example, Noggin signaling blocks both chondrogenesis and BMP activation causing increased osteogenesis in stem cells [82]. However, when Noggin null mice were studied, both accelerated and delayed mineralization was observed, suggesting complex tissue specific responses to Noggin/BMP stimulation [83]. Chordin is another signaling protein known to inhibit BMP signaling, but its expression is related to osteogenesis which accelerates when Chordin is knocked down [84]. EGF also signals the inhibition of chondrocyte differentiation and limb formation [110]. As mentioned before, it was suggested this inhibition is accomplished by EGF competing for Smad-1 with various BMP signals [107].

1.5 FGF signaling

As vital as Wnt and BMP signaling pathways are to the initiation of chondrogenesis, there is another family of signaling molecules that are necessary to regulate the hypertrophic differentiation of chondrocytes, that is, the Fibroblast Growth Factors (FGF's). FGF-2 is as potent initiator of chondrogenesis specifically in NCC's in the craniofacial region [73] but also functions in other areas of the body such as limb, nasal, and mandibular regions [68]. FGF-18 regulates chondrogenesis at every level, from early chondrocyte proliferation to hypertrophic differentiation and even vascular invasion of the growth plate [70]. FGF-18 is modulated by its interaction with the receptor, FGFR3, which exerts its affect on chondrogenesis and osteogenesis [71,72]. One of the most important roles of the FGF family is to regulate the patterning and inception of the limb bud by three key signaling molecules (FGF-8, FGF-9, and FGF-10). The primary role of FGF-8 during development is to induce patterning in craniofacial and limb bud regions [68] by modulating both FGF-10 and FGF-9 expression. FGF-9 helps to promote hypertrophy [69] while FGF-10 is crucial for joint patterning and development [74]. Interestingly, the most important member of this family in regards to limb bud formation may be FGFR2 which regulates the effects of both FGF-8 and FGF-10 [106]. While not as entwined in the process of chondrogenesis as some of the other signaling families; the FGF's are no less a vital and necessary component of cartilage formation.

1.6 Other regulators of chondrogenesis

In addition to these three signaling families there are several other critical regulators of chondrogenesis that have been identified. For example, N-cadherin, a calcium-dependent adhesion molecule, has long been linked to cell-cell adhesion that accompanies mesenchymal condensation [8]. Specifically, through interaction and regulation of the catenin cytosolic complex, an amalgamation including parts of the cell cytoskeleton, ß-catenin, and α-catenin, N-cadherin is able to facilitate the condensation of mesenchymal precursor cells that will differentiate into chondroblasts and proliferating chondrocytes. This role of N-cadherin has been observed both *in vitro* and *in vivo* [9,10].

Two members from the Hedgehog family have also been linked to chondrogenesis. Sonic Hedgehog (SHH) is a known potent patterning molecule; therefore it is no surprise that it has been found to signal limb formation and patterning [81]. Additional experiments also implicate SHH in early pre-chondrocyte stimulation [80]. Another family member, Indian Hedgehog (IHH) is a potent enhancer of cartilage formation as it helps to orient chondrocyte orientation within the matrix as well as stimulating proteoglycan production [78, 79]. Interestingly, while SHH and IHH have different temporal and spatial expression patterns during limb formation, when these two signals were switched and placed under the control of the opposite's promoter, it was shown that each could perform the other's function [75].

One rare opportunity for dedifferentiation in the process of chondrogenesis is offered in part by Parathyroid Hormone (PTH). PTH, by itself, acts to promote chondrocyte proliferation, however when working with PTH Related Protein (PTHrP) it can dedifferentiate hypertrophic chondrocytes back to the proliferating stage [65]. PTHrP by itself increases matrix production, but not hypertrophy [63]. Interestingly, when both of these signals are blocked, long bone chondrocyte hypertrophy is diminished during development [64].

Signaling molecules known to be influential in other biological processes play a role in chondrogenesis as well. Signals from both Hypoxia inducible factor (HIF-1α) and Vascular Endothelial Growth Factor (VEGF) seem to be necessary for chondrogenesis [88,89]. Unfortunately, except for the fact that HIF-1α seems to regulate Sox9 expression [87] and that VEGF and its receptors are up-regulated during BMP-2 treatment of chondrocytes *in vitro* [89] little is known of how these extracellular signals help coordinate this process.

Another important signaling molecule is Insulin-like growth factor-1 (IGF-1) that has been implicated in facilitating proliferation and differentiation of mesenchymal precursor cells during chondrogenesis [14]. Also, interleukin-1 (IL-1) is thought to be involved in inflammation and cartilage degradation, as was observed when *ex vivo* mandibular condyles from young and old mice were treated with IL-1 or TGFβ and compared to controls [15].

While each of these signaling molecules and pathways are strong regulators of chondrogenesis on their own, the true complexity of this system

cannot be realized until one considers the many different interactions that occur between these molecules/pathways during chondrocyte differentiation. BMP-2 initiation of cartilage formation requires the involvement of the aforementioned cell-cell adhesion via N-cadherin [11]. Additionally, chondrocytes activated by BMP-2/N-cadherin can be further regulated by the addition of various Wnt molecules. For example, treatment of murine C3H10T1/2 mesenchymal cells with Wnt-3a enhances BMP-2 activation of chondrocyte differentiation while exposure to BMP-2 is not sufficient to rescue chondrogenic differentiation when cultures are also treated with Wnt-7a, as would be expected by what is known of these genes individually [2,119].

Despite this wealth of knowledge regarding the molecular events responsible for regulating chondrogenesis, several questions remain unanswered. For example when cartilage is degraded *in vivo*, its regeneration happens very slowly, if at all; therefore, learning to reactivate this process could be of great benefit to the millions suffering from osteoarthritis as well as other cartilage injuries. Unfortunately, restarting this process in an acellular tissue matrix is only half the solution. How best to modulate this process while ensuring mature cartilaginous matrix continues to be produced is currently unknown. However, before we achieve the ability to manipulate chondrogenesis *in vivo*, we must first fully elucidate the molecular components of this process and their impact upon it. Unfortunately, there are likely many unknown or novel genes, whose individual and combined involvement in chondrogenesis remain to be elucidated. Research on one of

these genes, Mustn1, comprises the essence of this dissertation. Based on our data, Mustn1 appears to play a pivotal role in the early stages of chondrogenesis. By fully elucidating its function in cartilage formation it may be possible to gain a clearer understanding about the mechanism of chondrogenesis, and we hope that this will lead to greater understanding of this process.

1.7 Mustn1 cloning and cellular localization

Using transcriptional profiling in a mammalian bone regeneration model [120], as well as expressional analyses [121], previous work in our laboratory identified the **Mu**sculo**s**keletal **t**emporally **a**ctivated **n**ovel **g**ene (Mustang a.k.a. Mustn1) as up-regulated during fracture repair. Mustn1 encodes for a small (9.6 kDa) nuclear protein that shows amino acid homology when compared to mammals; however, homology is reduced in non-mammals, such as chick and zebrafish, and is not present in the genomes of invertebrates like *Drosophila* or *C. elegans*. Further, Mustn1 only contains a single motif, that of a nuclear localization signal that has been experimentally verified with Mustn1-GFP fusion experiments and found to localize to the nucleus, but neither the nuclear envelope nor nucleoli. Unfortunately, there are no other identifiable motifs found in Mustn1's sequence that offer any clues to its possible role. There are, however, a few sites for post translational modification: N-myristylation and phosphorylation. The activation of these sites may regulate conformational state and/or activity

however; no experimentation was performed to even validate that these modifications occur or what characteristics they impart on the Mustn1 protein. Myristylation is especially a curious finding as myristylation usually occurs on N-terminal amino acids and this site is found deep within the coding sequence, making it unlikely for this particular modification unless Mustn1 undergoes a cleavage event prior to modification. Further, it is unclear how the addition of a myristoyl group would affect a nuclear protein. Obviously, further elucidation of both the phosphorylation and myristylation sites is required.

1.8 Mustn1 temporal and spatial localization during fracture repair

The cellular localization of Mustn1 suggests this gene is probably involved in the few processes that occur within the nucleus, including DNA synthesis, chromatin remodeling, transcriptional regulation, post transcriptional modification, etc. However, since Mustn1 is only found in the musculoskeletal system in adult tissues [121] it is likely that Mustn1 is not involved in DNA synthesis, chromatin remodeling, or post transcriptional modification because these processes occur ubiquitously throughout different tissues. If Mustn1 were involved in one of these processes it would be expressed in more cell types/tissues than its expression pattern demonstrates. This leaves cell type specific transcriptional regulation as the likely role of the Mustn1 gene. Further, the lack of any RNA/DNA binding domains suggests that Mustn1 is likely a transcriptional co-regulator limited in its involvement to

musculoskeletal processes such as chondrogenesis, osteogenesis and myogenesis. However, no protein binding experimentation has yet been able to verify this hypothesis.

Indirect evidence for its involvement in osteogenesis and chondrogenesis is provided by Mustn1 transcriptional up-regulation in early stages of BFR, especially its expression by osteoprogenitor cells of the periosteum, osteoblasts and proliferating chondrocytes. Because it is well supported that BFR recapitulates bone development [122,123,124], spatial localization was also investigated in both developing limb buds and vertebra in mice as well as adult rat joints. The results from these studies revealed that Mustn1 expression was greatest in the perichondrium, proliferating pre-chondrocytes, and mesenchymal progenitor cells in developing mouse limb, intervertebral discs, and tail buds [121], thus implicating this gene in either proliferation and/or differentiation. Further experiments showed that there is no Mustn1 activity in the growth plate of long bones but expression in proliferating chondrocytes of articular cartilage. Taken together, these expression studies suggest that Mustn1 is involved in the differentiation of proliferating chondrocytes into mature cartilage producing hypertrophic chondrocytes and, as such, implicates Mustn1 in the process of chondrogenesis.

Overall hypothesis: Perturbation of Mustn1 will alter chondrogenic differentiation *in vitro* and chondrogenesis *in vivo*.

Specific Aim1:

Validate that BFR recapitulates bone development.

Hypothesis: Hox genes active during musculoskeletal development will be reactivated during BFR.

Rationale: As has been reported by others BFR recapitulates bone development [122,123,124]. Specifically, five Hox genes known to be active during musculoskeletal development (Msx-1, Msx-2, rHox, Hoxa-2, and Hoxd-9) should all become reactivated during BFR.

Specific Aim 2:

Characterize Mustn1 spatial expression during embryonic development.

Hypothesis: Mustn1 will be expressed in the developing musculoskeletal system.

Rationale: If fracture repair recapitulates development and since Mustn1 is expressed abundantly during the repair process, then it should also be expressed during development of the musculoskeletal system.

Specific Aim 3:

Determine the *in vitro* effects of Mustn1 overexpression on chondrocyte proliferation and differentiation.

Hypothesis: Overexpression of Mustn1 in chondrocytes will affect proliferation and/or differentiation.

Rationale: Previous data suggests that Mustn1 is a transcriptional co-activator or co-regulator [121] and as such, overexpressing it will affect either proliferation and/or differentiation.

Specific Aim 4:

Determine the *in vitro* effects of Mustn1 silencing of chondrocyte proliferation and/or differentiation.

Hypothesis: Silencing of Mustn1 will affect proliferation and differentiation.

Rationale: Previous data suggests that Mustn1 is a transcriptional co-activator or co-regulator [121] and as such, silencing it will affect proliferation and/or differentiation.

Specific Aim 5:

Elucidate the *in vivo* effects of Mustn1 silencing during *X. laevis* development.

Hypotheses: Mustn1 silencing will reduce or block the rate of musculoskeletal development *in vivo*.

Rationale: If Mustn1 is a co-activator of transcription it will be necessary and/or sufficient for transcription resulting in an impact on musculoskeletal development. If this is the case, then Mustn1 may influence chondrogenesis, osteogenesis, and muscle formation during development.

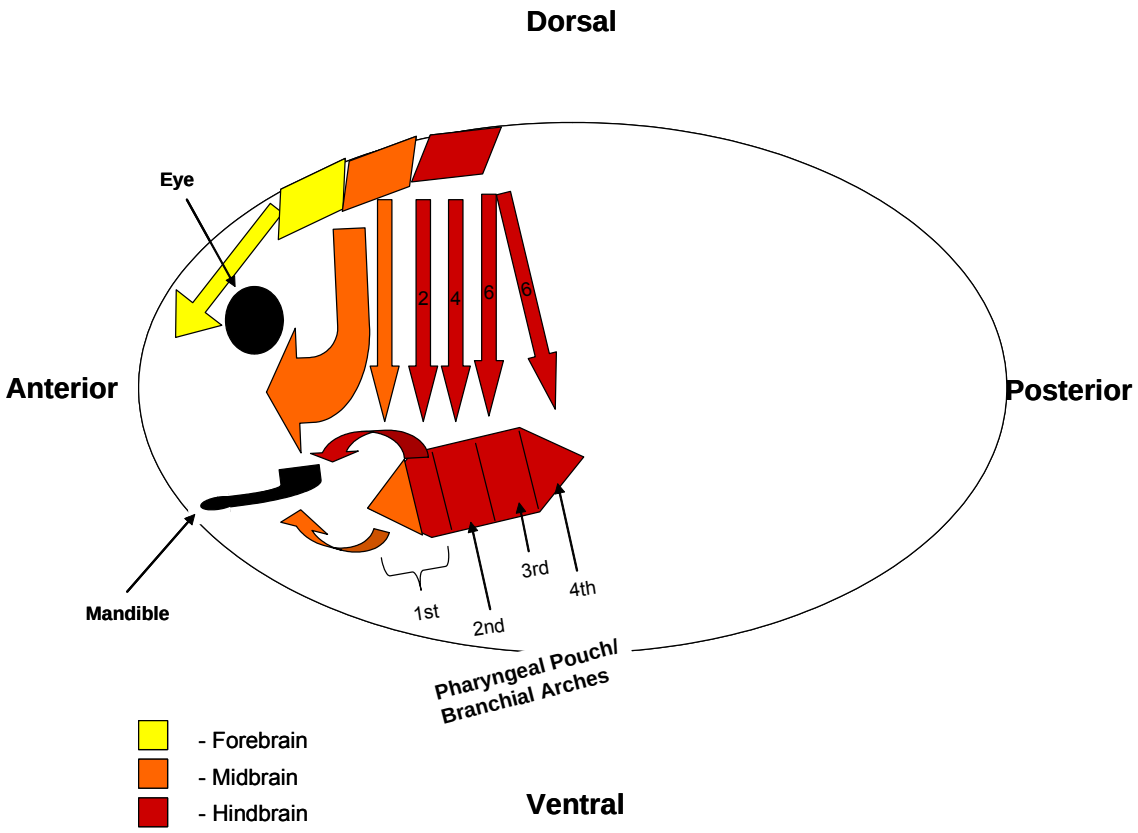

Figure 1. Cranial neural crest migration during X. laevis embryogenesis. Cranial NCC's originate between the neural and non neural ectoderm within the fore, mid, and hindbrain. As the neural tube closes, these cells migrate from their dorsal location in several distinct tracks. The NCC's of the forebrain migrate anteriorly to contribute to the development of the nasal process and palate. The NCC's located in the midbrain migrate ventrally and anteriorly to contribute to the development of the mandible and ear bones. The NCC's of the hindbrain migrate ventrally to populate the pharyngeal pouches and branchial arches.

2. Reactivation of Hox gene expression during bone regeneration

2.1 Summary

Previous studies have explored the link between bone regeneration and skeletogenesis. Although a great deal is known regarding tissue and cell based events, especially those involving ossification and chondrogenesis, much remains unknown about the molecular similarity of repair and development. Since the functional significance of Homeobox (Hox) genes in embryonic skeletogenesis has been well documented through knockout and deficiency studies, we chose to investigate whether members of this family are reactivated during fracture repair. Specifically, we examined the temporal and spatial expression of Msx-1, Msx-2, rHox, Hoxa-2, and Hoxd-9, because of their involvement in limb development. Utilizing quantitative reverse transcriptase RT-PCR (qPCR), mRNA levels from all five genes were shown to be up-regulated during fracture repair at all times tested (post-fracture day 3-21), as compared to intact bone. Further, using *in situ* hybridization and immunohistochemistry, spatial expression of these genes was localized to osteoblasts, chondrocytes and periosteal osteoprogenitor cells found within the fracture callus, the foremost cells responsible for the reparative phase of the healing process. Given the contribution of Hox genes in skeletal development, our results suggest that these genes are involved in either the

patterning or formation of the fracture callus, further supporting the notion that bone regeneration recapitulates skeletal development.

2.2 Introduction

It is well accepted that fracture repair is essentially a recapitulation of bone formation during development [7, 10, 11, 23, 33]. This connection is based on the notion that both processes involve similar molecular mechanisms that control cellular behavior and ultimately lead to the differentiation of mesenchymal cells into active osteoblasts and chondrocytes. Eventually, these cells direct the regeneration of skeletal tissues (bone and cartilage) that comprise the fracture callus and provide the ideal biomechanical environment for healing. Despite these marked similarities there are some clear differences, namely, the inflammatory response following a fracture, as well as remodeling, both processes which are absent during embryonic skeletal development.

In addition to these tissue and cell level morphological events, further similarities between embryonic bone development and regeneration can be found at the molecular level, especially in the activation patterns of specific genes. For example, the signaling genes Indian hedgehog (IHH) and Vascular Endothelial Growth Factor (VEGF), as well as matrix associated genes such as and Matrix Metalloprotease (MMP) 13, and transcription factors such as Core binding factor alpha 1 (Cbfa1/Runx2), and Glicentin 1 (Gli) all show related expression patterns throughout embryonic development

and fracture repair [7,33]. The same is true for members of the Transforming Growth Factor beta (TGFβ) superfamily [reviewed in 10]. Further, through global transcriptional profiling, our laboratory has also shown the expression of a large number of other genes that are up-regulated during both skeletal development and regeneration [11, 21], including novel genes [23].

Based on these results, we hypothesized that other genes important during skeletal embryogenesis, such as Hox genes, are also reactivated during fracture repair. Hox genes represent transcription factors that were originally identified in *Drosophila* and, along with their mammalian homologs, have been implicated in a wide variety of processes during embryogenesis [reviewed in 17]. Specifically, we focused on Hox genes that are known to be involved in limb bud formation during embryogenesis [15], such as Msx-1, Msx-2, Hoxa-2, and Hoxd-9. In addition, we analyzed the expression of another Hox candidate, rHox (also known as MHox, Prx1, Pmx, and Prrx), which was initially identified in osteoblasts [18] and found to be up-regulated during fracture repair [11]. Results from knockout studies suggest that some of these Hox genes play significant roles in bone development and as such, they may also have key roles in the fracture repair process. For example, Msx-2 mutant mice show abnormal cartilage and endochondral bone formation, reduced axial and appendicular skeletal length, as well as reduced numbers and altered morphology of osteoblasts and proliferating and hypertrophic chondrocytes [31]. Msx-1 and Msx-2 were also shown to play essential, and possibly redundant, roles in craniofacial development including

formation of sutures in the skull cap and tooth development [1]. Skeletal abnormalities were also observed for Hoxa-2 and Hoxd-9 deficiency. Specifically, absence of Hoxa-2 results in multiple cranial defects [9], while absence of Hoxd-9 creates malformations of the deltoid crest and reduction in humerus length. These observed effects suggest that Hoxd-9 and Hoxa-2 are involved in skeletal patterning [8, 5]. Lastly, rHox is thought to direct formation of pre-skeletal condensations from undifferentiated mesenchyme because of the observation that rHox -/- mice die shortly after birth with loss or malformations of all skeletal components, including craniofacial, limb, and vertebral structures [25].

Recently, using suppressive subtractive hybridization and microarray studies, our laboratory identified some of these genes to be up-regulated during bone regeneration [11]. In this study, we further explore the temporal and spatial expression patterns of five Hox genes: Msx-1, and Msx-2, rHox, Hoxa-2, and Hoxd-9, using qPCR, *in situ* hybridization and immunohistochemistry. Herein we reveal that all of these genes, known to participate in embryonic skeletal patterning, are reactivated during the development of a mammalian fracture callus.

2.3 Methods

Fracture Model

All methods and animal procedures were reviewed and approved by the University's Institutional Animal Care and Use Committee and met or exceeded all federal guidelines for the humane use of animals in research.

Controlled fixed fractures were generated in the right femurs of twenty-eight six-month old male Sprague Dawley rats by a procedure previously described [4] and routinely performed in our laboratory [11, 12, 13, 14, 21]. A set of five animals was euthanized by CO_2 inhalation at post fracture (PF) day 3, 5, 7 and 10, and a set of 4 animals at PF day 14 and 21. Both the fractured and intact contralateral (control) femurs were dissected free and processed for RNA, protein or immunohistochemistry.

RNA Isolation

Total RNA was isolated on PF days 3, 5, 7, 10, 14 and 21 from calluses as well as the contralateral control femurs. Calluses were harvested from diaphyses (approximately 5 mm proximal and distal to the fracture midpoint). These samples were homogenized in TriZol reagent (Invitrogen) or ToTALLY RNA (Ambion) as described previously [11-14, 21, 23]. As control, the intact femurs (including articular cartilage) were also homogenized in TriZol reagent (Invitrogen) or ToTALLY RNA (Ambion) as described above.

Quantitative reverse transcriptase real time polymerase chain reaction (qPCR)

mRNA, in equivalent amounts from four animals, was pooled to make the intact and PF day 3, 5, 7, 10, and 14 stock samples. Only two animals were combined to create the PF day 21 pool. Also, a reference pool (used in the calibration curve) was created by combining equal amounts of RNA from all samples of intact and PF day pools. Primers were custom-designed (Primer 3, http://frodo.wi.mit.edu/cgi-bin/primer3/primer3_www.cgi) to amplify 206-315 bp sequences within the coding sequences of the experimental genes Msx-1,

Msx-2, rHox, Hoxa-2, and Hoxd-9 (Table 1). All gene expression patterns were normalized to the expression pattern of β-actin (Table 1). All reactions utilized the One-Step QuantiTect SYBR Green RT-PCR kit (Qiagen) and were run using a Light Cycler (Roche). Optimization of reaction conditions was performed for each gene by altering annealing temperature (56-60^{o}C). Each run contained intact and PF day 3, 5, 7, 10, 14, and 21 RNA for both the experimental genes and ß-actin in addition to a five point calibration curve. The experimental gene values for all time points were normalized to their respective ß-actin levels. Each experimental gene was run 3 times and results are reported as average fold change in expression relative to intact levels with ± standard deviation (SD).

Histochemistry and Immunohistochemistry

Intact contralateral control and fractured femurs from each PF day were dissected free of soft tissue, fixed in 10% buffered formalin, decalcified in 5% formic acid, and embedded in paraffin (Polysciences). Serial longitudinal sections (10 μm) were then cut from each sample. Immunohistochemical analysis was performed on specific sections using primary polyclonal antibodies for Msx-1, Msx-2, Hoxa-2, and Hoxd-9 at a concentration of 1:50 (Santa Cruz Biotech) in conjunction with biotinylated anti-goat (Jackson Immunoresearch) or anti-rabbit (Zymed) secondary antibodies at a concentration of 1:200. Sections were incubated at 60^{o} C for 30 min, then deparafinized in xylene, and hydrated using an ethanol gradient. The sections were next permeabilized in PBS containing 0.2% Triton X-100 for 10

min, washed in PBS, and blocked (PBS with 3% horse serum) for 30 min. Sections were then incubated overnight at 4^{o} C with primary antibodies in blocking buffer. The following day, sections were washed in PBS and incubated with biotinylated secondary antibodies (Jackson Immunoresearch, Zymed) in blocking buffer for 30 min. After additional washing, ABC reagent (Vector) was added for 30 min and sections were washed again before detection with DAB reagent (Vector). Negative controls were generated on adjacent sections within the fracture callus by omitting the primary antibodies application. In addition Safranin O/fast green staining was performed on adjacent sections using standard staining procedures to indicate the areas of cartilage and bone. All sections were analyzed under bright field microscopy using a Zeiss microscope (Axiovert 200) and images were captured with a CCD camera (AxioCam MRc).

In situ hybridization:

In situ hybridization was carried out as previously described [23]. Briefly, prior to hybridization, all tissue sections were deparaffinized in xylene, washed, and hydrated using ethanol gradients. Protein digestion was accomplished by incubation in 1N HCl, followed by incubation with varying concentrations of proteinase K (1-100µg/mL, Roche). The sections were acetylated with 0.5% acetic anhydride in PBS (pH 8.0) for 10 min with continuous stirring. Riboprobes (antisense and sense) for rHox in hybridization buffer were heated at 80^{o}C for 3 min, followed by quick cooling in ice water. The hybridization mixture contained each riboprobe (1.0ng/µL),

50% deionized formamide, 10% dextran sulfate, 2X SSC, 0.02% SDS, 0.01% salmon sperm DNA. The slides were incubated for 16 hr at 60^{o} C in a humidified chamber. After hybridization the sections were washed and processed using an anti-DIG detection assay (Roche). Finally, the sections were rinsed with tap water, mounted, viewed under bright field microscopy using a Zeiss microscope (Axiovert 200) and images were captured with a CCD camera (AxioCam MRc).

2.4 Results

Temporal mRNA expression analyses:

Previous transcriptional profiling experiments from our laboratory identified rHox as differentially regulated during bone regeneration with mRNA levels in the fracture callus at 2.1, 3.8, 4, 5.2, 5.7, and 2.4-fold greater (relative to intact bone) for PF day 3, 5, 7, 10, 14 and 21, respectively [11]. To verify these results and to conclusively determine rHox expression pattern during callus progression, we carried out qPCR. This analysis revealed a similar trend in expression, that is, a steady increase in rHox expression peaking at 19.1-fold on PF day 10 followed by a decrease in expression, but still at much higher levels than intact bone, at PF day 14 (9.3 fold) and 21 (11.2 fold) (Figure 1A). Linear regression and correlation analysis of the two data sets yielded an R^2 value of 0.45, indicating that microarray data on its own is not very conclusive (although it did show a similar trend of up-regulation) and should be confirmed with more quantitative assays.

Similarly, we sought to determine the exact expression levels of the remaining Hox candidate genes. For simplification of presentation and analysis, data from Hoxa-2 and Hoxd-9 analysis are grouped together in a single graph (Figure 1B) while those for Msx-1 and Msx-2 are shown in Figure 1C. Hoxa-2 shows a steady increase (2.7-5.4 fold) in expression for the first 14 days and then a dramatic peak on PF day 21 with a 13.7 fold increase in expression relative to intact. In contrast, Hoxd-9 shows peaks in expression at PF days 3 and 10 (6.1 and 7.2 fold, respectively) (Figure 1B). In the case of Msx-1 and Msx-2, both genes exhibited peaks of mRNA expression on PF day 7 with 6.1 and 12.6-fold increases respectively, and again the level of up-regulation was evident throughout all points tested (Figure 1C). In summary, all of the genes monitored exhibited a clear increase in mRNA expression as compared to those detected in intact bone throughout the 21 post fracture days monitored.

Spatial mRNA/protein expression Analysis:

Given that the RNA isolated from fracture calluses was derived from a heterogeneous population of cells, we sought to determine which particular cell type(s) in the callus is/are responsible for specifically expressing each of the Hox genes tested. We utilized both *in situ* hybridization (for rHox) and immunohistochemistry (for Msx-1, Msx-2, Hoxa-2, and Hoxd-9,) to fulfill this objective.

Since no antibody was available for rHox, spatial localization analysis was performed via *in situ* hybridization on PF day 10 callus sections. We chose

PF day 10 because it is the time point where the highest level of rHox expression was detected. In addition, on PF day 10 many of the biological processes (i.e. intramembranous ossification, chondrogenesis, endochondral ossification,) are occurring simultaneously within the fracture callus. Strong hybridization was detected in areas of fibrocartilage, cartilage, periosteum, and woven bone as compared to sense control (Figure 2). More specifically, in areas of cartilage, proliferating and pre-hypertrophic chondrocytes stained much more robustly than terminally differentiated hypertrophic chondrocytes (Figure 2A, and C). Osteoprogenitor cells lining the periosteum also demonstrated strong staining (Figure 2D). Lastly, intense hybridization was detected in active osteoblasts found in areas of woven bone (Figure 2D, E, and F). In contrast, trapped osteoblasts that presumably differentiated into osteocytes, do not show robust reactivity to the rHox antisense riboprobe (Figure 2D, and F). Lastly, hybridization of an adjacent section within the fracture callus (to that shown in Figure 2A) with the control sense rHox riboprobe, showed no labeling (Figure 2B).

For the remaining genes, Msx-1, Msx-2, Hoxa-2, and Hoxd-9, immunohistochemistry was performed using polyclonal antibodies specific for each protein. Again, we chose callus sections from PF day 10 because they represent the multiple biological processes proceeding simultaneously during fracture repair. To help us histologically distinguish between these different tissues, Safranin O/fast green staining was used on adjacent callus sections

which stains areas of bone as blue/green and cartilage as red (Figure 3B, 3H, and 4B).

Hoxa-2 and Hoxd-9 showed very similar spatial expression patterns, especially when viewed at low magnification (Figure 3A and C) and as compared to the negative control (secondary antibody only) that is devoid of immunostaining (Figure 3E). Both Hoxa-2 and Hoxd-9 displayed strong protein expression in proliferating chondrocytes/pre-hypertrophic chondrocytes but strikingly diminished expression in hypertrophic chondrocytes typically found at the core of the soft callus (Figure 3D and F). In contrast, intense staining is detected in areas of fibrocartilage (Figure 3A and C). Similarly, strong immunoreactivity was also observed in osteoblasts found in the surrounding newly formed woven bone (Figure 3D, F, G and I), as well as in osteoprogenitor cells of the periosteum (Figure 3G and H). Lastly, Hoxa-2 and Hoxd-9 staining persists in osteoblasts/osteocytes that have been trapped in the newly made woven bone (Figure 3D, F, G and H).

Interestingly, Msx-1 and Msx-2 show similar pattern of protein expression to Hoxa-2 and Hoxd-9. Specifically, intense immunostaining in proliferating/pre-hypertrophic chondrocytes can be observed (Figure 4A, C, D, and F) as compared to the negative control that shows no immunostaining (Figure 4E). In contrast to Hoxa-2 and Hoxd-9, the expression pattern for both Msx-1 and Msx-2 persists even into the core cartilaginous regions where hypertrophic chondrocytes are predominantly found (Figure 4D and F). Although not all hypertrophic chondrocytes stained positively, a large number

of them are immunoreactive. It is worthwhile to mention that the staining of both of these transcription factors is concentrated within the nuclei of the stained cells as is expected (Figure 4D and F). Lastly, osteoprogenitor cells of the periosteum, as well as osteoblasts and osteocytes in areas of newly made woven bone were highly immunoreactive (Figure 4G and I). In contrast, no staining was detected in these cells on a control adjacent section (secondary antibody alone), as expected (Figure 4H).

2.5 Discussion

In this study, we chose to examine the temporal and spatial expression of five Hox genes, Msx-1, Msx-2, rHox, Hoxa-2 and Hoxd-9. We specifically focused on these genes since they have been implicated in limb bud formation during embryogenesis [15] and because other genes that are expressed during limb formation have also been found to be reactivated during fracture repair [7, 33]. Thus, we hypothesized that Hox genes, critical regulators of the embryonic skeleton, would also be reactivated during bone regeneration.

Hox gene expression was demonstrated as crucial to body segmentation and patterning during embryogenesis with specific Hox members involved in morphogenesis by activating other transcription factors and/or signaling molecules [17]. Mutations in these genes result in severe malformations of specific organs/tissues and even death [35]. More relevant to this study, Hox genes were also implicated in the process of embryonic skeletogenesis. For

example, Pbx-1 deficient mice showed defects in their axial and appendicular skeleton, while disruption of rHox resulted in deformity in, or lack of, craniofacial, limb, and vertebral skeletal structures [25, 32].

Mice deficient in rHox also revealed that this gene is active in regulating skeletal development and osteoblastic differentiation (binds to both collagen type I and osteocalcin promoters) [18, 19]. Upon further examination of the mutant phenotype, a defect in the formation and growth of chondrogenic and osteogenic precursors was identified and was suggested that rHox regulates the formation of pre-skeletal condensations from undifferentiated mesenchyme [25]. These conclusions are consistent with findings presented here, especially our *in situ* hybridization data that reveal increased rHox expression in periosteal osteoprogenitor cells and young active osteoblasts found in areas of woven bone. In addition, we also observed strong expression of rHox in proliferating/pre-hypertrophic chondrocytes, consistent with previous data that localized rHox in chondrocytes of developing long bones at embryonic day 15, as well as newborn mice [25]. Further, the steady increase of rHox expression through PF day 10, a time where chondrogenesis and intramembranous ossification are occurring simultaneously, also supports the notion that rHox serves as a regulator for both osteoblast and chondrocyte differentiation.

In the case of Msx-1 and Msx-2, homologous genes to the *Drosophila* muscle segment homeobox gene, (Msh) [16, 29], prior findings report that they may have redundant functions as transcriptional repressors [1]. This

similarity is linked to their identical DNA coding sequence, except for a discrepancy found in the N-terminus of each gene which bestows Msx-2 a greater affinity for DNA binding but makes Msx-1 a more effective repressor [1]. Both genes were found strongly expressed in developing craniofacial regions in an overlapping manner [24], with the exception that Msx-1 is expressed even during postnatal stages, whereas Msx-2 expression declines after birth. Consistent with these data, our results also indicate that both Msx-1 and Msx-2 are expressed by the identical cell types within the fracture callus. The expression of both genes was found to be very high (~3-13 fold) above mRNA levels seen in intact bone, and localized in periosteal osteoprogenitor cells, young active osteoblasts and proliferating/pre-hypertrophic chondrocytes. Furthermore, Msx-1 was showed to be downregulated in periosteal osteoblasts at birth but expressed postnatally in alveolar bone processes [27]. Although initially this might be contradictory to our results that show both Msx-1 and Msx-2 abundantly expressed by periosteum osteoblasts, when one considers the notion that fracture repair recapitulates embryonic development, reactivation of Msx-1 and 2 in periosteum-derived osteoblasts is then consistent and even expected since it is known that these cells originate from mesenchymal progenitors.

Lastly, Msx genes seem to promote proliferation while blocking terminal differentiation, as was shown by the downregulation of terminal differentiation markers osteocalcin and collagen type I through Msx-2 [6, 26] and cbfa/Runx2 by Msx-1 activity [3]. This is also supported by our data,

especially by the reduced expression of both Msx-1 and 2 detected in terminally differentiated osteocytes and hypertrophic chondrocytes. In contrast, robust expression of both genes was detected in active osteoblasts and proliferating chondrocytes. Further, suppression of terminal differentiation by Msx-1 and Msx-2 would explain the incomplete or delayed ossification of calvarial bones in Msx-2 deficient mice [31], as well as the complete deficiency of calvarial ossification in the Msx-1 and 2 double mutant mice [1]. This is probably due to the overall decrease in differentiated osteoblasts required to seal the cranial sutures. Lastly, abnormal cartilage and endochondral ossification were also observed in Msx-2 knockout mice leading to a reduction in both axial and appendicular skeletal lengths [31]. Clearly, additional experiments are required to conclusively determine the precise role(s) of Msx-1 and Msx-2, especially in periosteal osteoprogenitor differentiation during the progression of the fracture callus.

While Hoxa-2 knockouts and deletions were generated, studies on these animals primarily focused on the patterning of the branchial arches and the mammalian hindbrain [2, 9, 28]. However, even in these studies a link can be found between Hoxa-2 and skeletal development. The Hoxa-2 mutant mice exhibited multiple cranial defects, including duplication of ossification centers of middle ear bones as well as replacement of the second branchial arch elements with the first set [9]. In subsequent experiments it was demonstrated that Hoxa-2 directs proper formation of the second arch by preventing chondrogenesis and intramembranous ossification [20]. Our data

is in agreement with the fact that Hoxa-2 is involved in chondrogenesis and osteogenesis (ossification) during facture repair, since we mapped the up-regulated expression of this gene in both active osteoblasts and chondrocytes. In addition, osteoprogenitor cells in the periosteum also express high levels of Hoxa-2. However, an interesting inference may be made from the temporal peak in expression on PF day 21. Given the critical role of Hoxa-2 in skeletal patterning, this late peak in expression during fracture repair may indicate a yet undefined role of Hoxa-2 in endochondral ossification or bone remodeling, known to occur at this time in the callus.

While Hoxd-9 has been examined in systems ranging from locomotor behavior to cervical cancer [5, 22], its role has not been very well described during skeletogenesis. The single Hoxd-9 deficiency study conducted showed malformations of deltoid crest and reduction of the humerus in Hoxd-9 -/- mice [8]. In addition, a targeted disruption study of Hoxd-9 and Hoxd-10 found alterations in axial and appendicular skeletal structures, specifically the presence of an additional S1 vertebrae, as well as fusion of transverse processes with a high rate of four fused sacral vertebrae [5]. Collectively, these results support our findings that Hoxd-9 is involved in fracture callus development, especially the early stages (PF day 3-10), consistent with the spatial analysis where we mapped the expression of Hoxd-9 in proliferating chondrocytes and osteoblasts, as well as in the periosteum. These results suggest that Hoxd-9 plays a role in intramembranous ossification and

chondrogenesis rather than endochondral ossification which occurs at later times (PF 14 and 21).

The *in vivo* analyses of Msx-1, Msx-2, rHox, Hoxa-2, and Hoxd-9 described above, indicate that each gene is involved in skeletal development in a very specific way. As we expected, our hypothesis that Hox genes, critical regulators of the embryonic skeleton, will also be reactivated during bone regeneration was verified by the data presented here. To our knowledge, this study is one of the first to examine the reactivation of Hox genes during bone regeneration. Previously, another study showed that the rat homolog of the homeoprotein distal-less (Dlx) was found to be up-regulated during fracture at PF day 2-30 [34]. This was not a surprising finding since Dlx has been shown to regulate the expression of osteocalcin which promotes osteoblast differentiation [30]. Together with our results, these data indicate that all five Hox genes studied are reactivated during fracture repair and display differential up-regulated patterns of expression by specific callus cell types. It is clear from the expression studies that all of the Hox genes analyzed, as well as other members of their respective families (including Dlx), collectively function together to help control the regeneration of the various anatomical tissues of the callus as they develop, mature and eventually remodel into lamellar cortical bone. While the precise molecular mechanisms of action and functional contributions for these genes during fracture repair remains unknown, this study provides supplementary evidence strongly supporting the notion that bone regeneration recapitulates

development. Obviously, additional studies are needed to fully elucidate the exact roles of these genes in the fracture repair process.

Acknowledgments

I would like to thank Frank Lombardo and Scott McGovern for their contributions to the data presented within this report. Also, I would like to thank Alan Ka and Fayez Safadi for help in developing the *in situ hybridization* protocol, David Komatsu for insightful discussions, Jonathan Chiu for critically reading the manuscript and Rosemary Gaynor for secretarial support.

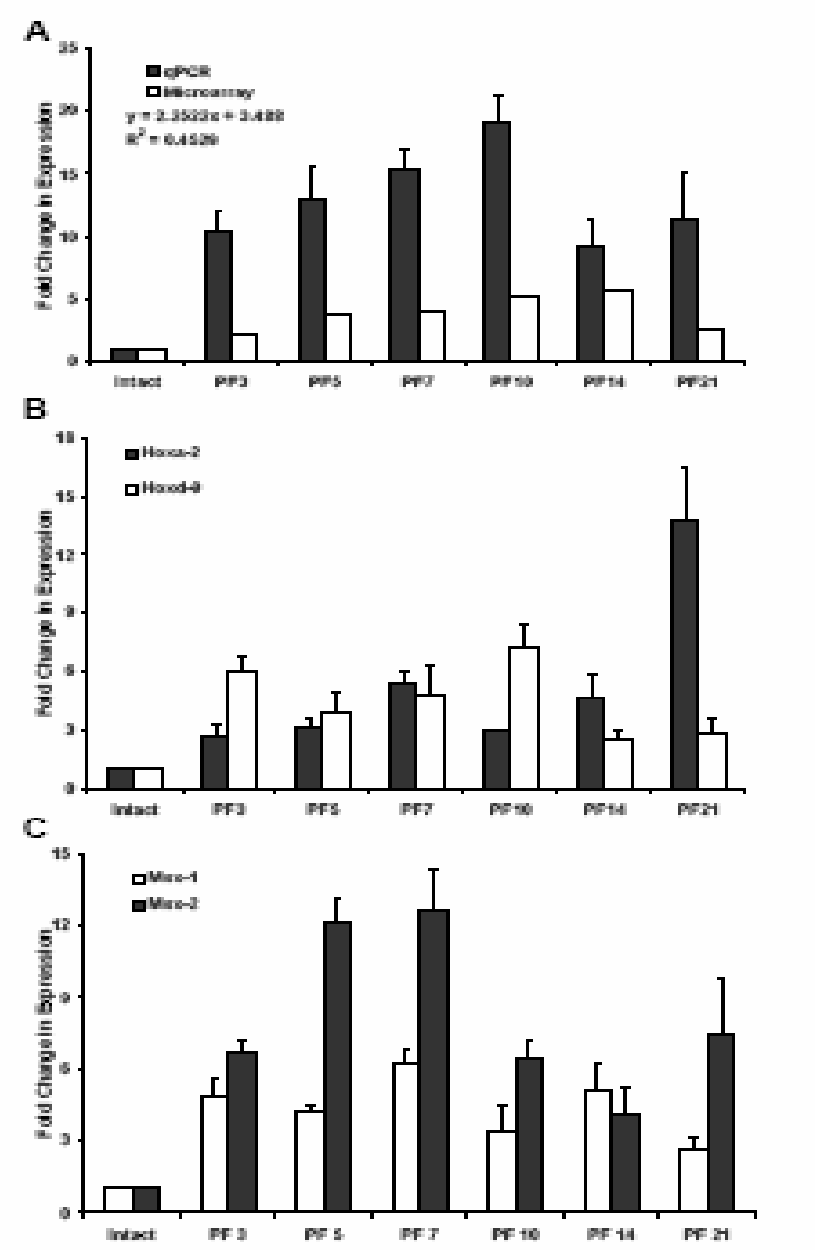

Figure 1. Transcriptional activation of Hox genes during fracture repair. All qPCR analyses were performed on pooled RNA samples (n=4 animals/time point) from intact femurs and post fracture days 3, 5, 7, 10, and 14. For PF day 21, n=2. All values represent average fold change relative to intact bone with error bars indicating standard deviation among replicates (n=3) in qPCR experiments. **A.** Temporal mRNA analysis of rHox by qPCR (Black) and microarray (white). Linear regression and correlation analysis was used to derive the R*2* value. **B.** Temporal mRNA analysis of Hoxa-2 (Black) and Hoxd-9 (White). **C.** Temporal mRNA analysis of Msx-1 (White) and Msx-2 (Black).

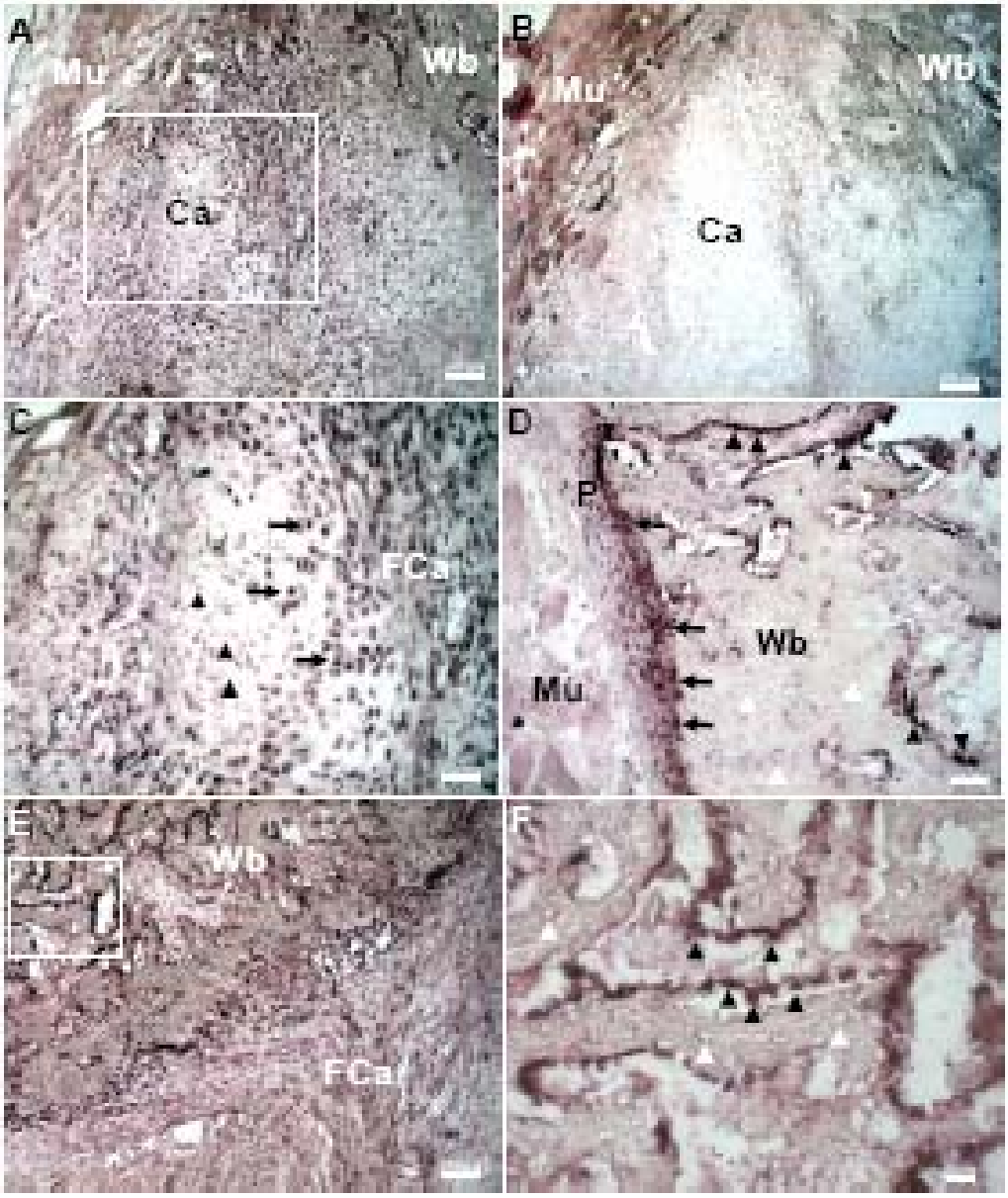

Figure 2. *In situ* hybridization of rHox during fracture repair. This figure was contributed by F. Lombardo. **A.** PF 10 callus section bordering the fracture site hybridized to rHox antisense riboprobe illustrating regions of muscle (Mu), woven bone (Wb), and cartilage (Ca). **B.** Adjacent section within the fracture callus to **A** hybridized with the sense rHox riboprobe as a control. **C.** Higher magnification view of the cartilaginous zone from **A** (white box) displaying fibrocartilage (FCa) with proliferating chondrocytes (arrows) seen staining strongly and hypertrophic chondrocytes (arrowheads) indicating little or no staining. **D.** rHox expression in periosteum (P) containing strongly staining osteoprogenitor cells (black arrows) and osteoblasts (black arrowheads). Very little or no staining is detected in osteoblasts/osteocytes within areas of woven bone (white arrowheads). **E.** Low magnification of rHox expression in areas of woven bone (Wb) and fibrocartilage (FCa) adjacent to fracture site. **F.** Higher magnification view of the region in **E** (white box) of woven bone signifying intensely stained osteoblasts (black arrowheads) and unstained osteocytes (white arrowheads). Scale bars represent 100μm in A, B, and E, 50 μm in C and D, and 20 μm in F.

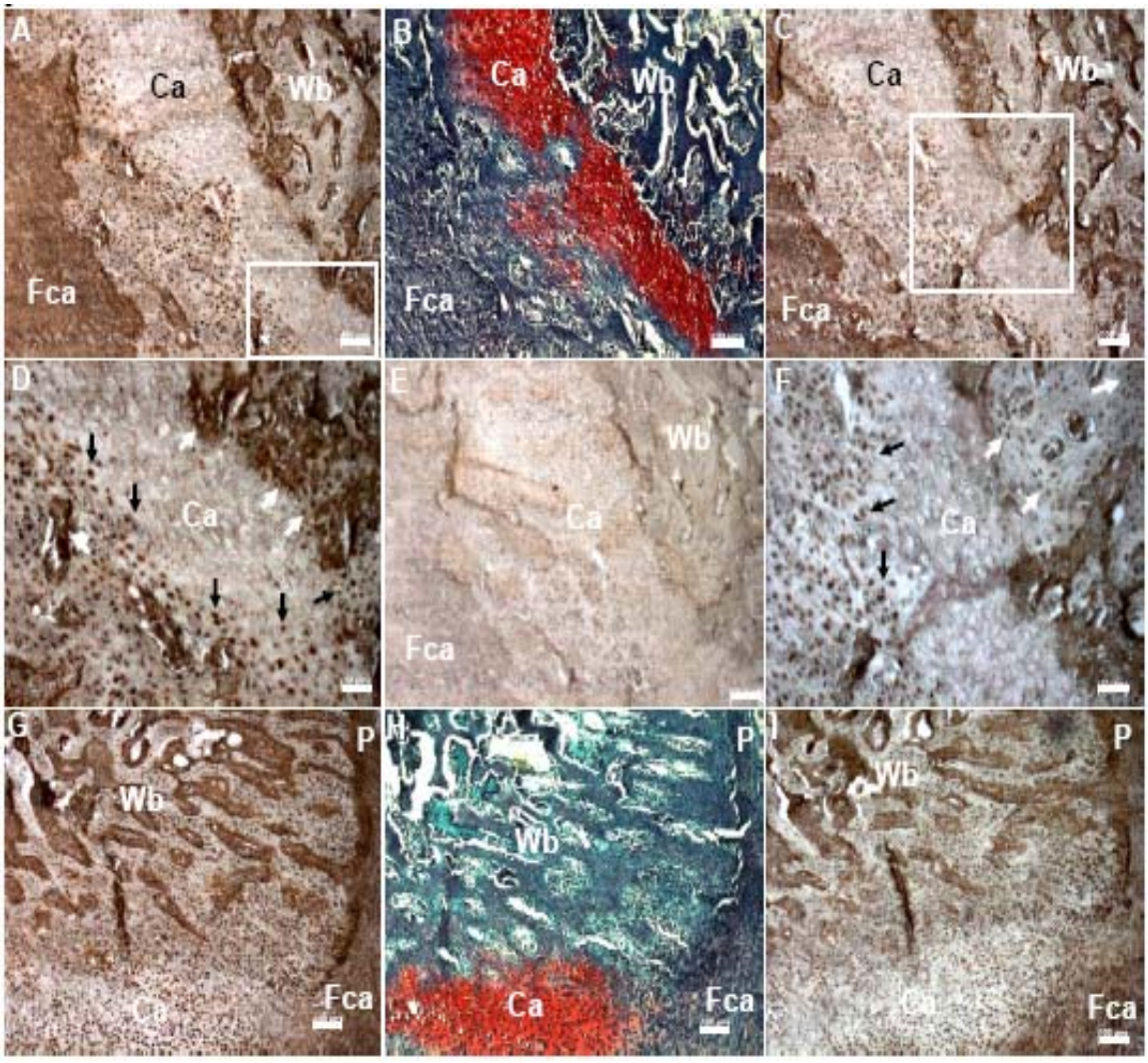

Figure 3. Spatial localization of Hoxa-2 and Hoxd-9. Immunohistochemical analysis of PF day 10 callus sections for Hoxa-2 and Hoxd-9. **A.** Low magnification view of Hoxa-2 staining adjacent to the fracture site with areas of woven bone (Wb), fibrocartilage (Fca), and cartilage (Ca) demonstrating intense staining. **B.** Safranin O fast/green staining of adjacent section from the same fracture callus with same regions identified. **C.** Low magnification view of adjacent section stained for Hoxd-9 with similar areas (fibrocartilage, cartilage, woven bone) stained. **D**. Higher magnification view of cartilaginous zone in **A** (white box) showing robustly stained proliferating chondrocytes (black arrows) and osteoblasts in areas of woven bone (white arrows). **E.** Adjacent section to **A** and **C** within the fracture callus stained with secondary antibody (negative control) section depicting no staining. **F.** Higher magnification view of cartilaginous zone in **C** (white box) showing robustly stained proliferating chondrocytes (black arrows) and osteoblasts/osteocytes trapped in areas of woven bone (white arrows). **G.** Low magnification view of the same section stained for Hoxa-2 and showing intense staining in the periosteum (P), as well as areas of woven bone (Wb), cartilage (Ca) and fibrocartilage (Fca). **H.** Adjacent section within the fracture callus stained with Safranin O fast/green depicting the same regions. **I**. Adjoining section to **G** and **H** stained for Hoxd-9 and showing intense staining in the periosteum (P), as well as areas of woven bone (Wb), cartilage (Ca) and fibrocartilage (Fca). Scale bars represent 100 μm in A, B, C, E, G, H, and I while scale bars in D and F represent 50 μm.

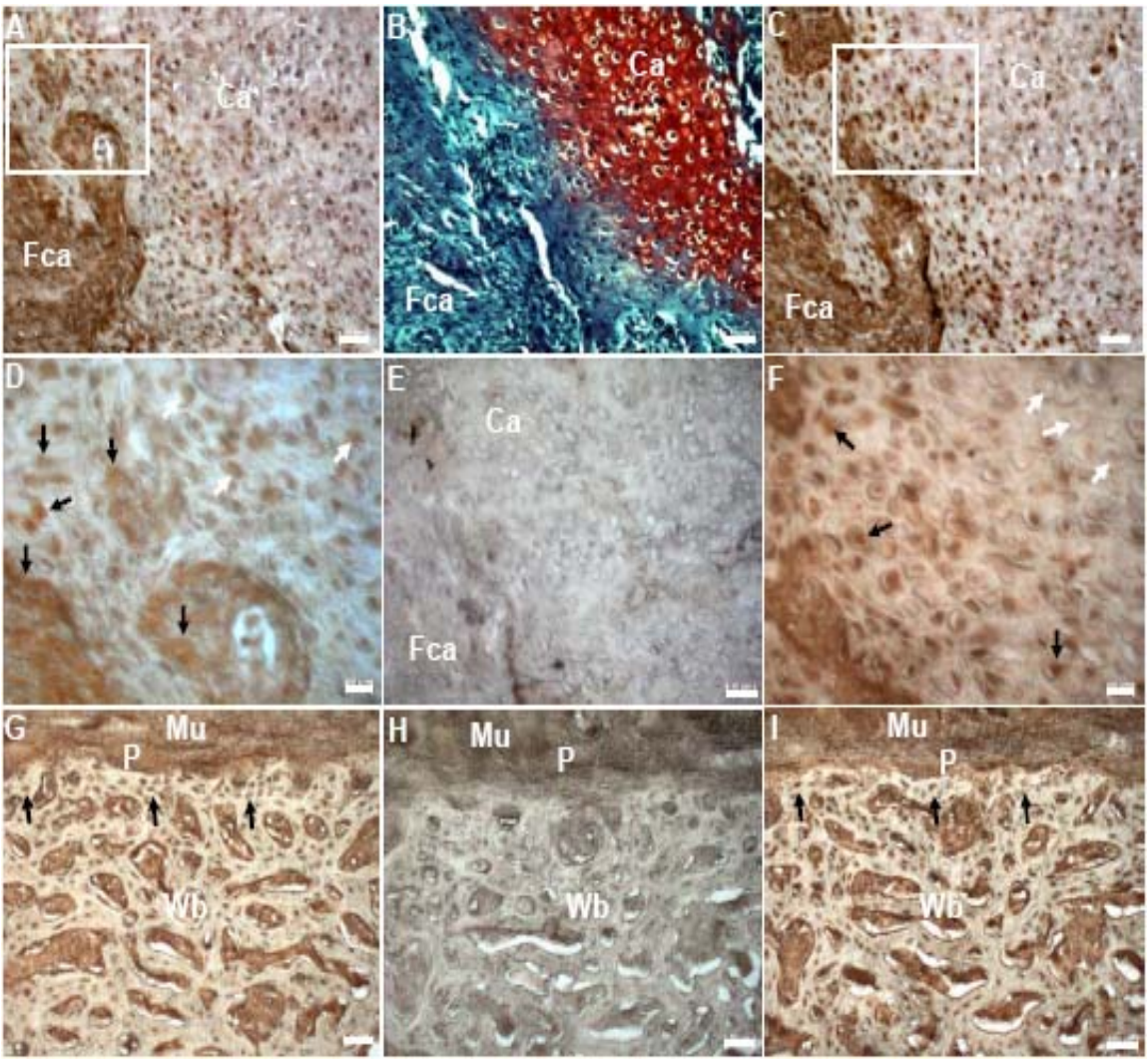

Figure 4 Spatial localization of Msx-1 and Msx-2. Immunohistochemical analysis of PF day 10 callus sections for Msx-1 and Msx-2. **A.** Section near fracture site stained for Msx-1 showing positive labeling in cartilage (Ca), and fibrocartilage (Fca). **B.** Safranin O fast/green staining of adjacent section within the fracture callus with same regions identified. **C.** Adjacent section to **A** within the fracture callus illustrating the same regions (cartilage, fibrocartilage) stained for Msx-2. **D.** Higher magnification view of cartilaginous zone in **A** (white box) demonstrating intense labeling in proliferating chondrocytes (black arrows) and pre-hypertrophic chondrocytes (white arrows). **E.** Adjacent section to **A** and **C** within the fracture callus stained with secondary antibody (negative control) section depicting no staining. **F.** Higher magnification view of cartilaginous area in **C** (white box) showing robust staining in proliferating/pre-hypertrophic chondrocytes (black arrows) but no/weak staining in hypertrophic chondrocytes (white arrows). **G**. Low magnification view of the callus (proximal to the fracture site) showing areas of muscle (Mu) and woven bone (Wb) with intense Msx-1 staining in periosteum (P) and osteoblasts, especially those that are still active below the periosteum (black arrows). Osteocytes that are found further away from the periosteum (bottom) do not express Msx-1 as strongly. **H.** Adjacent section to **G** and **I** stained with secondary antibody (negative control) and devoid of staining. **I.** Adjacent sections to **G** illustrating positive Msx-2 immunoreactivity in periosteum (P) and woven bone (Wb), particularly in osteoblasts (black arrows) and even osteocytes throughout the entire Wb region. Scale bars represent 50 μm in A, B, C, E, G, H, I, and 20 μm in D and F.

3. Mustn1 is Necessary for Chondrocyte Differentiation *in vitro*.

3.1 Abstract

Previously, we identified Mustn1; encoding a 9.6 kDa nuclear protein expressed specifically in the musculoskeletal system. Identification via *in situ* hybridization of developing limb and adult joints reveals strong Mustn1 expression in mesenchymal condensations and proliferating chondrocytes. Therefore, localization experiments were undertaken on developing mouse embryos. Whole mount *in situ* hybridization revealed Mustn1 expression in areas of chondrogenesis including limb buds, branchial arches, somites, and tail bud. To elucidate its function, experiments were carried out to functionally perturb Mustn1 by overexpression and silencing in the pre-chondrocytic RCJ cell line. Mustn1 was successfully overexpressed in RCJ cells by ~2-6 fold, and reduced in silenced cell lines to 32-52%, when compared to parental cell line Mustn1 expression levels. Overexpressing, silenced, control, and parental RCJ cell lines were assayed for proliferation and matrix production. No statistically significant changes were observed in either proliferation or proteoglycan production when Mustn1 overexpressing lines were compared to parental and control cells. In contrast, Mustn1 silenced cell lines were significantly reduced from parental and random control lines in both proliferation rate and matrix production. RNAi silenced cell lines showed average reductions in population of ~55-75%, and showed ~34-40% less

matrix ultimately produced when compared to parental and random control lines. Further, this reduction in matrix production was accompanied by significant reductions in the chondrogenic marker genes; Sox9, Collagen II, and Collagen X. Reintroduction of Mustn1 expression into these silenced cell lines rescued this phenotype, returning proliferation rate, matrix production, and marker gene expression back to parental levels. Taken together these data suggest that Mustn1 is a crucial regulator of chondrogenesis.

3.2 Introduction

Previous work in our laboratory has identified Mustn1 as a small (9.6kDa) protein that localizes predominantly to the musculoskeletal system in adult rodents [15]. Investigation of Mustn1's sequence revealed that it is highly homologous in vertebrates and contains a nuclear localization sequence but no other significant motifs, only potential phosphorylation and myristylation sites. Further, GPF fusion experiments show Mustn1 localization to the nucleus but not to the nuclear membrane or nucleoli indicating that Mustn1 possibly functions in a transcriptional complex [15].

In an effort to further characterize this gene, its promoter was identified and analyzed. Within the 1512bp region flanking Mustn1's 5' end several transcription factor binding sites were identified that belong to the Activator Protein (AP) family of proteins [14]. It was further shown that AP-1 family members (JunD, c-Fos, and Fra-2) bind to Mustn1's promoter during both proliferation and differentiation of C2C12 cells and are known as key

transcriptional regulators of musculoskeletal specific genes [14]. Knockout studies of these genes show varying degrees of phenotypic deficiency within the musculoskeletal system including osteoporosis, osteosarcoma, and chondrosarcoma as well as sterility, embryonic lethality, and ocular malformations [23]. However, because AP-1 members function within multiple signaling pathways, additional research is needed to determine which one(s) involve Mustn1 expression.

Although exploring Mustn1's sequence and temporal and spatial expression patterns provides useful information, conclusions on function cannot be drawn from these data alone. Fortunately, Mustn1 was initially identified by its differentially regulated expression pattern during the process of BFR. Mustn1 expression dramatically increases during the early phases of BFR culminating in a peak of ~55-fold over its intact level on post fracture (PF) day 5. After this peak; Mustn1 expression slowly returns to control (intact bone) levels throughout the remainder of the 28-day fracture healing process [15]. This differential expression pattern strongly suggests that Mustn1 plays a role in BFR. Complimentary experiments showed that Mustn1 is expressed by proliferating chondrocytes, osteoblasts and periosteal osteoprogenitor cells in a fracture callus. Further, Mustn1 expression was also seen within the developing intervertebral discs and limb bud during rat embryogenesis, as well as articular cartilage. Finally, while proliferating chondrocytes showed staining in all of these tissues; terminally differentiated hypertrophic chondrocytes within these samples did not show Mustn1 expression [15].

Mustn1's peak in expression correlates to BFR time points when mesenchymal precursor cells are migrating to the fracture site, differentiating into chondrocytes, and proliferating within the callus prior to hypertrophic differentiation. Therefore, functional perturbation of Mustn1 during chondrocyte proliferation and differentiation would help to clarify its role during chondrogenesis. To this end this study seeks to modulate Mustn1 expression in the pre-chondrogenic RCJ3.1C5.18 (RCJ) cell line. The RCJ line represents a heterogeneous cell population capable of differentiation into proliferating chondrocytes and ultimately terminally differentiated collagen X producing hypertrophic chondrocytes [2].

Because Mustn1 is highly expressed in the early stages of BFR and this process is known to recapitulate limb formation [5,6,7,8,22]; localization of Mustn1 during development should denote expression in areas of proliferating chondrocytes and musculoskeletal development, such as the developing branchial arches, somites, limb, and tail buds. If so, we seek to identify Mustn1 expression earlier in musculoskeletal development than previously reported [15]. This expression should correspond with data derived during RCJ differentiation. Based on previous data that suggests Mustn1 is a transcriptional co-regulator; alterations in Mustn1 basal levels will likely result in phenotypic changes in proliferation rate, differentiation, and/or matrix production.

3.3 Materials and Methods

Materials

The Anti-DIG Antibody was purchased from Roche (Indianapolis, IN). Dexamethazone and β-glycerophosphate were purchased from Sigma-Aldrich (St. Louis, MO). Bovine Calf Serum, DMEM medium and antibiotics were purchased from Gibco BRL (Gaithersburg, MD). G418 was purchased from Invitrogen (Carlsbad, CA). Oligonucleotides were designed against the coding regions of ß-2 Microglobulin, Mustn1, Collagen II, Collagen X, and Sox9 (See Table 1 for details).

Whole mount *in situ* hybridization

Riboprobes were created by using T7 and Sp6 primers to amplify the probe sequence. The product was then purified and labeled using the DIG RNA labeling Kit (Roche) creating sense and anti-sense riboprobes. The original PCR product was degraded using RNase free DNase 1 (Qiagen). This reaction was stopped using 0.2M EDTA (pH=8.0). The riboprobes were then purified using sephadex G-50 quick spin columns. The *in situ* analysis was completed following the protocol described by Hsieh et al (2003). Briefly, embryos were dissected out on 8.5, 9.5, 10.5, and 11.5dpc and fixed with 4% Paraformaldehyde for 1hr at room temperature. Larger embryos were then permeabilized with proteinase K and all embryos were then bleached with H_2O_2 and stored in 100% methanol at -20^{o}C. Embryos were then rehydrated through a methanol gradient and hybridized overnight at 65^{o}C in a probe

concentration of 250ng/ml. Embryos were then washed with MABT and blocked in MABT+20% Goat serum + 2% Boehringer Blocking Reagent (BM 1096 176). Embryos were incubated overnight in 1:2000 dilution anti-DIG 2^{o} antibody. Embryos were then washed with MABT and expression was visualized with NTMT/BCIP. Pictures were taken and embryos were stored in 80% glycerol/.1% NaAzide.

Cell culture

RCJ3.1C5 cells were maintained in Dulbecco's modified Eagle medium (DMEM) supplemented with 10% Bovine Calf Serum (BCS), 1% penicillin/streptomycin, and 10^{-7}M Dexamethasone. Cells were fed every 3-4 days and passaged prior to confluence.

RNA interference

Three 19-mer RNAi target sequences were designed (5'-AAGGAAGAAGACCTGAAGG -3', 5' – CCTGTGAAGGAAGAAGACC – 3', and 5' – TATTCAGCCGCAACCGCAC – 3') which correspond to three different regions of the Mustn1 coding sequence, however sequences 1 & 2 overlap. Oligonucleotides of hairpins containing these sequences (M2, M3, and M4 respectively) were generated (Invitrogen) and cloned into the pSuppressorRetro plasmid. A random control plasmid was generated by cloning a random 19-mer sequence (5' – GACTCCAGTGGTAATCTAC – 3'), which shows no similarity to any sequence within the *Mus musculus* genome,

into the same expression plasmid. A BLASTN (Basic Local Alignment Search Tool Nucleotide http;//www.ncbi.nlm.nih.gov/BLAST/) search was conducted to ensure that this random control sequence showed no homology to the rat genome. Using a Retroviral GeneSuppressor System kit (IMGENEX Corp) these plasmids were co-transfected along with a packaging vector designed to create an ectotropic retrovirus protein coat into 293 cells. Virus containing media was harvested and used to infect proliferating RCJ cells. After a 24hr infection period, RCJ cells were selected using G418 for one week. Surviving cells were plated at low density and colony forming units were allowed to grow up over several weeks. Homogeneous colonies were isolated and expanded. Five clones for each RNAi sequence were assayed for Mustn1 expression and the clones showing the most effectively reduced expression (M2-2, M3-5, and M4-4) were used in subsequent proliferation and differentiation experiments.

Transient transfection efficiency

The reintroduction of Mustn1 mRNA could not be stably selected; therefore efficiency of the transient transfection was tested by visualizing the GFP tag on the Mustn1 expression vector. A representative Mustn1 silenced cell line, M2-2, was transfected with tagged Mustn1 plasmid and viewed under bright field and fluorescence throughout the differentiation time course. Cell Populations were counted and the percentage of GFP positive cells was

determined. Five cell fields were chosen at random and counted, then averaged to provide standard deviation values.

Overexpression

The Mustn1 coding sequence was cloned into the pCDNA vector downstream of the CMV promoter. RCJ cells were transfected with this plasmid using Fugene 6 Transfection Reagent (Roche). After a 24hr transfection period, RCJ cells were selected using G418 for one week. Surviving cells were plated at low density and colony forming units were allowed to grow up over several weeks. Homogeneous colonies were isolated and expanded. Eight clones were assayed for Mustn1 expression and the three clones showing the highest Mustn1 overexpression (OE 3, OE 4, and OE 6) were used in subsequent proliferation and differentiation experiments.

Site-directed mutagenesis

Oligonucleotides were designed with alterations to the 3' nucleotide in each codon within the M2 RNAi sequence (M2 RNAi sense sequence 5' AAGGAAGAAGACCTGAAGG 3', Rescue sense sequence 5' AAAGAGGAGGATCTAAAAG 3'). These oligonucleotides were then used to amplify the original Mustn1 pCDNA plasmid using the QuikChange II Site-Directed Mutagenesis Kit (Stratagene). The original plasmid was then degraded using Dpn1 restriction digestion and the rescue plasmid was

transformed into XL1-Blue Supercompetent Cells. These cells were grown on Amp LB agar plates and colonies were expanded. The rescue plasmid was isolated via mini and midiprep kits (Qiagen). This rescue plasmid was then used to transiently transfect the RCJ M2-2 cell line prior to proliferation and differentiation analysis.

Proliferation analysis

RCJ cells were seeded in 96-well plates (Falcon) at low density (~2,000 cells/well). The regular RCJ media was removed and 2.5%BCS RCJ media was added at the 0hr time point. Triplicate wells for each cell line were assayed during a 72hr time course (at 2hr, 24hr, 48hr, and 72hr) via MTS reagent (Promega). 5µl of MTS reagent was added to each well containing 100µl media. The plates were then incubated at 37^{o}C for 1hr in the dark. The MTS/media solution was then diluted in 400ul dH_2O and analyzed by spectrophotometer (BioRad) at 490nm. Values were normalized to MTS/media solution from wells that did not contain cells. Values were further normalized to the 2hr time point to reflect population doublings. The triplicate values for each cell line at each time point were then averaged and standard deviation bars were created.

Matrix production analysis

RCJ cells from each cell line were seeded in 24-well plates (Falcon) at high density (~20,000cells/well). At near confluence the regular RCJ media

was removed and replaced with differentiation media (DMEM with 10% BCS, 1% penicillin/streptomycin, 10^{-7}M dexamethasone, 50µg/ml ascorbic acid, and 10mM β-glycerol-phosphate) on Day 0. Differentiation media was removed and replaced with fresh on Day 3, 6, 9, and 12. Samples were taken throughout a 14 day time course (on Day 0, 2, 5, 7, 10, and 14). On these time points triplicate wells for each cell line were fixed for 4 min with 10% Buffered Formalin Phosphate (Fisher) and stored in PBS at 4^{o}C. On Day 14, all plates were stained with a 1% Alcian blue solution for 45min at room temperature. Wells were washed with PBS and the Alcian blue was eluted in 4%Guanidine Hydrochloride in PBS for 30min at room temperature. Samples were then diluted 1:2-1:4 in dH_2O and analyzed at 600nm via spectrophotometer (BioRad) and normalized to the Guanidine Hydrochloride/dH_2O solution. The triplicate values for each cell line at each time point were then averaged and standard deviation bars were created. Values were then further normalized to the Day 0 time point to reflect fold change.

RNA isolation

RCJ cells were seeded in 24-well plates (Falcon) at high density (~20,000cells/well). At near confluence the regular RCJ media was removed and replaced with differentiation media (DMEM with 10% BCS, 1% penicillin/streptomycin, 10^{-7}M dexamethasone, 50µg/ml ascorbic acid, and 10mM β-glycerol-phosphate) on Day 0. Differentiation media was removed

and replaced with fresh on Day 3, 6, and 9. Samples were taken throughout a 14 day time course (on Day 0, 2, 5, 7, 10, and 14). On these time points triplicate wells for each cell line were lysed using TriZol reagent (Invitrogen), pooled, and stored at -80^{o}C. Upon completion of the time course RNA was extracted using chloroform and 100% isopropanol using Invitrogen protocols. The RNA was then resuspended and diluted in dH_2O in preparation for quantitative real-time RT-PCR experimentation.

Quantitative real-time RT-PCR (qPCR)

RNA isolated from Day 0, 2, 5, 7, 10, and 14 of the differentiation time course was treated with DNase 1 (Qiagen). RNA was quantified using a ND-1000 Spectrophotometer (Nano Drop). The qPCR experiments were carried out using a QunatiTect SYBR Green RT-PCR Kit (Qiagen) on a LightCycler system (Roche) as previously described (Komatsu et al 2004). Primer pairs for Mustn1, Collagen II, Collagen X, and Sox9 were designed to anneal at 58^{o}C and RNA concentrations of 4-20ng/reaction (Table 1). Each run consisted of mRNA from Day 0, 2, 5, 7, 10, and 14 (for Mustn1) or Day 0, 5, 10, 14 (for marker genes) assayed for the gene of interest and the housekeeping gene β 2-Microglobulin, as well as 5 point calibration curves (1.25-20ng/reaction). The calculated concentration values for each gene of interest were normalized to its corresponding β 2-Microglobulin values. All qPCR products were checked via agarose gel electrophoresis to assess

amplification. Each run was replicated 3 times and results are reported as expression level ± standard deviation.

Statistical analysis

The quantitative data shown throughout this report were the average results of three or more independent experiments with standard deviation indicated by error bars. Significance was determined in all analysis by One way ANOVA followed by a Holm-Sidac Post-hoc when comparing to initial (Day 0 or 2hr) time points and Mann-Whitney tests when values from a single time point was compared.

3.4 Results

Whole mount *in situ* hybridization

In order to elucidate the Mustn1 expression pattern during mouse development, we performed whole mount *in situ* hybridization. Mouse embryos incubated with the antisense riboprobes showed staining in several key tissues at different time points (Figure 1). In 8.5dpc embryos, a diffuse staining within the interior of the embryo, the site of several tissues such as paraxial mesoderm, developing organs and musculoskeletal elements, showed strong staining (Figure 1A). At 9.5dpc embryos, staining expanded throughout the embryo, possibly in musculoskeletal tissues such as the paraxial mesoderm on either side of what appears to be the unstained neural tube as well as craniofacial structures (Figure 1B). In 10.5dpc embryos,

staining became localized to several areas of chondrogenesis and bone formation. The craniofacial region showed intense staining as well as the branchial arches (Figure 1C, black arrows). The forelimb and hind limb buds also showed significant staining when compared to the sense control embryo (Figure 1C, white arrows). While the somites showed light staining in a rayed pattern perpendicular to the spinal column, deeper color was evident at the developing posterior tip of the tail (Figure 1C). In the 11.5dpc embryos, staining was again observed along the entirety of both the fore and hind limb buds however, more intense staining was observed in the hind limb (Figure 1D, white arrows). Again staining was observed in the craniofacial region, particularly the developing branchial arches (Figure 1D, black arrows). Both anterior somites and posterior tail region showed staining as well. Mouse embryos incubated with a sense control riboprobes for Mustn1 showed little or no staining at any time point (Figure 1 E-G). Mild coloration was observed both in the fore and midbrain as well as the otic vesicle in individual embryos; however, this staining likely indicates trapping of the staining agent within these cavities.

Mustn1 & marker gene expression in RCJ cells

In order to get a baseline expression pattern for Mustn1 and the three cartilage marker genes used in later experiments (Sox9, Collagen II, and Collagen X), we quantified mRNA levels in parental unaffected RCJ cells via qPCR and normalized to expression levels of the housekeeping gene ß 2-

Microglobulin. Mustn1 expression in RCJ cells shows a peak of ~5.2 fold at Day 2 of differentiation when compared to Day 0 values. Mustn1 expression then falls back to Day 0 levels for the remainder of the time course (Figure 2A). When Sox9 was assayed, a steady increase was observed throughout the time course culminating in a peak in expression of ~4.7 fold over Day 0 values on Day 14 (Figure 2B). Collagen II showed a similar expression pattern, increasing to a peak of ~51.4 fold over Day 0 values on Day 14. Finally, Collagen X showed an increase in expression later in the time course, beginning on Day 10 and peaking on Day 14 with a value of ~21.1 fold over Day 0 values (Figure 2B).

Overexpression and silencing

Next we sought to alter Mustn1 expression in RCJ cells via functional perturbation resulting in overexpression or silenced cell lines. Overexpression of Mustn1 by stable transfection resulted in multiple homogeneous clones. Three clones were selected and showed an increase of Mustn1 expression of 6.1, 3.1, and 2.1 fold when normalized to the parental cell line (OE 3, OE 4, and OE 6 respectively, Figure 3A). Transfection of the empty expression vector into the parental RCJ cell line as control caused no significant alteration in Mustn1 expression levels (Figure 3A).

Silencing of Mustn1 by RNAi infection also resulted in multiple homogeneous clones. Three clones, one resulting from each of the three

different RNAi target sequences, were selected and their Mustn1 expression was analyzed via qPCR. These clones showed that Mustn1 expression was reduced to 37%, 32%, and 58% of the parental cell line expression levels (in M2-2, M3-5, and M4-4, respectively, Figure 3B). Infection of a random control sequence into the parental cell line showed no significant difference in Mustn1 expression (Figure 3). M2-2 was chosen as a representative silenced cell line, both for cell type and because of representative affects on cell proliferation and differentiation, to become the Rescue cell line by reintroducing Mustn1 expression via transient transfection of the modified sequence which returned Mustn1 expression levels to parental control levels (Figure 3B).

Transient transfection efficiency

Because transient transfection was required to rescue Mustn1 expression, efficiency experiments were undertaken to ensure protein reintroduction. The average number of GFP positive cells was determined at regular time points throughout the duration of cell differentiation. At Day 0 the cell population was 41.4% positive for GFP; on Day 2 – 45.3%, on Day 5 – 53.7%, on Day 7 – 36.0%, on Day 10 – 34.2%, and on Day 14 – 37.0% (Figure 4).

Proliferation assay

To identify any effects caused by overexpressing or silencing Mustn1 on chondrocyte proliferation rate, we assayed RCJ population growth in low

density cell culture. When the proliferation rate of overexpressing cell lines (OE 3, OE 4, and OE 6) were compared to both the parental cell line and the empty vector control, there were no significant differences found at any time point (Figure 5A). In contrast, when the proliferation rate of the silenced cell lines (M2-2, M3-5, and M4-4) were compared to both the parental and the random control cell lines, significant differences were observed at several time points (Figure 5B). Specifically, at the 24hr time point; the random control, M2-2, M3-5, and rescue cell lines (with averages of ~2.2, 1.5, 1.7, & 2.3 respectively) showed no significant differences from parental (avg. ~2.2). However, the M4-4 cell line (~1.1) showed significant reduction in population level when compared to parental ($p<.01$). Furthermore, returning Mustn1 mRNA rescues the silenced cell line's proliferation rate as is shown by the lack of significant difference in population size between the rescue and parental cell lines ($p<.05$ at all time points). At the 48hr time point; the random control, M3-5, and rescue cell lines (with averages of ~4.0, 1.7, & 2.5 respectively) showed no significant differences from parental (avg. ~3.88). However, the M2-2 & M4-4 cell lines (with averages of ~1.8 and 1.7, respectively) showed significant reduction in population level when compared to parental ($p<.05$, Figure 5B). At the 72hr time point; random control, and rescue cell lines (with averages of ~5.7, and 4.3, respectively) showed no significant differences from parental (avg. ~5.6). However, M2-2, M3-5, and M4-4 cell lines (with averages of 2.44, 2.54, 1.41 respectively) all showed significant reduction in population levels when compared to parental ($p<.001$

for M2-2 & M4-4 and p<.01 for M3-5, Figure 4). Furthermore, there was a significant difference in population size between the M2-2 and rescue cell lines (p<.01, Figure 5B).

Matrix production assay

To determine if altering Mustn1 expression affected proteoglycan production, matrix was quantified via Alcian blue staining in confluent cell cultures to normalize for cell number. When Alcian blue staining was assayed in the two overexpressing cell lines showing the highest and lowest up-regulation of Mustn1 (OE 3 and OE 6 respectively) and compared to both the parental cell line and the empty vector control, there was no significant difference found at any time point (Figure 6A). In contrast, when Alcian blue binding was quantified in silenced cell lines (M2-2, M3-5, and M4-4) and compared to both the parental and the random control cell lines significant differences were found at all time points (Figure 6B). Specifically, on Day 5, the random control cell line (avg. ~5.7) showed no significant difference from the parental cell line (avg. ~5.3). However, the M2-2, M3-5, M4-4 and rescue cell lines (with Alcian blue quantification averages of ~3.5, 3.6, 3.7, and 4.9 fold over Day 0 levels, respectively) showed significant differences in matrix production (p<.001 for M2-2, M3-5, and M4-4 and p<.03 for the rescue cell line when compared to parental). On Day 7, the random control cell line (avg. ~7.3 fold change) showed no significant difference from the parental cell line (avg. ~6.8 fold change). However, the M2-2, M3-5, M4-4, and rescue cell

lines (with averages of 4.0, 4.6, 4.0, and 5.8 fold change respectively) showed significant differences in matrix production ($p<.001$ for M2-2, M3-5, and M4-4 and $p<.02$ for the rescue line when compared to parental). On Day 10, the random control and rescue cell lines (with averages of ~9.3 and 8.2 fold change) showed no significant difference from the parental cell line (avg. ~9.5 fold change). However, the M2-2, M3-5, and M4-4 cell lines (with averages of 5.4, 5.9, and 6.4 fold change respectively) showed significant reduction in matrix production ($p<.001$ for all three cell lines when compared to parental). Lastly, on Day 14, the random control and rescue cell lines (with averages of ~9.3 and 9.7 fold change) showed no significant difference from the parental cell line (avg. ~8.7 fold change). However, the M2-2, M3-5, and M4-4 cell lines (with averages of ~5.4, 5.8, and 5.3 fold change respectively) showed significant reduction in population level ($p<.001$ for M3-5 and M4-4 and $p<.03$ for M2-2 when compared to parental). A significant difference was found when M2-2 was compared to the Rescue cell line on Day 7 ($p<.05$) as well as Days 10 & 14 ($p<.01$) (Figure 6B).

qPCR analysis

To determine if cell differentiation was affected by modulating Musnt1 expression, experiments to qauntitate marker gene expression on confluent cell populations were undertaken. Mustn1 and marker gene mRNA levels were determined via qPCR and compared to Random control, to account for any affects infection and subsequent selection had on gene expression.

When Mustn1 was analyzed, the representative RNAi cell line (M2-2) was reduced to only 47% expression when compared to Random control whereas Rescue showed 89% expression when compared to Random levels (Figure 7). No significant differences were found between the Random and Rescue cell lines at any time point and each peaked on Day 2 with increases of ~4.5 and 5.3 fold over Day 0, respectively. However, the RNAi cell line, M2-2, lacked this Mustn1 expression peak on Day 2, only achieving a 3.8 fold increase over its significantly reduced Day 0 Mustn1 expression value. This peak did not occur until Day 10. While the only significant difference between the Random control and M2-2 cell lines was on Day 2, this discrepancy was very dramatic ($p<.001$, Figure 7).

When Sox9 was assayed the Random, and Rescue cell lines showed steady increase in expression culminating in peaks on Day 14 with ~5.6 and 9.4 fold increases over Day 0, respectively. The M2-2 cell line did not show this increase in expression and instead peaked on Day 10 with only a ~1.2 fold increase prior to a reduction of expression to only .52 of Day 0 expression on the final day of the time course (Figure 7).

When Collagen II was assayed the Random and Rescue cell lines showed steady increase in expression culminating in peaks on Day 14 of ~100.7, and 54.7 fold increases over Day 0, respectively. Again, the M2-2 cell line lacked this level of increase in expression; instead peaking at only ~2.6 fold on Day 14 (Figure 7).

When Collagen X was assayed the Random and Rescue cell lines showed steady increase in expression culminating in peaks on Day 14 of ~4.8 and 10.7 respectively. The M2-2 cell line actually showed a reduction in expression throughout the time course culminating in an expression level of only 15% of Day 0 expression at the conclusion of the time course (Figure 7).

3.5 Discussion

The expression pattern of Mustn1 during embryogenesis suggests that this gene is active in areas of cartilage, bone and muscle formation. Although this correlation does not mean Mustn1 is involved in these processes, its expression strongly localizes to areas of chondrogenesis such as the limb bud and somites as observed by Lombardo et. al. Throughout the embryo, tissues containing differentiating mesenchymal cells, particularly limb and tail buds, branchial arches, and somites, show Mustn1 expression. These findings add support to the idea the Mustn1 plays a role in musculoskeletal development *in vivo*.

That Mustn1 is involved in the early phases of chondrogenesis is further supported by the *in vitro* analyses. The fact that overexpressing Mustn1 did not cause any significant deviation in either proliferation rate or proteoglycan production, can simply be explained by the notion that a modest increase in Mustn1 expression in RCJ3.1 cells (~2-6 fold) was not enough to alter the proliferation rate or matrix production when compared to the parental or control cell lines even though the parental RCJ cell line only shows a ~5-fold

up-regulation in Mustn1 expression during differentiation. It is, of course, possible that no matter how high Mustn1 is expressed, it will have no impact on either proliferation or differentiation in chondrocytes. In contrast, the silencing experiments indicate that Mustn1 is necessary for both the proliferation and differentiation of chondrocytes. In cell lines that were silenced and showed only 33.7-58.2% Mustn1 expression when compared to the parental cell line, proliferation rate and matrix production were both clearly suppressed. This decrease was accompanied by the dramatic reduction in the expression of the three chondrogenic marker genes (Sox9, Collagen II, and Collagen X) assayed.

While the proliferation and matrix production analyses do not elucidate the role of Mustn1, the suppression of Sox9, Collagen II, and Collagen X expression does provide a greater understanding of Mustn1's function during chondrocyte differentiation. For example, the observation that matrix production is reduced in Mustn1 RNAi cell lines, could simply be a result of the reduced proliferation rate. However, not only was matrix formation tested on confluent cells ensuring a similar number of cells in each population, but the suppression of Collagen X (Figure 7), a marker of hypertrophy [9,19,20] observed in populations suggests that the lack of matrix production is caused by the inability of these cells to differentiate into terminal hypertrophic chondrocytes and not the reduced proliferation rate. Further, the parallel suppression seen in the Collagen II expression (Figure 7) indicates that the RNAi cell lines do not progress even to the proliferating chondrocyte stage in

their differentiation lineage and therefore cannot subsequently reach hypertrophic differentiation [18,20,21], placing inhibition of differentiation of these silenced cell lines prior to proliferating chondrocytes.

While this idea may seem counterintuitive given the fact that even silenced cell cultures are binding Alcian blue, even pre-chondrocytes create minimal levels of extracellular matrix. This ~38% reduction in the staining of Alcian blue when compared to the parental control cell line may also occurring because Mustn1 expression is still present even in the RNAi cell lines (as evident by the measurement in Mustn1 expression). Further, Alcian blue only stains the glycosaminoglycans (GAGs) within cartilage which is why it is only used in these experiments as a measurement of proteoglycan production [17]. Even though GAGs are still being produced, the main component of the cartilage matrix is collagen. Collagen makes up 2/3 of cartilage dry weight with over 75% of that comprised of collagen II [4,12]. The dramatic suppression of collagen II mRNA suggests that the matrix produced by silenced cell lines is imperfect and structurally deficient when compared to matrix produced by parental or random cell lines.

The most interesting result of these molecular analyses is the suppression of Sox9 observed in the silenced cell lines which is rescued when Mustn1 is reintroduced into the cells via transient transfection. These data indicate that Mustn1 functions earlier in chondrocyte differentiation (prior to Sox9 activation), as Sox9 is responsible for the transcriptional activation of Collagen II in multiple chondrogenic and osteogenic tissues [1,3,16]. Thus,

the reduction in Sox9 expression likely causes the subsequent suppression of Collagen II levels. Sox9 activation itself has been shown to be both required and sufficient for chondrogenesis alone or with Sox5 and Sox 6 [3,11,13]. The vital role of Sox9 during chondrocyte differentiation makes Mustn1's affect on this gene's expression an interesting avenue to explore. Although these data implicate Mustn1 in the activation of Sox9, this data alone does not help narrow down the signaling pathway in which Mustn1 functions, as several pathways affect Sox9 expression.

When these data are taken in conjunction with our previous results on Mustn1, i.e. its musculoskeletal system specificity and the fact that it is a nuclear protein [15], a clearer picture of Mustn1's function begins to form. This research suggests that Mustn1 works within the nucleus, possibly as part of the transcription initiation complex although protein binding experiments have yet to validate this idea. The lack of a DNA binding motif within its sequence precludes Mustn1 from being a transcription factor *per se* and thus supports the notion that Mustn1 possibly functions as a musculoskeletal co-activator or co-repressor. Further, results from these experiments seem to propose that Mustn1 is a co-activator of a transcriptional complex involved in both proliferation and differentiation in chondrocytes as both processes are negatively affected when Mustn1 is silenced *in vitro*. However, that Mustn1 helps to repress a repressor of these processes is still a possibility. If Mustn1 is indeed a transcriptional co-activator, the identification of its target genes holds much promise in the elucidation of chondrogenesis. Further, because

Mustn1 is active very early in chondrocyte differentiation, BFR, and bone formation (Figure 1, Figure 2, and [15]), finding the direct targets of this gene may identify the early initiators of each of these vital processes. While Mustn1 itself is not sufficient for chondrocyte differentiation, it is possible that its target gene(s) may be. Although these results are promising, further research must be preformed to clearly elucidate Mustn1's role in chondrogenesis.

Target Gene	Accession Number	Primer Sequence	Amplicon Size	Tm(oC)
B-2microglobulin	NM 012512	5’ - TGGTGTGCTCATTGCTATTC 3’ - CTCTGAAGGAGCCCAAAAC	152	58
Mustn1	NM 181390	5’ - GCTTTTCCTCTGCCACCTC 3’ - ATTCCCCGACCCACCTC	129	58
Collagen II	NM 012929	5’ - TGTGCTTCTTCTCCTTGCTC 3’ - GACCTGAAACTCTGCCACC	187	58
Collagen X	AJ131848	5’ - ACCTGGGGCAACTTAGAAAA 3’- CAGTGGAATAGAAGGCACACA	179	58
Sox9	AB073720	5’ - CCGACACGGAGAACACAC 3’ - CAGTCATAGCCCTTCAGCAC	98	58

Table 1. List of primers and conditions used for qPCR amplification

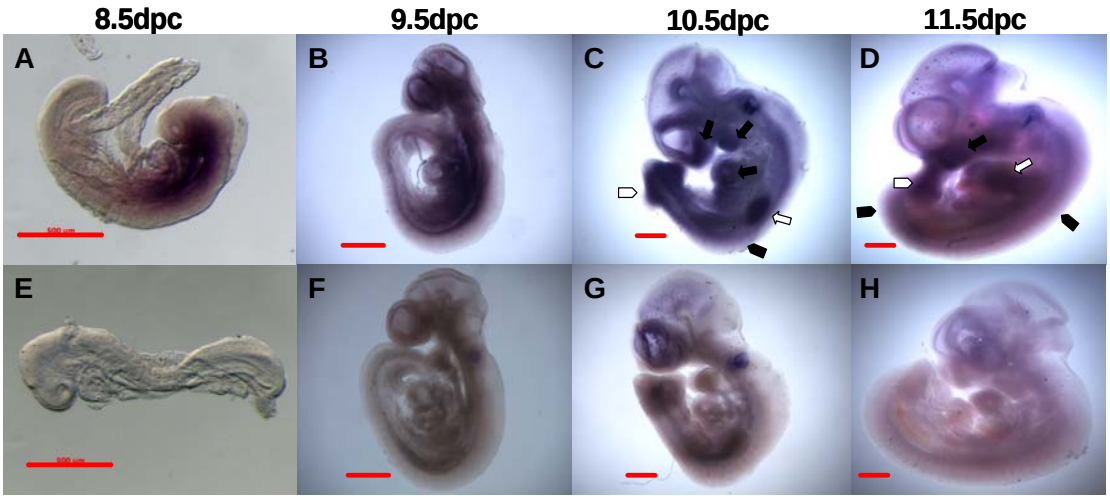

Figure 1. Mustn1 expression localizes to areas of chondrogenesis and myogenesis during mouse embryogenesis. Whole mount embryos at 8.5, 9.5, 10.5 and 11.5dpc were hybridized with, sense and antisense riboprobes for Mustn1. Antisense probe hybridization are shown in **A.** 8.5 dpc, **B.** 9.5dpc, **C.** 10.5dpc and **D.** 11.5dpc while sense probes are shown in **E.** 8.5dpc, **F.** 9.5dpc, **G.** 10.5dpc and **H.** 11.5dpc. A and B show embryos that express Mustn1 throughout mesodermal tissues, while C and D show embryos with distinct staining in forelimbs (white arrows), hindlimb (white arrowheads), branchial arches (black arrows), somites (black arrowheads) and posterior tail bud. Scale bars=.5µm.

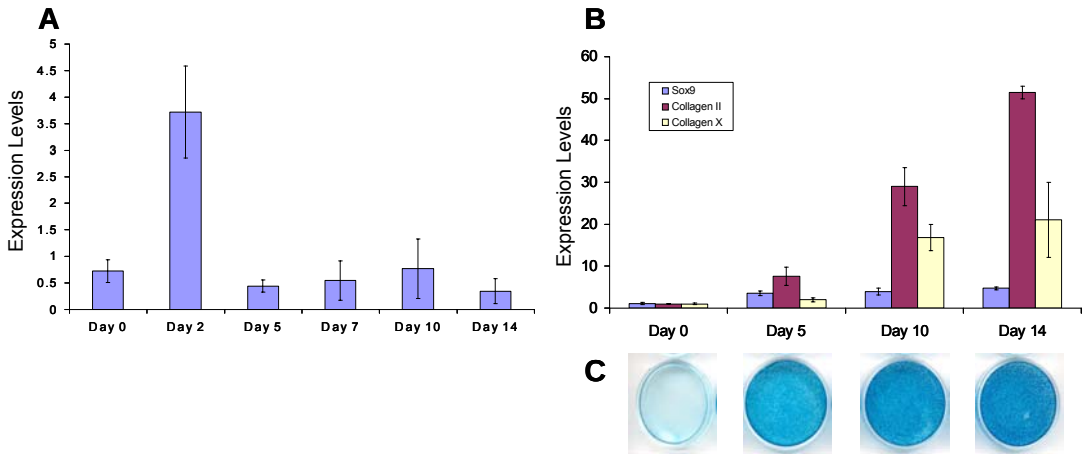

Figure 2. Mustn1 and marker gene expression is differentially regulated during RCJ cell differentiation. Graphs show expression of Mustn1 (**A**), and Sox9, a pre-chondrocyte cell marker, Collagen II, a proliferating chondrocyte cell marker, and Collagen X, a hypertrophic chondrocyte cell marker (**B**) as assayed via qPCR during RCJ differentiation. Confluent RCJ cells were stimulated to differentiate at Day 0 and mRNA was isolated and assayed at the days indicated. All bars represent average values of raw gene expression normalized to ß2-Microglobulin expression in pooled mRNA (n=3). Error bars indicate standard deviation of mechanical variation between qPCR runs (n=3). **C**. Differentiation was also monitored via Alcian blue (stains proteoglycans within the extracellular matrix) on Day 0, 5, 10, &14. The darkness of the color corresponds to greater Alcian blue binding and subsequently more proteoglycans/matrix present.

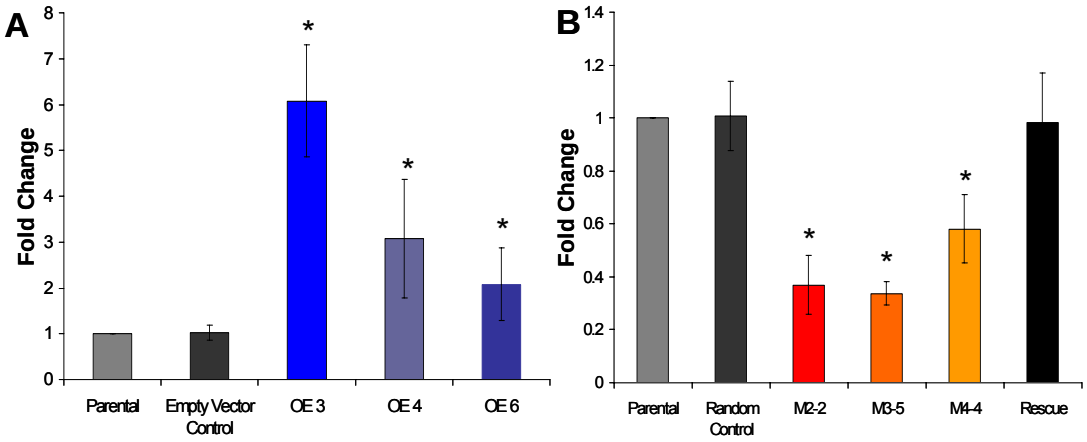

Figure 3. Modulation of Mustn1 expression via overexpression and silencing. A. Mustn1 was overexpressed in RCJ cells (cell lines - Over Expression (OE) 3 – 608% of parental expression, 4 – 307%, 6 – 208%) via stable plasmid transfection and an empty vector plasmid was transfected as a control. **B.** Mustn1 was silenced in proliferating cell lines (Mustn1 (M)2-2 – 48% of parental expression, M3-5 – 34%, and M4-4 – 58%) via stable viral infection of siRNA into RCJ and a random sequence with no homology to the rat genome was infected as control. The Rescue cell line was created by transiently transfecting the RNAi cell line M2-2 with a Mustn1 containing plasmid. Mustn1 expression was assayed by qPCR in proliferating RCJ cells and normalized to ß2-Microglobulin. Fold change was then determined by normalizing values to those of parental cells (raw value=.720). All bars represent average values of raw gene expression normalized to ß2-Microglobulin expression in pooled mRNA (n=3). Error bars indicate standard deviation (N=3). * p<.01 determined by Mann-Whitney test vs. Parental.

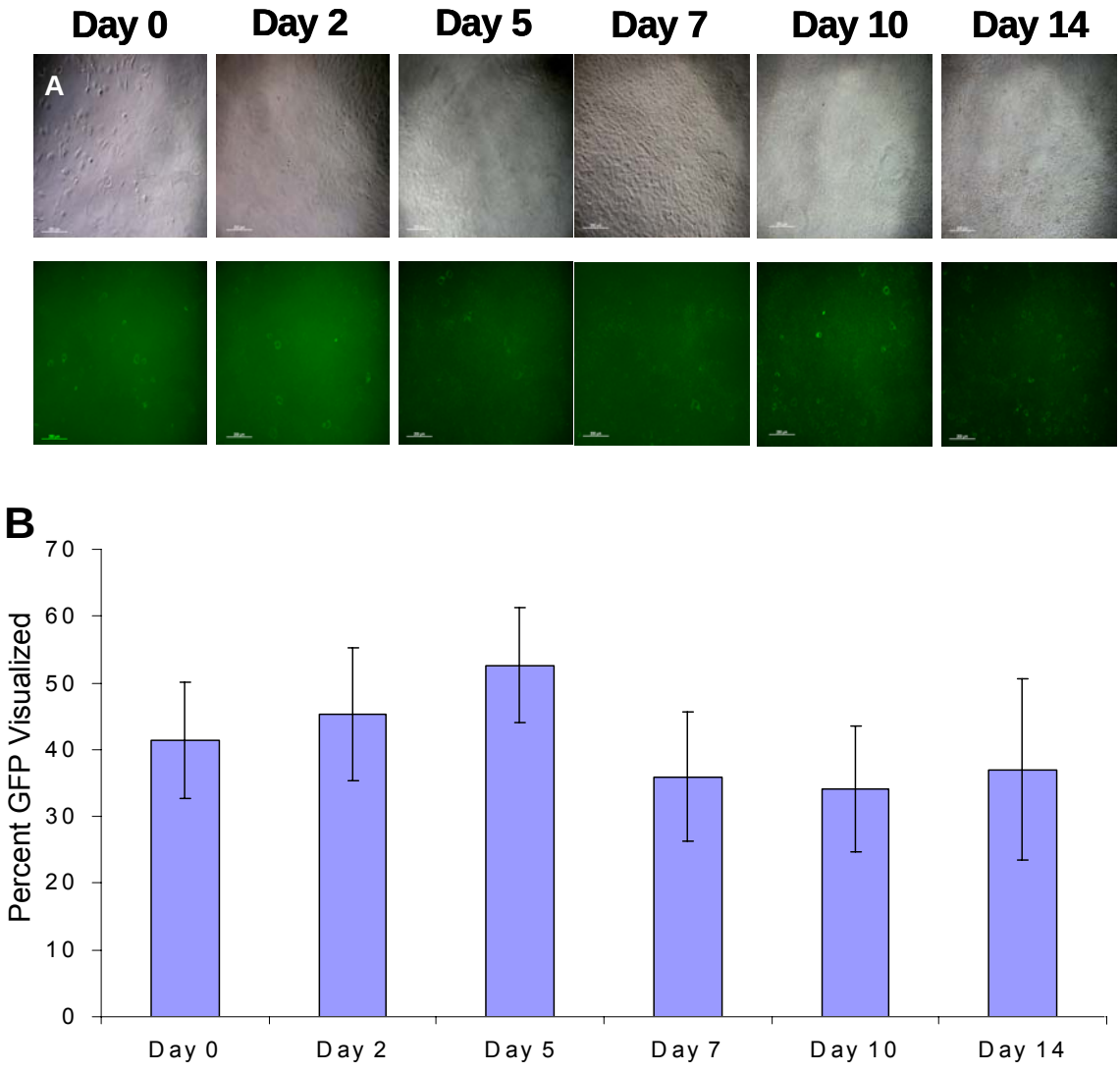

Figure 4. Transfection efficiency of rescue Mustn1 plasmid in M2-2 RNAi cell line. Mustn1 silenced cell line M2-2 was transfected with a Mustn1 containing plasmid tagged with GFP. **A.** Representative fields were observed under bright field and fluorescent conditions. Scale bars= 200µm **B.** Diagram representing the quantification of GFP positive cells as percent of total cell populations determined by counting representative fields as average ± SD. (n=5).

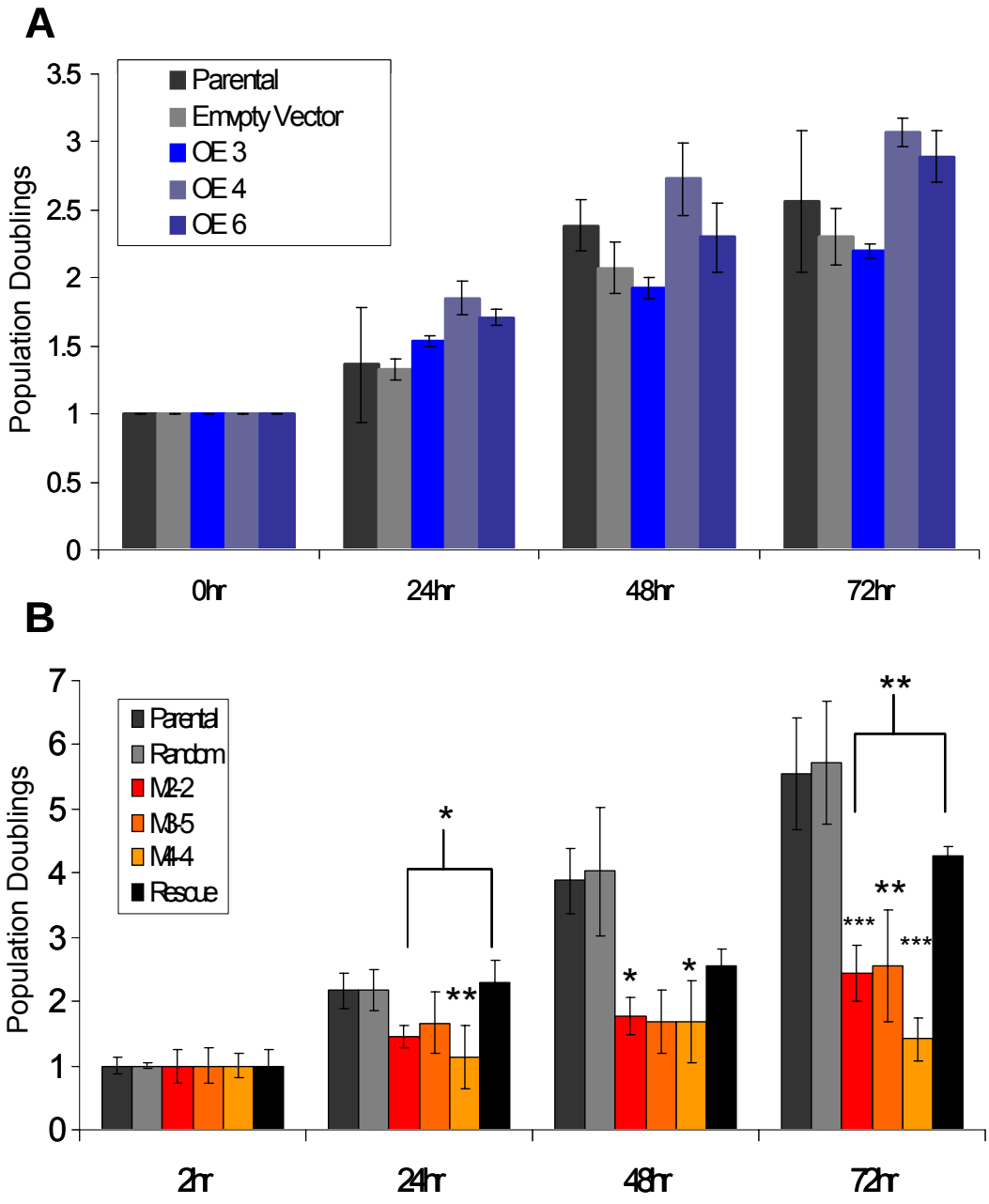

Figure 5. Cell Proliferation rate is unchanged when Mustn1 is overexpressed but is reduced in Mustn1 silenced cell lines. A. Graph showing cell proliferation measurements in parental, empty vector, OE 3, 4, & 6 cell lines via MTS over a 3 day time course. There was no statistical significance between parental, empty vector, or any OE cell line at any time point (all p >.05). **B.** Similar analysis of silenced cell lines (parental, random control, M2-2, M3-5, & M4-4, and rescue). There was no statistical difference between empty vector, random control, or rescue and parental cell lines at any time point. Each data point represents the average of triplicate MTS experiments (n=3) preformed on low density plated proliferating RCJ cell lines. Error bars represent Standard Deviation of biological variability. Each line was normalized to the 0hr time point to show population doublings. All statistical significance was determined by ANOVA on ranks with Tukey post-hoc. Significant difference was only observed in the silenced cell lines and between silenced cell line M2-2 and rescue. * - p< .05, ** - p<.01, *** - p<.001

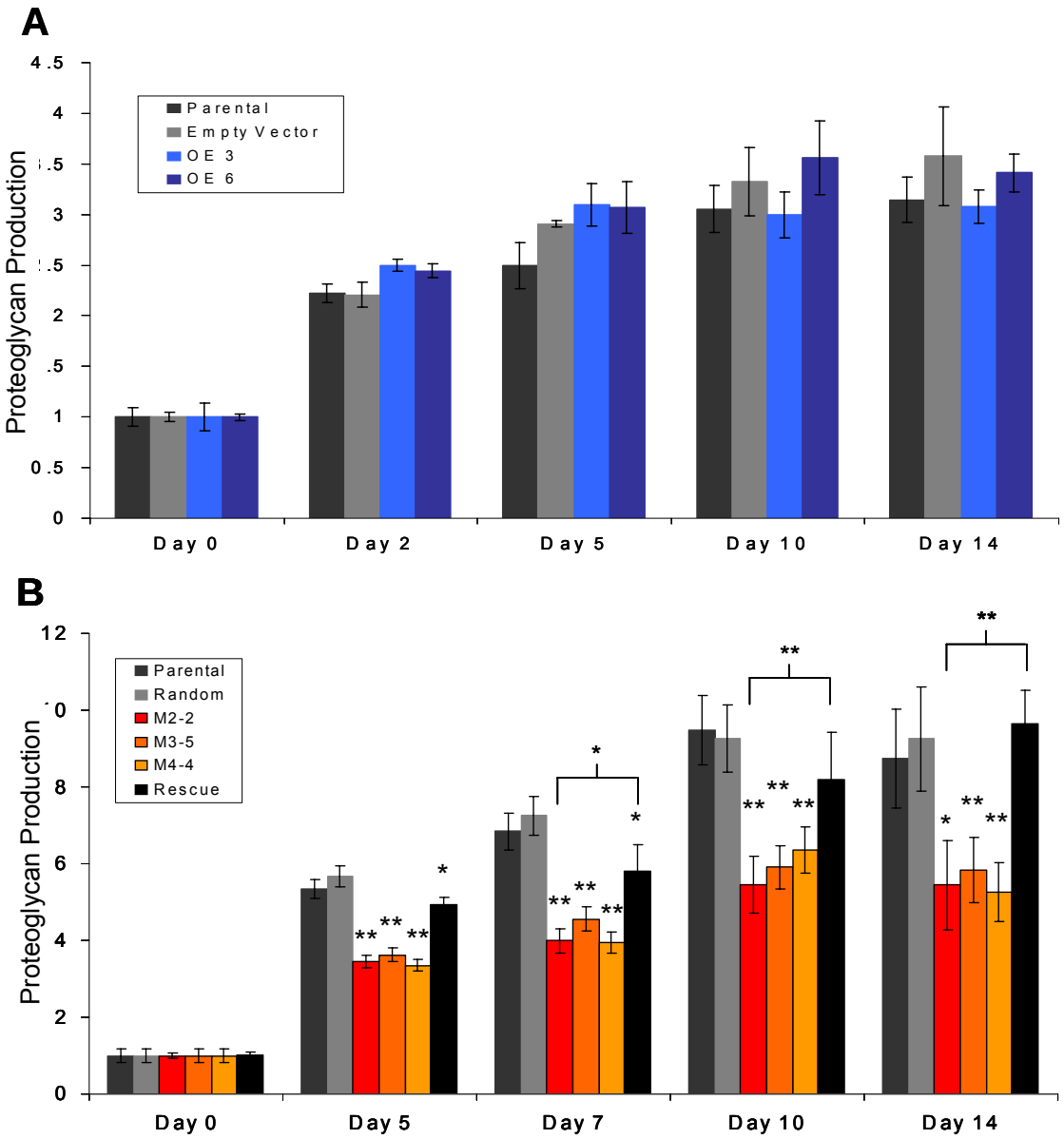

Figure 6. Matrix production is unaffected when Mustn1 is overexpressed, but is reduced in Mustn1 silenced cell lines. Confluent cells from each line were stimulated to differentiate on Day 0. At specific times during differentiation the cell lines were fixed and stained with Alcian blue. This dye was then eluted and quantified via spectrophotometery to determine the amount of matrix produced at each time point. **A.** Parental, OE 3, 6 and empty vector cell lines were assayed at Day 0, 2, 5, 10, & 14. **B.** Parental, random, M2-2, M3-5, M4-4, and rescue cell lines on Day 0, 5, 7, 10 & 14. All bars indicate average of triplicate experiments ± Standard Deviation. Significance was determined by ANOVA on ranks with a Tukey Post-hoc vs. Parental cell line levels or Mann-Whitney to compare M2-2 to Rescue. Significant difference was only observed in the silenced cell lines and between silenced cell line M2-2 and rescue. * p<.05 and ** p<.01.

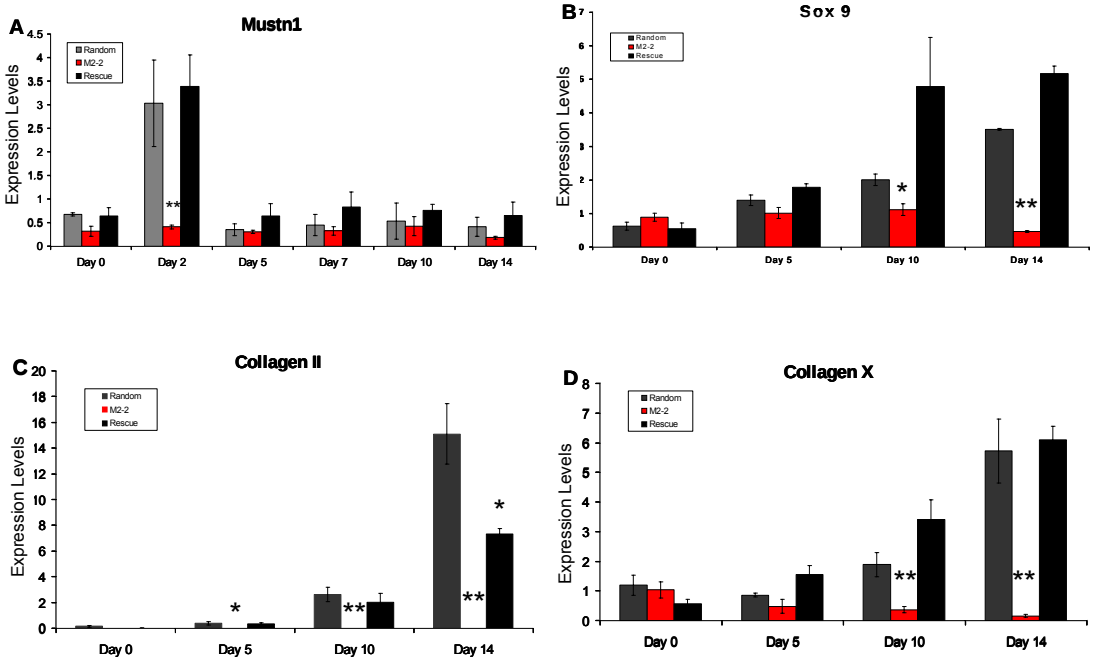

Figure 7. Mustn1 and chondrogenic marker gene expression is reduced in Mustn1 silenced cells. Graphs show gene expression as assayed via qPCR throughout a differentiation time course. Confluent RCJ cells were stimulated to differentiate at Day 0 and mRNA was isolated and assayed (normalized to ß2-Microglobulin) at Day 0, 5, 10 & 14. Results are shown for **A.** Mustn1, **B.** Sox9, a pre-chondrocyte cell marker, **C.** Collagen II, a proliferating chondrocyte cell marker, and **D.** Collagen X, a hypertrophic chondrocyte cell marker. All bars represent average raw gene expression values of pooled mRNA (n=3). Error bars indicate standard deviation of mechanical variation between qPCR runs (n=3). Significance was determined by Mann-Whitney test vs. Random Expression levels. * - p<.05, ** - p<.01.

4. *In vivo* Downregulation of *Mustn1* mRNA Leads to Morphological Defects and Downregulation of Sox9 Expression.

I would like to acknowledge Arif Kirmizitas for his help in performing the embryo injections described below.

4.1 Abstract

Previously, our lab reported on the isolation and characterization of Mustn1, a 9.6 kDa nuclear protein that is involved in fracture repair. We further determined that Mustn1 is necessary but not sufficient for pre-chondrocyte proliferation, differentiation, and matrix production *in vitro* via overexpression and RNA interference experiments. These data suggest that Mustn1 may play a crucial role in the early stages of chondrogenesis, both during fracture repair as well as development. In the case of the latter, whole mount *in situ* analysis of Mustn1 in wild type mice at stages 8.5-11.5dpc reveal expression the developing musculoskeletal system. These experiments were repeated in *Xenopus laevis* and showed similar patterning of expression, with Mustn1 localizing predominately to the craniofacial region and somites. Further analysis of Mustn1 temporal expression revealed an increase during neurulation stages, corresponding to somite production and mesodermal development before reaching a plateau through stage 35. To evaluate Mustn1's function during development, Mustn1 antisense morpholino oligonucleotides were injected into *X. laevis* embryos. While control morpholino injected embryos were unaffected, gross morphological

defects were observed in the Mustn1 morpholino injected (Mustn1-MO-injected) embryos including small or lack of eyes, shortened body axis, and tail/body kinks. Further, the myogenic and chondrogenic markers MyoD and Sox9 were assayed via whole mount *in situ* hybridization. While no alteration of MyoD pattern was associated with Mustn1 depletion, Sox9 expression was severely reduced in the Mustn1-MO-injected embryos. When this expression was quantified Sox9 expression was downregulated by ~40% in Mustn1-MO-injected embryos during later stages in development. Reintroduction of Mustn1 expression rescued both the morphological phenotype and Sox9 expression. Finally, when Mustn1 was overexpressed in *X. laevis* embryos, no phenotype was observed when compared to control injected groups either in morphology or Sox9 expression. Taken together, these experiments suggest that Mustn1 expression is necessary for musculoskeletal development and Sox9 expression *in vivo*.

4.2 Introduction

Previous work in our laboratory has identified the Mustn1, as a small (9.6kDa) nuclear protein that is expressed in the musculoskeletal system in adult rodents as well as bone, muscle, proliferating chondrocytes and periosteum in developing embryos [1 & unpublished observations]. Previous analyses with Mustn1 sought to functionally characterize this gene *in vitro* during both chondrogenic and myogenic differentiation. Mustn1 was silenced via RNAi in the pre-chondrocyte RCJ as well as a myogenic cell line, C2C12.

When Mustn1 expression was reduced, proliferation and differentiation in RCJ cells and differentiation of C2C12 cells were reduced as well [chapter 3 & unpublished data]. Matrix production by hypertrophic chondrocytes and myotube formation by muscle cells were both disrupted and dramatically depressed. In addition, when both chondrogenic (Sox9, Collagen II, and Collagen X) and myogenic markers (MyoD, Myogenic, MHC, Desmin) were assayed, their expression was found to be suppressed as well [chapter 3 & unpublished data]. These experiments suggest that Mustn1 is critical for the differentiation of these two different cell types and thus it may serve as a vital molecule for cartilage and skeletal muscle development. Thus investigating Mustn1's role during development would be of great benefit.

We chose to functionally perturb Mustn1 *in vivo* via silencing during *Xenopus laevis* development so that we can investigate its effects during cartilage and skeletal muscle formation. Historically, this approach offers insight into a gene's role, especially since *X. laevis* is an ideal model system for studying embryogenesis as it undergoes the relatively rapid development of a clear embryo and it is easy to deliver antisense morpholinos to blocks translation [15,17]. *X. laevis* also develops very similarly to higher vertebrates such as mouse and human in regards to cartilage formation. At the tissue level; *X. laevis* develop many of the same precursors during craniofacial development as higher vertebrates. Cranial components such as the branchial arches, Meckel's Cartilage, and palatoquadrate show similar

expansion and result in similar structures produced in both *X. laevis* and higher vertebrates [2,8].

Further, several of the molecules (i.e. Sox 9, Collagen II, MyoD, myogenin) affected by our previous *in vitro* Mustn1 silencing experiments play important roles during frog development as well. Sox genes including Sox9 have been implicated in neural crest development and chondrogenesis just as in mammalian embryogenesis [6,7]. Sox9's main target gene, collagen II, has also been well documented and visualized throughout development in *X. laevis* as well [3,4,5]. Similarly, MyoD and myogenin have also been well described during *X. laevis* embryogenesis [13,14]. Thus silencing of Mustn1 during *X. laevis* development should provide direct evidence of its function *in vivo*.

4.3 Results

Mustn1 shows homology among vertebrates.

To build upon the homology experiment of previous work, homology experiments were preformed on several lower vertebrates. Mustn1 protein sequence analysis for mouse, viper, frog, and zebrafish show high homology. Specifically, when compared to mouse; viper, frog, and zebrafish show a 77%, 69%, and 59% homology respectively. The NLS motif was particularly conserved; however the potential phosphorylation and myristylation sites did show some amino acid differences (Figure 1 yellow highlights).

Mustn1 expression temporally and spatially localized to craniofacial development and somitogenesis.

To determine at which time point and in which tissues Mustn1 is expressed in *X. laevis*, localization experiments were undertaken. Temporal analysis of Mustn1 expression via qPCR revealed a slight peak just prior to gastrulation followed by a steady increase prior to a plateau during neurulation as compared to the expression of housekeeping gene Ornithine decarboxylase (Figure 2A). While multiple qPCR analysis validate this peak was present, when we used *in situ* hybridization to determine the spatial location of Mustn1 expression, the slight peak corresponding to late blastula was not consistently detected, but in later developmental stages; expression was originally observed in the paraxial mesoderm followed by craniofacial regions as well as somites (Figure 2B-E) when compared to sense probe controls (Figure 2F-I). The increase in size of the stained regions corresponded appropriately to the increase in expression observed in the temporal analysis.

Mustn1 silencing results in multiple morphological defects.

To determine if Mustn1 was necessary for musculoskeletal development, silencing experiments were undertaken. These experiments involved the injection of either a control morpholino (not coding for any sequence within the X. *laevis* genome) or Mustn1 morpholino (an antisense morpholino

oligonucleotide which binds Mustn1 mRNA preventing translation) dorsal of the midline in animal blastomeres at the 4-cell stage to target dorsal and anterior regions of the developing embryo. Co-MO-injected embryos showed no significant developmental defects throughout the investigated time course (Figure 3A&B left). In contrast, Mustn1-MO-injected embryos showed several morphological defects that include: small, or lack of, eye(s), reduced body axis length, and kinks within the body/tail. These defects were observed at both stages 37-38 and 40 (Figure 3A&B middle). When Mustn1 expression was reintroduced via co-injection of Mustn1 morpholino embryos with modified mRNA (Rescue injected), the severity of these defects was significantly reduced or ablated completely (Figure 3A&B right).

These defects were quantitatively determined for all groups by scoring affected individuals and plotting the data as a function of population percentage. In the case of eye defects, while 96% (of 176 total) of Co-MO-injected embryos showed two normal eyes, only 32% (of 184 total) did in Mustn1-MO-injected embryos (Figure 4A). Returning Mustn1 mRNA back to the Mustn1-MO-injected embryos (Rescue injected group) increased the number of normal embryos to 61% (of 158 total). Further, the Co-MO-injected group also contained 3% of embryos that had two small eyes, 0.5% of embryos that only had one eye and 0% of embryos with no eyes at all. In contrast, the Mustn1-MO-injected embryos showed 27% of embryos with two small eyes, 28% of embryos with only one eye, and 15% of embryos with no eyes. Finally, the Rescue injected group showed 22% of embryos with small

eyes, 13% of embryos with only one eye, and 4% of embryos with no eyes (Figure 4A).

Regarding body axis defects, the Co-MO-injected group showed 90% of embryos with normal body axis length and 10% with shortened axis, as defined by a disruption in the body to tail length ratio (Figure 4B). The Mustn1-MO-injected embryos showed 51% of embryos with normal body axis length and 49% of embryos with shortened axis. The Rescue injected group showed 70% of embryos with normal body axis length and 30% with shortened axis.

In the case of tail defects, these were divided into 3 groups, tail development with no defect, mild defects consisting of slight curvature, and severe defects in which the tail curvature showed a greater than 90^{o} bend. For Co-MO-injected embryos 88% showed no tail defect while the remaining 12% showed a mild tail phenotype. For Mustn1-MO-injected embryos 31% showed no tail defect, 45% of embryos showed mild defects, and the remaining 25% exhibited a severe phenotype. In the Rescue injected group 47% of embryos showed no tail defect, 41% showed mild phenotype, and the remaining 18% of embryos showed a severe phenotype (Figure 4C).

Control and Mustn1 morpholinos localize to craniofacial regions and somites.

To determine which tissues were affected by antisense morpholino injection, localization experiments were undertaken. The control and Mustn1

morpholinos were both co-injected with Fluorescein dextran amine (FDA). Under fluorescent light, this dye fluoresces allowing the visualization of FDA diffusion and consequently, the corresponding morpholino with which it was co-injected. When Co-MO-injected embryos were observed under fluorescence, the FDA was localized throughout the entire embryo but predominately to the craniofacial region and somites as directed (Figure 5A). In contrast, with Mustn1-MO-injected embryos localization of the FDA was detected in more defined areas; especially those that correspond strongly to areas showing morphological defects such as the craniofacial region and somites (Figure 5B & C). In addition the modified Mustn1 mRNA designed to rescue Mustn1 expression was co-injected with mRNA coding for mCherry protein (a fluorescent protein similar to red fluorescent protein originally designed to optimize FRET by reducing photobleaching) [21] localized to comparable regions as the FDA (Figure 5D).

Silencing Mustn1 *in vivo* does not alter MyoD expression patterning.

To determine if Mustn1 silencing was affecting myogenesis similarly to *in vitro* data, expression analysis experiments of MyoD were undertaken. Co-MO-injected, Mustn1-MO-injected, and Rescue injected embryos were assayed for the somite marker MyoD via *in situ* hybridization. All groups showed similar staining for MyoD with only a mild observable variation in this gene's patterning at Stage 24, 33, or 38 (Figure 6A-C). When MyoD

expression was determined via qPCR, no significant differences were found between Co-MO-injected and either Mustn1-MO-injected or Rescue injected levels at stage 25, 34, or 39 (Figure 7A). Other muscle markers, including later markers such as Heavy Muscle Actin, myogenin, and Desmin were not assayed.

Silencing Mustn1 *in vivo* reduces Sox9 expression patterning.

To determine if Musnt1 silencing was affecting chondrogenesis similarly to *in vitro* data, expression analysis of Sox9 were undertaken. Co-MO-injected, Mustn1-MO-injected, Rescue injected embryos were assayed for the chondrocyte marker Sox9 via *in situ* hybridization. Results with whole mount Co-MO-injected embryos showed the majority of Sox9 staining is localized to the craniofacial region at stage 40 (Figure 6D). High magnification of a representative Co-MO-injected embryo showed Sox9 expression, specifically, in dorsal elements, likely the NCC's along the dorsal boundary of the head, as well as in the brachial arches ventral to the eye and in anterior tissues (Figure 6E). The eye itself also showed staining in the periphery although this may be caused by trapping of the staining agent within the ocular cavity. In a representative Mustn1-MO- injected embryo, Sox9 expression is almost completely ablated leaving only a narrow band of light staining anterior and ventral to where the eye would normally be located (Figure 6F). In a representative Rescue injected embryo, Sox9 expression shows similar patterning to that of Co-MO-injected embryos (Figure 6G). Staining can be

observed again in the branchial arches as well as the NCC's and eye periphery. Further, when Sox9 expression was quantified via qPCR, significant differences were found between Co-MO-injected and Mustn1-MO-injected embryos at stage 34 & 39 in which Mustn1-MO-injected embryos showed reductions in expression of 33.4% (p=.025) and 38.7% (p=.021), respectively, when compared to Co-MO-injected embryos (Figure 7B). No significant differences in expression were found in Sox9 expression between Rescue injected and Co-MO-injected embryos at stage 25, 34, or 39.

Overexpressing Mustn1 does not cause morphological defects or alterations in Sox9 expression.

To determine if increasing Mustn1 expression during development caused any phenotype, overexpression experiments were undertaken. When 3ng Mustn1 or mCherry was injected into 2-cell *X. laevis* embryos (1.5ng/blastomere), no significant morphological defects were detected when embryos were observed at stages 37 or 40 (Figure 8A&D). When Sox9 expression was investigated via *in situ* hybridization, no alteration in the expression pattern was visualized when compared to mCherry mRNA injected control (Figure 8B-F). In all embryos expression can be seen in the same tissues as Co-MO-injected, namely, branchial arches, neural crest, eye periphery, and anterior tissues such as the nasal process and palate.

4.4 Discussion

Mustn1 homology and localization suggests a role in vertebrate development.

Previously, our laboratory identified Mustn1 as a small musculoskeletal specific, nuclear protein that localizes to periosteal osteoprogenitors, osteoblasts and proliferating chondrocytes during bone development and regeneration [1]. Subsequent experiments on pre-chondrocytes *in vitro* determined that silencing Mustn1 resulted in strong reduction of proliferation rate, matrix production, and chondrogenic marker expression. Therefore, it is not surprising that in *X. laevis* Mustn1's temporal and spatial localization correlates to musculoskeletal development. As somitogenesis and skeletogenesis begin during *X. laevis* development, Mustn1 expression shows a mild peak prior to steady increase and ultimately resulting in a plateau that extends throughout neurulation. While this early peak in Mustn1 expression is intriguing because it occurs just prior to gastrulation, our inability to visualize this expression via *in situ* hybridization, suggest that it's too low to be detected or alternatively, it is located in some unobservable area of the embryo. Instead, we chose to focus on the observable expression during later stages of development. Spatially, Mustn1 localizes to the developing somites as well as the craniofacial region, similar to the pattern observed during mammalian development. Further, Mustn1 protein sequence homology in vertebrates suggests that this gene's structure and function is highly conserved among vertebrates.

Mustn1 depletion leads to multiple morphological defects.

When Mustn1 expression was reduced via antisense morpholino injection, multiple developmental defects were observed. These defects included malformations in the craniofacial region leading to small or loss of eyes, altered body axis and tail length, and curvature or kinks in the body/tail as compared to Co-MO-injected embryos. When Mustn1 was reintroduced in Rescue injected embryos the severity of these defects was reduced. This result was consistent even when multiple stages were examined and when the concentration of morpholino injected was varied from 30-40ng/embryo, however, the severity of the defects were less severe at lower concentrations prior to rescue showing dose dependence. Further, localization experiments demonstrate that FDA in both Co-MO-injected and Mustn1-MO-injected embryos localizes to the craniofacial regions as well as the somites. While in Co-MO-injected embryos, FDA did not localize to any morphological defects, in Mustn1-MO-injected embryos the FDA shows strong localization to areas where defects occurred. In Rescue injected embryos both FDA and mCherry, co-injected with Mustn1 mRNA, localize to the same areas suggesting that this reintroduction of Mustn1 is indeed rescuing the phenotype observed in Mustn1-MO-injected embryos. While FDA and mCherry localization does not directly identify morpholino localization, this lineage tracing to defective areas does suggest that the morpholino is correlated with these defects.

While craniofacial regions were severely affected, the presence and size of the cement gland remained largely unchanged between groups. This may suggest that the craniofacial defect observed may be attributed to impaired dorsal developmental element, such as the lack of proper migration of NCC's, and not ventral elements. However, because this observation could be the end result of a number of defective processes such as lack of proliferation of these cells, failure of these elements to properly differentiate, or even defective communication between neighboring tissues such as NCC's and the developing eye placode, further research is required to elucidate the mechanism causing this phenotype.

A number of previously published morpholino experiments bear similarities to the defects observed in these experiments. Not surprisingly, when Sox9 was depleted in developing *X. laevis* embryos eye size was reduced and anterior matrix production, visualized via Alcian blue binding, was similarly affected [7]. Given the effect of Mustn1 silencing on Sox9 expression, the similarity of these observed effects is in agreement. However, Sox9 is not the only gene which, when depleted, yields similar experimental results to the ones described herein. For example, when Runx2 is silenced via morpholino injection, cartilage formation is almost completely ablated, resulting in craniofacial deformities [19] similar to those seen with Mustn1 downregulation. Further, FoxN3, a member of subclass N of fork head/winged helix transcription factors, causes a reduced eye phenotype when silenced. Closer

examination of this phenotype suggests that this smaller eye is likely caused by a disruption in cranial crest cell migration [20].

Interestingly, the craniofacial phenotype is not the only similarity found between the Mustn1 morphant and previous research. While MyoD has yet to be depleted in *X. laevis* embryos, Xtbx6r, a novel T-box gene which is also expressed in the paraxial mesoderm, shows similar body/tail kink when altered [18]. While aspects of the phenotype shown here are mirrored in other studies, none of the aforementioned studies observe the severity and/or combination of defects that occur with Mustn1 depletion. While it goes beyond the scope of this report, determining the effects of Mustn1 depletion on these critical chondrogenic/myogenic molecules is a promising avenue to elucidating the molecular interactions of these genes.

Mustn1 depletion reduces Sox9 expression but does not similarly affect MyoD.

When the expression pattern of MyoD was assayed via *in situ* hybridization only slight observable alterations in localization patterns were reported at stage 24, 33, or 38 (Figure 6 & data not shown). These alterations were predominately localized craniofacially in regions that would become jaw muscle. Unfortunately, MyoD expression is very time sensitive at these time points and the variability even within the Co-MO-injected embryos suggest that this observation may simply be temporal variation between embryos selected. Therefore, to validate this finding mRNA levels from

anterior dissections were quantified and no significant differences were found between Co-MO-injected and Mustn1-MO-injected or Rescue injected embryos at stage 24, 34, or 39 suggesting that the variation seen *in situ* is indeed temporal variation between embryos selected. Previous work in our laboratory conducted *in vitro* with the C2C12 myogenic cell line does suggest that silencing Mustn1 significantly diminishes MyoD expression as well as other marker genes. In addition to impacting gene expression, myotube formation was also reduced when Mustn1 was silenced [unpublished data]. These data suggest Mustn1 plays a role in muscle differentiation *in vitro* but may act redundantly *in vivo* masking the affect of silencing in these *X. laevis* experiments.

When Mustn1 was overexpressed in *X. laevis* embryos, no alteration in Sox9 expression pattern is observed via *in situ* hybridization when compared to mCherry injected control. However, in Mustn1-MO-injected embryos Sox9 expression is severely reduced. Sox9 expression, which is predominately found within the craniofacial region of the embryo, becomes restricted to a thin streak of weak staining anterior and peripheral to the presumptive eye position. When mRNA isolated from injected embryo anterior dissections was quantified, Sox9 expression demonstrates a ~40% reduction in Mustn1-MO-injected embryos when compared to Co-MO-injected embryos at stages 34 & 39. With the reintroduction of Mustn1 mRNA this reduction is rescued and Rescue injected embryos show no difference in Sox9 when compared to Co-MO-injection. Interestingly, in Co-MO-injected embryos, this staining is

localized ventral and anterior, with strong dorsal and posterior expression, but this dorsal expression is largely absent when Mustn1 is silenced. This again suggests that Mustn1 silencing affects the NCC development as they originate posteriorly and dorsal to the craniofacial region and migrate both ventrally toward the branchial arches and to the anterior regions of the eye. However, more resolution is needed in the localization experiments to determine which tissues are expressing Mustn1 and Sox9 at these stages. When Mustn1 is reintroduced Sox9 expression extends back into both dorsal regions and branchial arches as similar to Co-MO-injected embryos.

Overexpressing Mustn1 does not result in morphological defects or alter Sox9 expression pattern.

Overexpressing Mustn1, even at a relatively high concentration, seems to have no effect on development. This is consistent with both the *in vitro* research preformed previously on pre-chondrocytic and myogenic cell lines [unpublished data]. Overexpressing Mustn1 in these cells failed to yield any appreciable proliferation or differentiation phenotype. This suggests that while Mustn1 may be necessary for proper Sox9 expression and subsequently development, it is not sufficient to cause ectopic proliferation and/or differentiation to take place reaffirming the current hypothesis that Mustn1 is necessary but not sufficient for chondrogenesis.

As presented in this report Mustn1 depletion causes a variety of severe morphological defects as well as disruption in Sox9 expression during *X.*

laevis development. These data are consistent with results from our *in vitro* experiments which suggests that Mustn1 silencing negatively affects proliferation rate, matrix production, and down-regulates chondrogenic marker genes in the pre-chondrocytic RCJ cell line. Taken together with overexpression analysis, this research implies that Mustn1 is a vital protein necessary for chondrogenesis both *in vitro* and *in vivo*. While this report represents only an initial investigation into Mustn1's role during development, the preliminary results are dramatic and make Mustn1, and its role in chondrogenesis, worthy of further research.

4.5 Experimental procedures

Antisense morpholino oligonucleotide and rescue plasmid

A Mustn1 antisense morpholino oligonucleotide (Mustn1-MO) derived from 25 nucleotides located toward the 3' terminus within coding sequence has the sequence 5' GGGAATGTCCCAACCACAGGATGCC 3' (Gene Tools). Doses of 30-40ng were injected dorsal of the midline of 2- or 4-cell stage embryos. A standard scrambled morpholino oligonucleotide (Gene Tools) was used as control and injected under identical conditions. A rescue plasmid was created by modifying the coding sequence of Mustn1 at the site of morpholino binding using a site directed mutagenesis Sp6/T7 kit (Roche). The modified sequence at the site of morpholino was changed to 5' GGAATTCTCTGGTTAGGCCACTCAC 3' where red indicates mutations made. Arif Kirmizitas preformed all embryo morpholino and mRNA injection.

qPCR analysis

Quantification of gene expression via qPCR was preformed using kits and protocols from either Roche or Qiagen. Briefly, RNA was extracted from either whole wild-type embryos or anterior dissections of Co-MO-injected, Mustn1-MO-injected, and Rescue injected embryos via degradation with proteinase K in TNES buffer followed by phenol/chloroform extraction. RNA from wild-type embryos was reverse transcribed to cDNA (via Invitrogen kit) prior to qPCR for Mustn1 using a Lightcycler 480 and one-step qPCR SYBR green kit (Roche). The RNA from morpholino injected embryos became template for qPCR of Sox9 and MyoD using Lightcycler 2.1 (Roche) and two-step qPCR SYBR green kit (Qiagen). In both cases target gene expression was normalized to the expression level of Ornithine Decarboxylase.

Whole mount *in situ* hybridization

Whole mount *in situ* hybridizations were done according to standard procedures [15]. Briefly, embryos were fixed at specific stages with 4% paraformaldehyde for 1hour and stored in 100% Methanol prior to hybridization. The embryos were re-hydrated in a methanol/PBST gradient and permeabilized with proteinase K for 5 min. Embryos were pre-hybridized prior to incubation overnight in hybridization buffer with 1µg/ml probe at 60^{o}C. Embryos were washed in a SSC gradient before being blocked with MABT + 10% Lamb serum +2% blocking reagent (Roche). Embryos were then

incubated in Anti-DIG overnight at 4^{o}C prior to detection with BM Purple (Roche). Digoxigenin-labeled antisense probes were synthesized using Mustn1, MyoD and Sox9 cDNAs.

Embryo manipulation

In vitro fertilization and embryo culture were done according to standard protocols. Embryonic stages were determined according to Nieuwkoop and Faber (1967).

Scoring of morphological defects

Criteria were designed for each of the defect categories. For eye defects, embryo eyes were considered normal if they did not demonstrate any of the following: small eye(s) showed an observable reduction in eye circumference when compare to average Co-MO-injected embryos; they may have also shown disruption in the eye tissue, 1-eyed embryos showed little to no eye tissue unilaterally, embryos with a no eyed phenotype did not display any observable eye tissue on either side of the head. For Axis defects, an embryo body axis was considered normal if, at stage 40, the body and tail were approximately equal length. If this body: tail ratio was observably divergent from 1:1 resulting in a truncation of body axis; then the embryo was considered to have a shortened body axis. For tail defects, embryo bodies/tails were considered normal if they contained no kinks. If the embryo showed kinks in the body/tail that caused less than a 90^{o} change in body axis,

they were considered mild defects. If the embryo body/tail contained kinks causing a greater than 90^{o} change in body axis, they were considered severe defects.

Overexpressing Mustn1 *in vivo*

1.5ng of mRNA derived from the Mustn1 Rescue plasmid was injected into each blastomere at the 2-cell stage in the same manor as the morpholino injections. mCherry mRNA was injected as a control at the same concentration. Embryos were allowed to develop normally and were fixed and observed at stage 40.

Statistical analysis

Statistical significance between gene expression levels was determined via Mann-Whitney analysis between Co-MO-injected and Mustn1-MO-injected as well as Co-MO-injected and Rescue injected embryos. Significance was achieved when $p<.05$.

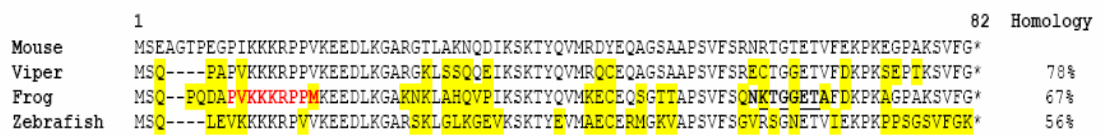

Figure 1. Mustn1 protein sequence homology between vertebrate species. Mustn1 amino acid sequences from Mouse, Viper, frog, and Zebrafish are compared and the % similarity (to mouse) is shown on the right. Changes in the primary sequence are denoted in yellow. Amino acids found in mouse but not other species are denoted by dashes. Analysis of motifs and potential modification sites within the *X. laevis* Mustn1 coding sequence are highlighted. The frog Nuclear Localization Sequence (NLS) is shown in red (aa8-16) and potential myristylation and phosphorylation sites are denoted by underlining (aa 62-67) and bold (aa 61-64 and aa 65-68) respectively.

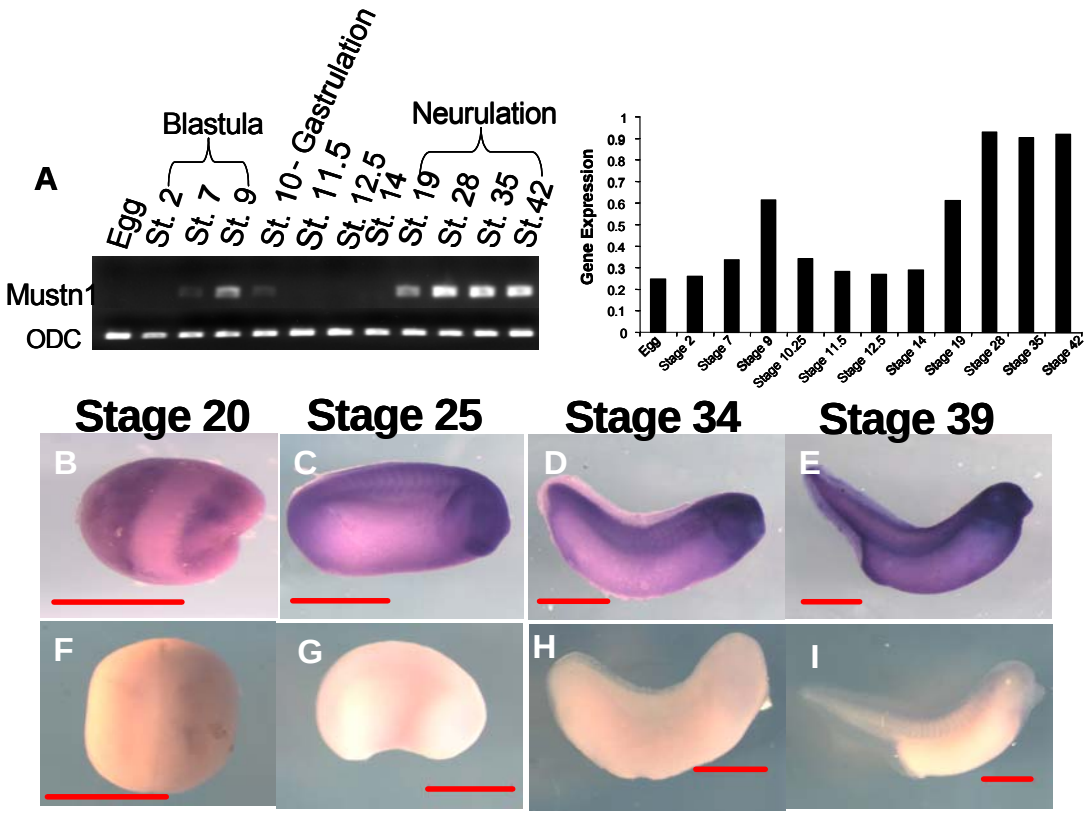

Figure 2. Mustn1 is differentially expressed both temporally and spatially during *X. laevis* development. A. Differential Mustn1 expression via qPCR shows a slight peak prior to gastrulation followed by an increase and plateau of expression during later developmental stages corresponding to neurulation. Analysis of spatial Mustn1 expression in wild-type embryos via *in situ* hybridization during development is shown by dorsal view of representative antisense Mustn1 hybridized St. 20 embryo, **B** and lateral views at **C**. St. 25, **D.** St. 34, and **E.** St. 40. Control (sense hybridized) embryos are shown **F.** St. 20, **G.** St. 23, **H.** St. 34, and **I.** St. 39. Scale bars=1mm.

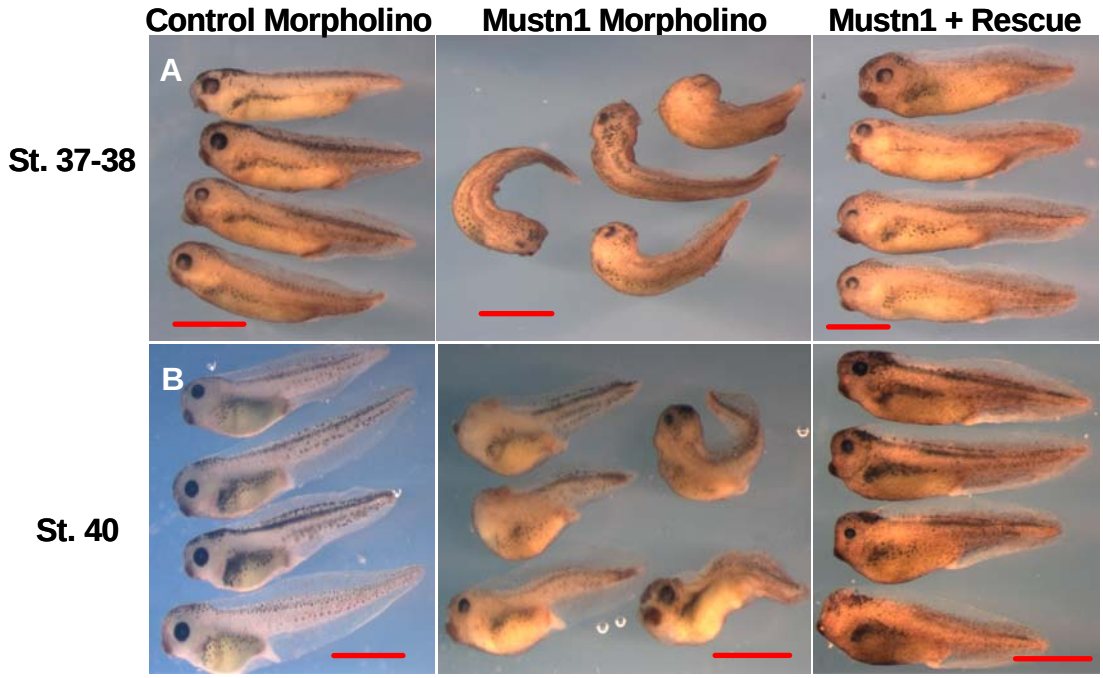

Figure 3. Qualitative analyses of morphological defects in Mustn1 morphants. Xenopus embryos were injected with morpholinos (35 ng/embryo) dorsal to the midline at the 4-cell stage and allowed to develop similarly. **A.** Comparison of Co-MO-injected embryos (left), Mustn1-MO-injected embryos (middle) and Rescued embryos (right side) at stage 37-38, lateral view. The Mustn1-MO-injected embryos reveal smaller eyes, truncated body axis, and tail kinks. **B.** Same analysis at stage 40. The control embryos (left side) grow normally, while Mustn1-MO-injected embryos (middle) show severe defects. The eyes shrink or disappear; the body length is also reduced along with curvature of the tail. Rescued embryos (right) show reduced severity of these defects. All scale bars = 1mm.

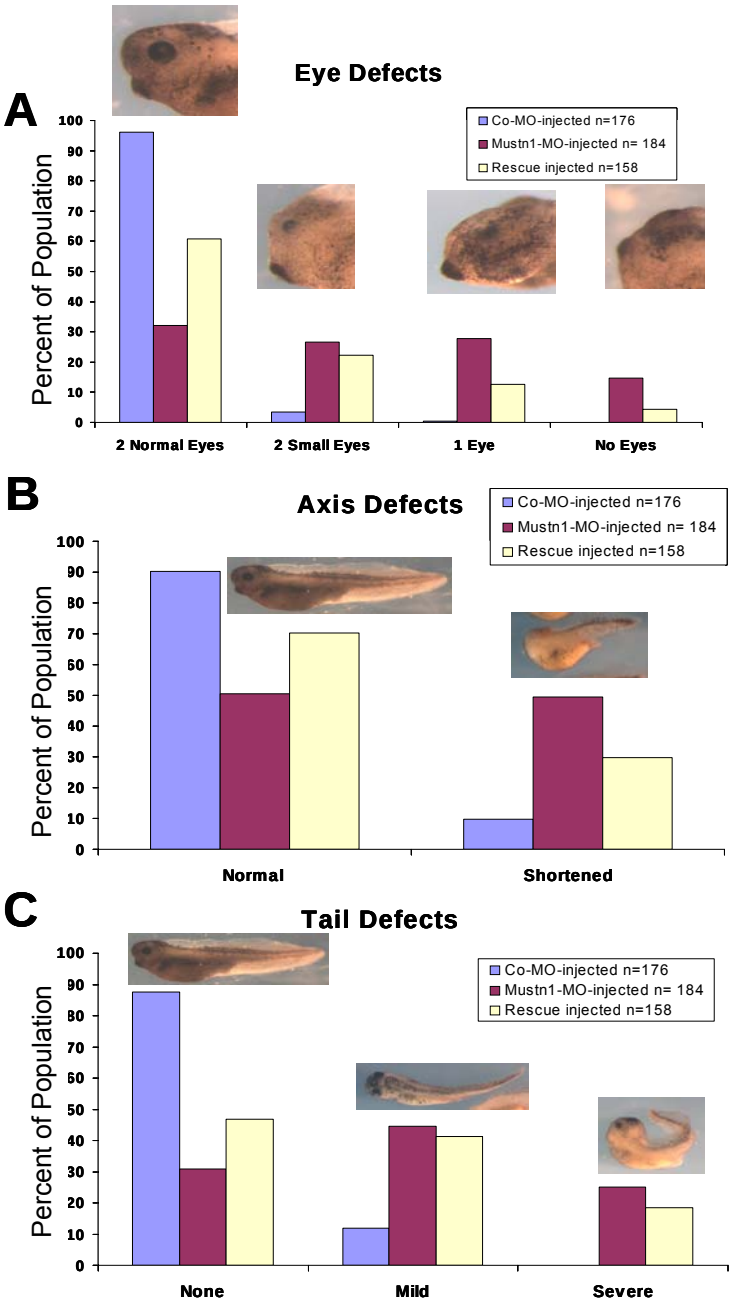

Figure 4. Quantitative analyses of morphological defects in Mustn1 morphants. Xenopus embryos from each group were fixed at stage 37-41 and were scored for each defect. **A.** Graphs of eye phenotypes presented in injected embryos. Labels correspond to phenotypes represented in the images (all lateral views except the dorsal view for the 1 Eye, Mild, and severe Tail phenotype) accompanying each category's quantification of Co-MO-injected, Mustn1-MO-injected, and Rescued embryos by percent of total population. **B.** Same analysis for Body axis length defects. Embryos were categorized as having either a normal (left) or shortened (right) body axis. **C.** Same analysis for Tail Kink defects. Embryos were categorized as having a normal (left), mild (middle), or severe (right) tail curvature.

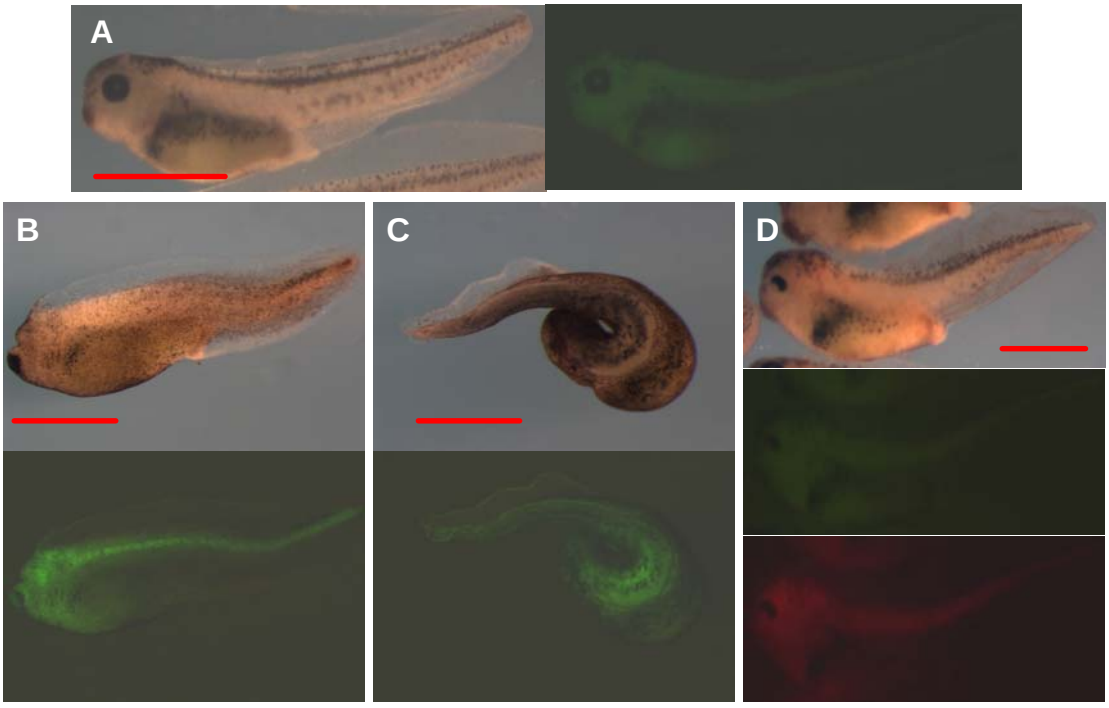

Figure 5. Localization of Mustn1 morpholino to areas of morphological defects. Embryos were injected with morpholinos (35 ng/embryo) dorsal to the midline at the 4-cell stage. Control and Mustn1 morpholino injected embryos were co-injected with Fluorescent Dextran Amine (FDA). Modified mRNA injected into the Rescued embryos was co-injected with mCherry mRNA. **A.** Lateral view of Co-MO-injected embryos under bright field (left) and at 470nm (right). FDA shows localization to craniofacial regions and somites. **B&C.** Lateral and Dorsal views of Mustn1-MO-injected embryos under bright field (top) and at 470nm (bottom). FDA co-injected with Mustn1 morpholino show localization to areas of morphological defects such as craniofacial regions (**B**) and affected areas of the somites (**C**). **D.** Lateral view of rescued embryos under bright field (top), 470nm (middle) and 600nm (bottom). FDA and mCherry mRNA show co-localization throughout the embryo. All Scale bars = 1mm.

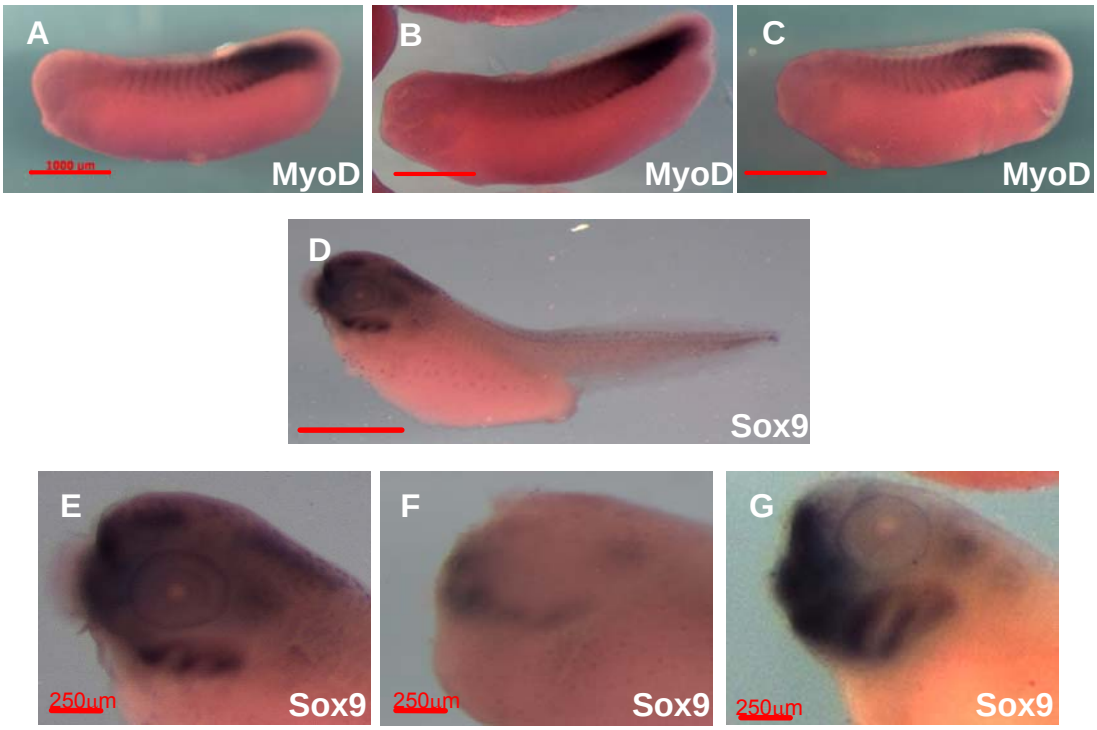

Figure 6. Mustn1 depletion affects chondrogenic but not myogenic marker expression. *In situ* hybridization was used to monitor the expression of the chondrogenic and myogenic markers, Sox9 and MyoD, respectively. Lateral view of MyoD expression in stage 24 embryos injected with Co-MO (**A**), Mustn1-MO (**B**) and rescued (**C**). Sox9 expression in Co-MO-injected embryo at stage 40 (**D**). Also high Magnification lateral view of Sox9 expression in stage 40 embryos injected with Co-MO (**E**), Mustn1-MO (**F**) and rescued (**G**). While no differential expression is observable in MyoD expression, Sox9 shows severe reduction in craniofacial cartilaginous elements. Scale bars = 1mm (**A-D**) or 250µm (**E-G**).

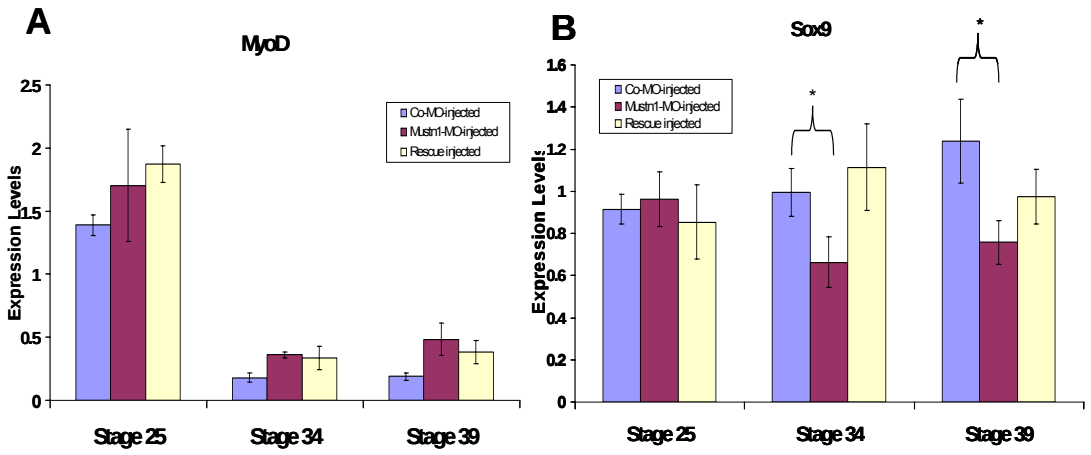

Figure 7. Mustn1 depletion reduces of Sox9 but not MyoD expression *in vivo*. mRNA was isolated from anterior regions of injected embryos and pooled (n=5) at stages 25, 34, & 39. qPCR for each of the marker genes was used to determine the exact expression levels. **A.** Graph of MyoD expression for Co-MO, Mustn1-MO, and Rescue injected embryos at indicated stages. No significant differences in MyoD expression were detected between any of the groups at any time point. **B.** Graph of Sox9 expression for Co-MO, Mustn1-MO, and Rescue injected embryos at indicated stages. No significant difference was found between Co-MO-injected and Rescue injected groups at any time point. A significant difference between Co-MO-injected and Mustn1-MO-injected embryos was found at stages 34 and 39. All bars represent average values of pooled mRNA (n=3). Error bars indicate standard deviation of mechanical variation between qPCR runs (n=3). Significance was determined by Mann-Whitney test vs. Co-MO-injected levels. *- $p<.05$.

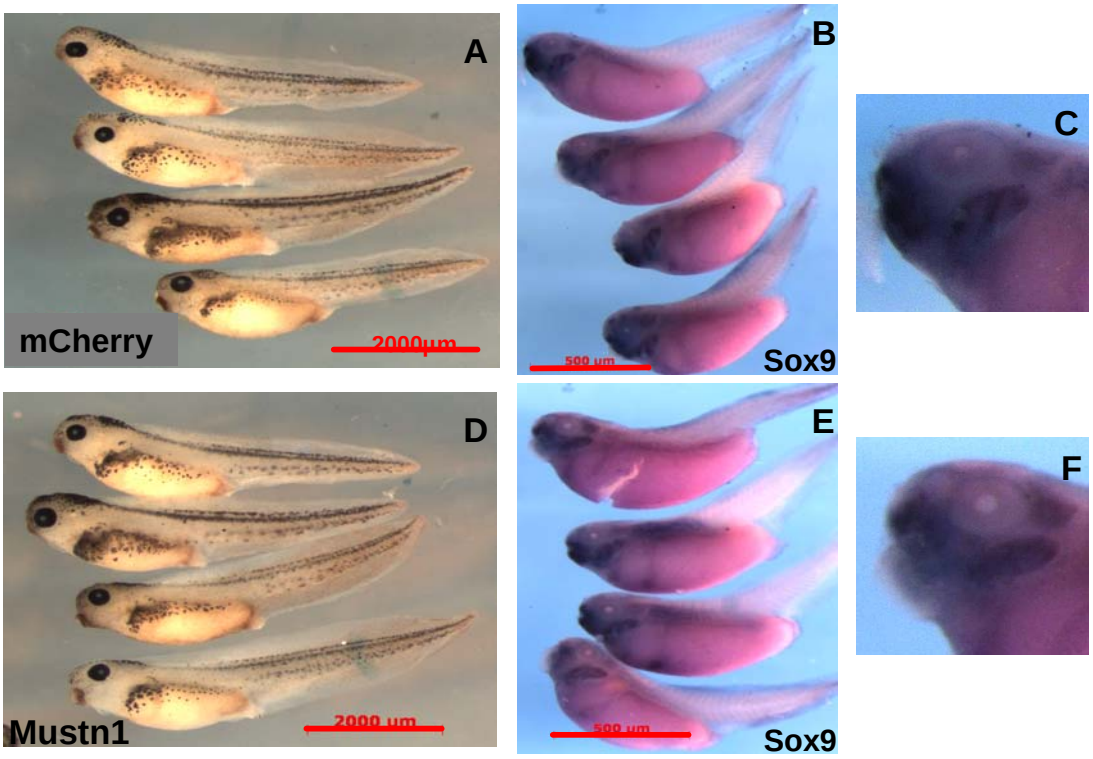

Figure 8. Overexpression of Mustn1 has no effect on chondrogenesis or Sox9 expression. Lateral views of embryos injected with either 1.5ng Mustn1 mRNA or 1.5ng mCherry mRNA as control into each blastomere at the 2-cell stage. *In situ* hybridization was used to monitor the expression of Sox9. Embryos were grown up under identical conditions and fixed at stage 40. **A.** Lateral view of mCherry mRNA injected embryos. **B.** Lateral view of mCherry mRNA injected embryos after *in situ* hybridization for Sox9. **C.** High Magnification lateral view of Sox9 expression in a representative mCherry mRNA injected embryo. **D.** Lateral view of Mustn1 mRNA injected embryos. **E.** Lateral view of Mustn1 mRNA injected embryos after *in situ* hybridization for Sox9. **F.** High Magnification lateral view of Sox9 expression in a representative Mustn1 mRNA injected embryo.

5. Conclusions

5.1 Bone fracture repair recapitulates development

The idea that BFR recapitulates bone development has been well supported both on the cellular and molecular levels [4,6,7,21]. However, because Mustn1 was originally identified as a differentially regulated molecule during BFR [13] and this report aims to elucidate its expression during development, we chose to validate this hypothesis by analyzing the expression patterns of genes critical to development during BFR. Specifically, we chose five Homeobox (Hox) transcription factors (Msx-1, Msx-2, rHox, Hoxa-2, and Hoxd-9) that were well documented during musculoskeletal development and analyzed them during fracture repair to determine if they were reactivated and, if so, in which cells/tissues within the callus.

As documented in Specific Aim #1, all five of these genes were up-regulated during BFR at all time points tested. Further these five genes showed similar expression patterns when fracture callus was spatially analyzed. Within the callus, rHox showed expression in osteoprogenitor cells and osteoblasts but not differentiated osteocytes. This expression pattern is consistent with research conducted on this gene during development which suggests that not only does rHox regulate osteogenic differentiation by binding osteocalcin and collagen I promoters [8,9] but, when rHox is mutated, defects in early phases of chondrogenesis and osteogenesis are observed [15].

When Msx-1 and Msx-2 were analyzed similar up-regulation was observed. Also, spatial localization experiments showed strong staining for these genes in proliferating and hypertrophic chondrocytes as well as osteoblasts and osteocytes. These data are again consistent with research linking these genes to chondrogenesis and osteogenesis during development [3,17].

Finally, Hoxa-2 and Hoxd-9 also showed an increase in expression throughout fracture repair but each showed peaks in expression at early stages within the time course. While this expression also localized to proliferating chondrocytes and osteoblasts/osteocytes there was no expression observed in terminally hypertrophic chondrocytes. Once again, these results are logical when considering data collected regarding these two genes during development suggesting that both Hoxa-2 and Hoxd-9 are necessary for proper chondrogenesis and osteogenesis particularly in early phases of these processes [5,10].

The reactivation of these five Hox genes during BFR, especially at time points and in cell types consistent with their roles during embryogenesis, strongly supports the current hypothesis that BFR recapitulates bone development. This validation suggest that since Mustn1 has been identified during BFR, in addition to likely regulating the components of BFR such as chondrogenesis, this gene is also likely involved in musculoskeletal development during embryogenesis.

5.2 The function of Mustn1 in chondrogenesis

Mustn1 is likely a nuclear co-activator of chondrogenesis and myogenesis.

Previous work done in our laboratory has provided indirect evidence as to the role Mustn1 plays *in vivo*. The first piece of evidence is derived from analyzing Mustn1 amino acid sequence for potential motifs and modification sites. This analysis identified a single known motif, a nuclear localization sequence (NLS), as well as potential myristylation and phosphorylation sites. When the NLS was verified via GFP-Mustn1 fusion construct, it was determined that Mustn1 localizes primarily to the nucleus, however, it is not found in the nucleoli or the nuclear membrane [13]. This data already significantly narrows down the list of possible functions of Mustn1 to such nuclear roles as DNA repair, transcriptional activation, DNA synthesis, RNA modification, etc. It is unlikely that Mustn1 plays a role in ribosomal rRNA transcription due to its lack of activity in the nucleoli and it is unlikely that this gene plays a role in nuclear transport because it does not contain a nuclear export sequence.

To elucidate this novel gene, one of the first experiments was to test for Mustn1 expression in different tissues. These data showed that Mustn1 expression is specific to the musculoskeletal system in adult tissues as its mRNA was identified only in bone, skeletal muscle, trachea, and tendon [13]. This finding was further supported by the results presented in Specific Aims #2 & 5 of this dissertation which showed that Mustn1 expression localizes to

areas of musculoskeletal development during vertebrate embryogenesis. This specificity suggests that Mustn1 does not play a housekeeping role in the nucleus, such as DNA replication or repair, because if it did it would be ubiquitous throughout all tissue types. This strongly suggests that Mustn1 is involved in the transcriptional regulation of musculoskeletal genes. Because its sequence does not contain a DNA binding motif, Mustn1 cannot be considered a transcription factor in the traditional sense and instead is likely either a co-activator or co-repressor.

Finally, experiments preformed in Specific Aims #3 & 4 of this dissertation in the pre-chondrocyte RCJ cell line found that while overexpressing Mustn1 cause no significant alterations in cell proliferation or differentiation, refuting our hypothesis, silencing of Mustn1 caused significant reductions in both of these processes as well as severe reductions in three major chondrogenic marker genes (Sox9, Collagen II, and Collagen X). When other research was preformed on the myogenic C2C12 cell line, a similar result was found. While overexpressing Mustn1 caused no cellular phenotype, silencing Mustn1 via RNAi caused a lack of myotube formation and reduced expression of several myogenic marker genes (MyoD, Myogenic, Myh4, and Desmin) [unpublished data]. Because these experiments show that marker gene expression is adversely affected when Mustn1 is silenced they suggest that Mustn1 could be a crucial part of a transcriptional complex allowing for differentiation of these cell types. It should be noted that it has yet to be determined if these reductions in marker gene expression are direct or indirect effects of Mustn1

silencing however, the early temporal activation of both Sox9 and MyoD suggest that Mustn1 silencing is closely related to these gene's subsequent downregulation.

Mustn1 likely regulates chondrogenesis and myogenesis *in vivo*.

Again, previous work preformed in our laboratory provides early evidence of Mustn1's function *in vivo*. Specifically, the localization of Mustn1 to periosteal osteoprogenitor cells, osteoblasts and proliferating chondrocytes during BFR begs further investigation. During development, multiple areas of mesenchymal condensations in limb buds, vertebral perichondrium, and intervertebral discs show Mustn1 expression; particularly in proliferating but not terminally differentiated hypertrophic chondrocytes [13]. This pattern of expression is consistent with data reported in this dissertation identifying areas of Mustn1 expression earlier in development.

Again, Specific Aims #2 & 5 of this dissertation reports *in situ* hybridization of whole mount mouse and *X. laevis* embryos, where we see evidence of Mustn1 expression in limb buds, branchial arches, tail bud, and somites during time points when all of these areas are undergoing either chondrogenesis or myogenesis. Indeed, *in vitro* analysis in pre-chondrocytes shows a sharp peak in Mustn1 expression during early differentiation followed by return to normal expression levels suggesting this gene acts early in the chondrocyte cellular progression. However, localization and *in vitro* analysis

simply correlate Mustn1 expression with these developmental processes and do not provide adequate causal evidence. For stronger support we undertook functional perturbation experiments *in vivo*.

In Specific Aim #5 of this dissertation we chose to investigate Mustn1 function *in vivo*. First a model organism, the *Xenopus laevis* embryo, was chosen since it shows similar temporal Mustn1 activation during developmental time points corresponding to musculoskeletal development. Localization experiments show Mustn1 expression in tissues consistent with the mouse embryo, namely developing somites and the craniofacial region. When Mustn1 is silenced in *X. laevis* embryos via antisense morpholino injection, several morphological defects are observed. As reported earlier, these defects are relegated predominately to the regions of Mustn1 expression and include small or missing eyes, truncated body axis, and body/tail kink or curvature.

It is interesting to note that these defects are not observable prior to mid-neurulation, when chondrogenesis and muscle development have begun. This observation further refutes the idea that the temporal peak in Mustn1 expression prior to gastrulation is significant; otherwise it is likely that earlier defects would be observed. However, while this early expression suggests Mustn1 is active in the earliest differentiation of mesoderm; validation of this hypothesis is needed. Additional experiments, including higher resolution *in situ* and sectioning, should be able to verify if this is the case.

Further, concentrating on the observable phenotype we find that reintroduction of Mustn1 mRNA rescues these defects. These defects give us rare insight into Mustn1's function during development. For example, in many cases, the small or missing eyes seem to be a by-product of severely malformed craniofacial regions in Mustn1-MO-injected embryos. While the eye itself is not part of the musculoskeletal system, it is possible that this observable defect is caused by a lack of eye cup or vesicle development, which is in part created via interactions between ectodermal NCC's and craniofacial mesenchyme, rather than failure of the eye placode to form normally. The tissues affected are formed primarily by differentiation and development of either ventral branchial arches or dorsal NCC's. Disrupting chondrogenesis in either of these areas could result in the severely malformed craniofacial structures observed.

Interestingly, when the cement gland located ventrally to the head was scored for truncation or loss, no difference was found between Mustn1-MO-injected embryo and control (data not shown), suggesting that ventral structures remain relatively intact despite Mustn1 depletion. Further, a truncated body axis may represent either reduced chondrogenesis or inferior ossification. This could be a defect in intramembranous ossification and therefore bypass any effects in chondrogenesis. However, the fact that tail and body vertebra in *X. laevis* develop via independent mechanisms require further investigation of this phenotype, perhaps in addition model systems.

Finally, the kink observed in both tail and body with regular frequency may be caused by imperfect muscle formation. While MyoD expression was not altered either spatially or quantitatively in Mustn1-MO-injected embryos, it is possible that this defect is the result of other muscle development mechanisms or that the techniques employed were unable to adequately elucidate Mustn1's impact. Again, while this makes for interesting speculation, further research into the molecular regulation of muscle development, such as analysis of later muscle marker genes (Myogenin, Desmin, & Heavy Muscle Actin) as well as muscle patterning experimentation, is required. Overall, the severity and combination of these three defects as well as the temporal and spatial localization of Mustn1 during development strongly suggest that this gene plays a role in musculoskeletal development. This conclusion is only further supported by the disruption of Sox9 expression in Mustn1-MO-injected embryos.

Mustn1 regulates chondrogenesis via regulating Sox9 expression *in vivo*.

Both *in vitro* and *in vivo* analysis presented herein suggest that silencing Mustn1 causes a downregulation of Sox9 expression. While this data only represents a cursory examination of Mustn1 expression, the notion that this gene seems to affect Sox9 expression, the master regulator of chondrogenesis, offers insights into the molecular mechanism. Unfortunately, many signaling molecules associated with chondrogenesis exert effects on

Sox9 expression. For example, as described in the introduction to this dissertation, TNF-α, NF-κB, HIF-1α, and ß-catenin all regulate Sox9 expression. Both TNF-α and NF-κB have been shown to block Sox9 expression [16]. HIF-1α has recently been found to regulate Sox9 expression in hypoxic environments during early skeletogenesis [2,14]. The interaction between ß-catenin and Sox9 is thought to balance the developmental processes of ossification and chondrogenesis linking this master regulator of chondrogenesis with the Wnt signaling pathway [1]. BMP stimulation of chondrogenesis operates via modulation of Sox9 expression as well [20] and repressors of the BMP pathway, such as Smad-b, inhibit it by targeting Sox9 expression [20]. Indeed, FGF's, SHH, IHH and PTH/PTHrP have all been recently suggested as likely Sox9 regulators [11,22,23]. Given the vast number of Sox9 regulating pathways, identifying the molecular function of Mustn1 simply from this interaction alone is impossible. Still, the regulation of such a potent modulator of chondrogenesis should not be overlooked.

While we cannot currently narrow down the specific pathway(s) in which affects Mustn1 function in the context of it's regulation of Sox9, recent research in our laboratory has identified promoter elements that may help to shed light on its regulation. Liu and Hadjiargyrou, 2006 have identified regulators of Mustn1 expression via deletion experiments on its promoter. They determined that AP-1 family members c-Fos, Fra-2, and JunD are required for Mustn1 activation in proliferating and differentiating C2C12 cells. These genes have been linked to the regulation of BMP-2 induced

chondrogenesis via a density dependent mechanism [18], but exactly how is unknown and further localization experiments are being pursued for all of these genes in articular cartilage [19]. While this is indeed an exciting result, promoter activation was only tested in the muscle cell line C2C12 and it is possible that regulation in chondrocytes is governed by different transcription factors. Still, this work represents the continuing elucidation of Mustn1 role in musculoskeletal development. While many questions of Mustn1 function remain unanswered, the research presented herein strongly suggests Mustn1 is a crucial regulator of chondrogenesis *in vitro* and *in vivo*.

Bibliography

Chapter 1

1. Rudnicki JA, Brown AM. Inhibition of chondrogenesis by Wnt gene expression in vivo and in vitro. Dev Biol. 1997 May 1;185(1):104-18.

2. Fischer L, Boland G, Tuan RS. Wnt-3A enhances bone morphogenetic protein-2-mediated chondrogenesis of murine C3H10T1/2 mesenchymal cells. J Biol Chem. 2002 Aug 23;277(34):30870-8. Epub 2002 Jun 20.

3. Hartmann C, Tabin CJ. Dual roles of Wnt signaling during chondrogenesis in the chicken limb. Development. 2000 Jul;127(14):3141-59.

4. Kawakami Y, Wada N, Nishimatsu SI, Ishikawa T, Noji S, Nohno T. Involvement of Wnt-5a in chondrogenic pattern formation in the chick limb bud. Dev Growth Differ. 1999 Feb;41(1):29-40.

5. Stott NS, Jiang TX, Chuong CM. Successive formative stages of precartilaginous mesenchymal condensations in vitro: modulation of cell adhesion by Wnt-7A and BMP-2. J Cell Physiol. 1999 Sep;180(3):314-24.

6. Chen H, Johnson RL. Interactions between dorsal-ventral patterning genes lmx1b, engrailed-1 and wnt-7a in the vertebrate limb. Int J Dev Biol. 2002;46(7):937-41.

7. Hartmann C. Wnt-signaling and skeletogenesis. J Musculoskelet Neuronal Interact. 2002 Mar;2(3):274-6.

8. Delise AM, Tuan RS. Analysis of N-cadherin function in limb mesenchymal chondrogenesis in vitro. Dev Dyn. 2002 Oct;225(2):195-204.

9. Oberlender SA, Tuan RS. Spatiotemporal profile of N-cadherin expression in the developing limb mesenchyme. Cell Adhes Commun. 1994 Dec;2(6):521-37.

10. Oberlender SA, Tuan RS. Expression and functional involvement of N-cadherin in embryonic limb chondrogenesis. Development. 1994 Jan;120(1):177-87.

11. Fischer L, Boland G, Tuan RS. Wnt signaling during BMP-2 stimulation of mesenchymal chondrogenesis. J Cell Biochem. 2002;84(4):816-31.

12. Schmitt B, Ringe J, Haupl T, Notter M, Manz R, Burmester GR, Sittinger M, Kaps C. BMP2 initiates chondrogenic lineage development of adult human mesenchymal stem cells in high-density culture. Differentiation. 2003 Dec;71(9-10):567-77.

13. Stott NS, Jiang TX, Chuong CM. Successive formative stages of precartilaginous mesenchymal condensations in vitro: modulation of cell adhesion by Wnt-7A and BMP-2. J Cell Physiol. 1999 Sep;180(3):314-24.

14. Fukumoto T, Sperling JW, Sanyal A, Fitzsimmons JS, Reinholz GG, Conover CA, O'Driscoll SW. Combined effects of insulin-like growth factor-1 and transforming growth factor-beta1 on periosteal mesenchymal cells during chondrogenesis in vitro. Osteoarthritis Cartilage. 2003 Jan;11(1):55-64.

15. Livne E, Laufer D, Blumenfeld I. Differential response of articular cartilage from young growing and mature old mice to IL-1 and TGF-beta. Arch Gerontol Geriatr. 1997 Mar-Apr;24(2):211-21.

16. Gaur T, Rich L, Lengner CJ, Hussain S, Trevant B, Ayers D, Stein JL, Bodine PV, Komm BS, Stein GS, Lian JB. Secreted frizzled related protein 1 regulates Wnt signaling for BMP2 induced chondrocyte differentiation. J Cell Physiol. 2006 Jul;208(1):87-96.

17. Morello R, Bertin TK, Schlaubitz S, Shaw CA, Kakuru S, Munivez E, Hermanns P, Chen Y, Zabel B, Lee B. Brachy-syndactyly caused by loss of Sfrp2 function. J Cell Physiol. 2008 Apr 29. [Epub ahead of print].

18. Daumer KM, Tufan AC, Tuan RS. Long-term in vitro analysis of limb cartilage development: involvement of Wnt signaling. J Cell Biochem. 2004 Oct 15;93(3):526-41.

19. Tufan AC, Daumer KM, Tuan RS. Frizzled-7 and limb mesenchymal chondrogenesis: effect of □ignaling□s□on and involvement of N-cadherin. Dev Dyn. 2002 Mar;223(2):241-53.

20. Ladher RK, Church VL, Allen S, Robson L, Abdelfattah A, Brown NA, Hattersley G, Rosen V, Luyten FP, Dale L, Francis-West PH. Cloning and expression of the Wnt antagonists Sfrp-2 and Frzb during chick development. Dev Biol. 2000 Feb 15;218(2):183-98.

21. Wada N, Kawakami Y, Ladher R, Francis-West PH, Nohno T. Involvement of Frzb-1 in mesenchymal condensation and cartilage differentiation in the chick limb bud. Int J Dev Biol. 1999 Sep;43(6):495-500.

22. Hwang SG, Yu SS, Lee SW, Chun JS. Wnt-3a regulates chondrocyte differentiation via c-Jun/AP-1 pathway. FEBS Lett. 2005 Aug 29;579(21):4837-42.

23. Jin EJ, Park JH, Lee SY, Chun JS, Bang OS, Kang SS. Wnt-5a is involved in TGF-beta3-stimulated chondrogenic differentiation of chick wing bud mesenchymal cells. Int J Biochem Cell Biol. 2006 Feb;38(2):183-95. Epub 2005 Sep 12.

24. Loganathan PG, Nimmagadda S, Huang R, Scaal M, Christ B. Comparative analysis of the expression patterns of Wnts during chick limb development. Histochem Cell Biol. 2005 Feb;123(2):195-201.

25. Akiyama H, Kamitani T, Yang X, Kandyil R, Bridgewater LC, Fellous M, Mori-Akiyama Y, de Crombrugghe B. The transcription factor Sox9 is degraded by the ubiquitin-proteasome system and stabilized by a mutation in a ubiquitin-target site. Matrix Biol. 2005 Jan;23(8):499-505. Epub 2004 Dec 8.

26. Rabie AB, She TT, Harley VR. Forward mandibular positioning up-regulates SOX9 and type II collagen expression in the glenoid fossa. J Dent Res. 2003 Sep;82(9):725-30.

27. Kim JH, Do HJ, Yang HM, Oh JH, Choi SJ, Kim DK, Cha KY, Chung HM. Overexpression of SOX9 in mouse embryonic stem cells directs the immediate chondrogenic commitment. Exp Mol Med. 2005 Aug 31;37(4):261-8.

28. Bi W, Deng JM, Zhang Z, Behringer RR, de Crombrugghe B. Sox9 is required for cartilage formation. Nat Genet. 1999 May;22(1):85-9.

29. Yingst S, Bloxham K, Warner LR, Brown RJ, Cole J, Kenoyer L, Knowlton WB, Oxford JT. Characterization of collagenous matrix assembly in a chondrocyte model system. J Biomed Mater Res A. 2008 May 21. [Epub ahead of print]

30. Tchetina EV, Kobayashi M, Yasuda T, Meijers T, Pidoux I, Poole AR. Chondrocyte hypertrophy can be induced by a cryptic sequence of type II collagen and is accompanied by the induction of MMP-13 and collagenase activity: implications for development and arthritis. Matrix Biol. 2007 May;26(4):247-58.

31. Shen G, Rabie AB, Zhao ZH, Kaluarachchi K. Forward deviation of the mandibular condyle enhances endochondral ossification of condylar cartilage indicated by increased expression of type X collagen. Arch Oral Biol. 2006 Apr;51(4):315-24.

32. Rodríguez-Niedenführ M, Dathe V, Jacob HJ, Pröls F, Christ B. Spatial and temporal pattern of Wnt-6 expression during chick development. Anat Embryol (Berl). 2003 May;206(6):447-51. Epub 2003 Apr 15.

33. Miljkovic ND, Cooper GM, Marra KG. Chondrogenesis, bone morphogenetic protein-4 and mesenchymal stem cells. Osteoarthritis Cartilage. 2008 Apr 10. [Epub ahead of print]

34. Bandyopadhyay A, Tsuji K, Cox K, Harfe BD, Rosen V, Tabin CJ. Genetic analysis of the roles of BMP2, BMP4, and BMP7 in limb patterning and skeletogenesis. PloS Genet. 2006 Dec;2(12):e216.

35. Boskey AL, Paschalis EP, Binderman I, Doty SB. BMP-6 accelerates both chondrogenesis and mineral maturation in differentiating chick limb-bud mesenchymal cell cultures. J Cell Biochem. 2002;84(3):509-19.

36. Hennig T, Lorenz H, Thiel A, Goetzke K, Dickhut A, Geiger F, Richter W. Reduced chondrogenic potential of adipose tissue derived stromal cells correlates with an altered TGFbeta receptor and BMP profile and is overcome by BMP-6. J Cell Physiol. 2007 Jun;211(3):682-91.

37. Shintani N, Hunziker EB. Chondrogenic differentiation of bovine synovium: bone morphogenetic proteins 2 and 7 and transforming growth factor beta1 induce the formation of different types of cartilaginous tissue. Arthritis Rheum. 2007 Jun;56(6):1869-79.

38. Gooch KJ, Blunk T, Courter DL, Sieminski AL, Vunjak-Novakovic G, Freed LE. Bone morphogenetic proteins-2, -12, and -13 modulate in vitro development of engineered cartilage. Tissue Eng. 2002 Aug;8(4):591-601.

39. Nochi H, Sung JH, Lou J, Adkisson HD, Maloney WJ, Hruska KA. Adenovirus mediated BMP-13 gene transfer induces chondrogenic differentiation of murine mesenchymal progenitor cells. J Bone Miner Res. 2004 Jan;19(1):111-22.

40. Blunk T, Sieminski AL, Appel B, Croft C, Courter DL, Chieh JJ, Goepferich A, Khurana JS, Gooch KJ. Bone morphogenetic protein 9: a potent modulator of cartilage development in vitro. Growth Factors. 2003 Jun;21(2):71-7.

41. Solloway MJ, Dudley AT, Bikoff EK, Lyons KM, Hogan BL, Robertson EJ. Mice lacking Bmp6 function. Dev Genet. 1998;22(4):321-39.

42. Gamer LW, Ho V, Cox K, Rosen V. Expression and function of BMP3 during chick limb development. Dev Dyn. 2008 Jun;237(6):1691-8.

43. Reinhold MI, Kapadia RM, Liao Z, Naski MC. The Wnt-inducible transcription factor Twist1 inhibits chondrogenesis. J Biol Chem. 2006 Jan 20;281(3):1381-8.

44. Mikels AJ, Nusse R. Purified Wnt5a protein activates or inhibits beta-catenin-TCF signaling depending on receptor context. PloS Biol. 2006 Apr;4(4):e115.

45. Church V, Nohno T, Linker C, Marcelle C, Francis-West P. Wnt regulation of chondrocyte differentiation. J Cell Sci. 2002 Dec 15;115(Pt 24):4809-18.

46. Geetha-Loganathan P, Nimmagadda S, Huang R, Scaal M, Christ B. Role of Wnt-6 in limb myogenesis. Anat Embryol (Berl). 2006 Jun;211(3):183-8.

47. Später D, Hill TP, O'sullivan RJ, Gruber M, Conner DA, Hartmann C. Wnt9a signaling is required for joint integrity and regulation of Ihh during chondrogenesis. Development. 2006 Aug;133(15):3039-49.

48. Dell'accio F, De Bari C, Eltawil NM, Vanhummelen P, Pitzalis C. Identification of the molecular response of articular cartilage to injury, by microarray screening: Wnt-16 expression and signaling after injury and in osteoarthritis. Arthritis Rheum. 2008 May;58(5):1410-21.

49. Hill TP, Später D, Taketo MM, Birchmeier W, Hartmann C. Canonical Wnt/beta-catenin signaling prevents osteoblasts from differentiating into chondrocytes. Dev Cell. 2005 May;8(5):727-38.

50. Chen Y, Whetstone HC, Youn A, Nadesan P, Chow EC, Lin AC, Alman BA. Beta-catenin signaling pathway is crucial for bone morphogenetic protein 2 to induce new bone formation. J Biol Chem. 2007 Jan 5;282(1):526-33.

51. Goldring MB, Tsuchimochi K, Ijiri K. The control of chondrogenesis. J Cell Biochem. 2006 Jan 1;97(1):33-44.

52. Chi SS, Rattner JB, Sciore P, Boorman R, Lo IK. Gap junctions of the medial collateral ligament: structure, distribution, associations and function. J Anat. 2005 Aug;207(2):145-54.

53. Akiyama H, Lyons JP, Mori-Akiyama Y, Yang X, Zhang R, Zhang Z, Deng JM, Taketo MM, Nakamura T, Behringer RR, McCrea PD, de Crombrugghe B. Interactions between Sox9 and beta-catenin control chondrocyte differentiation. Genes Dev. 2004 May 1;18(9):1072-87.

54. Kirton JP, Crofts NJ, George SJ, Brennan K, Canfield AE. Wnt/beta-catenin signaling stimulates chondrogenic and inhibits adipogenic differentiation of pericytes: potential relevance to vascular disease? Circ Res. 2007 Sep 14;101(6):581-9.

55. Galceran J, Fariñas I, Depew MJ, Clevers H, Grosschedl R. Wnt3a-/--like phenotype and limb deficiency in Lef1(-/-)Tcf1(-/-) mice. Genes Dev. 1999 Mar 15;13(6):709-17.

56. Murakami S, Lefebvre V, de Crombrugghe B. Potent inhibition of the master chondrogenic factor Sox9 gene by interleukin-1 and tumor necrosis factor-alpha. J Biol Chem. 2000 Feb 4;275(5):3687-92.

57. MacRae VE, Farquharson C, Ahmed SF. The restricted potential for recovery of growth plate chondrogenesis and longitudinal bone growth following exposure to pro-inflammatory cytokines. J Endocrinol. 2006 May;189(2):319-28.

58. Muddasani P, Norman JC, Ellman M, van Wijnen AJ, Im HJ. Basic fibroblast growth factor activates the MAPK and NfkappaB pathways that converge on Elk-1 to control production of matrix metalloproteinase-13 by human adult articular chondrocytes. J Biol Chem. 2007 Oct 26;282(43):31409-21.

59. Zhang P, Jimenez SA, Stokes DG. Regulation of human COL9A1 gene expression. Activation of the proximal promoter region by SOX9. J Biol Chem. 2003 Jan 3;278(1):117-23.

60. Smith GN Jr, Brandt KD. Hypothesis: can type IX collagen “glue” together intersecting type II fibers in articular cartilage matrix? A proposed mechanism. J Rheumatol. 1992 Jan;19(1):14-7.

61. Dreier R, Opolka A, Grifka J, Bruckner P, Grässel S. Collagen IX-deficiency seriously compromises growth cartilage development in mice. Matrix Biol. 2008 May;27(4):319-29.

62. Yingst S, Bloxham K, Warner LR, Brown RJ, Cole J, Kenoyer L, Knowlton WB, Oxford JT. Characterization of collagenous matrix assembly in a chondrocyte model system. J Biomed Mater Res A. 2008 May 21.

63. Kim YJ, Kim HJ, Im GI. PTHrP promotes chondrogenesis and suppresses hypertrophy from both bone marrow-derived and adipose tissue-derived MSCs. Biochem Biophys Res Commun. 2008 Jun 11. [Epub ahead of print]

64. Lanske B, Amling M, Neff L, Guiducci J, Baron R, Kronenberg HM. Ablation of the PTHrP gene or the PTH/PTHrP receptor gene leads to distinct abnormalities in bone development. J Clin Invest. 1999 Aug;104(4):399-407.

65. Harrington EK, Roddy GW, West R, Svoboda KK. Parathyroid hormone/parathyroid hormone-related peptide modulates growth of avian

sternal cartilage via chondrocytic proliferation. Anat Rec (Hoboken). 2007 Feb;290(2):155-67.

66. Zerega B, Cermelli S, Bianco P, Cancedda R, Cancedda FD. Parathyroid hormone [PTH(1-34)] and parathyroid hormone-related protein [PTHrP(1-34)] promote reversion of hypertrophic chondrocytes to a prehypertrophic proliferating phenotype and prevent terminal differentiation of □ignaling□s-like cells. J Bone Miner Res. 1999 Aug;14(8):1281-9.

67. Melnick M, Witcher D, Bringas P Jr, Carlsson P, Jaskoll T. Meckel's cartilage differentiation is dependent on hedgehog signaling. Cells Tissues Organs. 2005;179(4):146-57.

68. Bobick BE, Thornhill TM, Kulyk WM. Fibroblast growth factors 2, 4, and 8 exert both negative and positive effects on limb, frontonasal, and mandibular chondrogenesis via MEK-ERK activation. J Cell Physiol. 2007 Apr;211(1):233-43.

69. Hung IH, Yu K, Lavine KJ, Ornitz DM. FGF9 regulates early hypertrophic chondrocyte differentiation and skeletal vascularization in the developing stylopod. Dev Biol. 2007 Jul 15;307(2):300-13.

70. Liu Z, Lavine KJ, Hung IH, Ornitz DM. FGF18 is required for early chondrocyte proliferation, hypertrophy and vascular invasion of the growth plate. Dev Biol. 2007 Feb 1;302(1):80-91.

71. Liu Z, Xu J, Colvin JS, Ornitz DM. Coordination of chondrogenesis and osteogenesis by fibroblast growth factor 18. Genes Dev. 2002 Apr 1;16(7):859-69.

72. Davidson D, Blanc A, Filion D, Wang H, Plut P, Pfeffer G, Buschmann MD, Henderson JE. Fibroblast growth factor (FGF) 18 signals through FGF receptor 3 to promote chondrogenesis. J Biol Chem. 2005 May 27;280(21):20509-15.

73. Ido A, Ito K. Expression of chondrogenic potential of mouse trunk neural crest cells by FGF2 treatment. Dev Dyn. 2006 Feb;235(2):361-7.

74. Lovinescu I, Koyama E, Pacifici M. Roles of FGF-10 on the development of diathrodial limb joints. Penn Dent J (Phila). 2003;103:5, 9.

75. Young B, Minugh-Purvis N, Shimo T, St-Jacques B, Iwamoto M, Enomoto-Iwamoto M, Koyama E, Pacifici M. Indian and sonic hedgehogs regulate synchondrosis growth plate and cranial base development and function. Dev Biol. 2006 Nov 1;299(1):272-82.

76. Smits P, Dy P, Mitra S, Lefebvre V. Sox5 and Sox6 are needed to develop and maintain source, columnar, and hypertrophic chondrocytes in the cartilage growth plate. J Cell Biol. 2004 Mar 1;164(5):747-58.

77. Ikeda T, Kamekura S, Mabuchi A, Kou I, Seki S, Takato T, Nakamura K, Kawaguchi H, Ikegawa S, Chung UI. The combination of SOX5, SOX6, and SOX9 (the SOX trio) provides signals sufficient for induction of permanent cartilage. Arthritis Rheum. 2004 Nov;50(11):3561-73.

78. Mak KK, Kronenberg HM, Chuang PT, Mackem S, Yang Y. Indian hedgehog signals independently of PTHrP to promote chondrocyte hypertrophy. Development. 2008 Jun;135(11):1947-56.

79. Karp SJ, Schipani E, St-Jacques B, Hunzelman J, Kronenberg H, McMahon AP. Indian hedgehog coordinates endochondral bone growth and morphogenesis via parathyroid hormone related-protein-dependent and –independent pathways. Development. 2000 Feb;127(3):543-8.

80. Hattori H, Mizutani H, Ueda M. Sonic hedgehog. Clin Calcium. 2002 Feb;12(2):233-7.

81. Zhu J, Nakamura E, Nguyen MT, Bao X, Akiyama H, Mackem S. Uncoupling Sonic hedgehog control of pattern and expansion of the developing limb bud. Dev Cell. 2008 Apr;14(4):624-32.

82. Nifuji A, Kellermann O, Noda M. Noggin inhibits chondrogenic but not osteogenic differentiation in mesodermal stem cell line C1 and skeletal cells. Endocrinology. 2004 Jul;145(7):3434-42.

83. Tylzanowski P, Mebis L, Luyten FP. The Noggin null mouse phenotype is strain dependent and haploinsufficiency leads to skeletal defects. Dev Dyn. 2006 Jun;235(6):1599-607.

84. Kwong FN, Richardson SM, Evans CH. Chordin knockdown enhances the osteogenic differentiation of human mesenchymal stem cells. Arthritis Res Ther. 2008 Jun 4;10(3):R65.

85. Watanabe H, Yamada Y, Kimata K. Roles of □ignalin, a large chondroitin sulfate proteoglycan, in cartilage structure and function. J Biochem. 1998 Oct;124(4):687-93.

86. Nagase H, Kashiwagi M. Aggrecanases and cartilage matrix degradation. Arthritis Res Ther. 2003;5(2):94-103.

87. Amarilio R, Viukov SV, Sharir A, Eshkar-Oren I, Johnson RS, Zelzer E. HIF1alpha regulation of Sox9 is necessary to maintain differentiation of

hypoxic prechondrogenic cells during early skeletogenesis. Development. 2007 Nov;134(21):3917-28.

88. Malladi P, Xu Y, Chiou M, Giaccia AJ, Longaker MT. Hypoxia inducible factor-1alpha deficiency affects chondrogenesis of adipose-derived adult stromal cells. Tissue Eng. 2007 Jun;13(6):1159-71.

89. Bluteau G, Julien M, Magne D, Mallein-Gerin F, Weiss P, Daculsi G, Guicheux J. VEGF and VEGF receptors are differentially expressed in chondrocytes. Bone. 2007 Mar;40(3):568-76.

90. Oldershaw RA, Tew SR, Russell AM, Meade K, Hawkins R, McKay TR, Brennan KR, Hardingham TE. Notch signaling through Jagged-1 is necessary to initiate chondrogenesis in human bone marrow stromal cells but must be switched off to complete chondrogenesis. Stem Cells. 2008 Mar;26(3):666-74.

91. Chen Y, Whetstone HC, Youn A, Nadesan P, Chow EC, Lin AC, Alman BA. Beta-catenin signaling pathway is crucial for bone morphogenetic protein 2 to induce new bone formation. J Biol Chem. 2007 Jan 5;282(1):526-33.

92. Grotewold L, Rüther U. Bmp, Fgf and Wnt □ignaling in programmed cell death and chondrogenesis during vertebrate limb development: the role of Dickkopf-1. Int J Dev Biol. 2002;46(7):943-7.

93. Rich JT, Rosová I, Nolta JA, Myckatyn TM, Sandell LJ, McAlinden A. Upregulation of Runx2 and Osterix during in vitro chondrogenesis of human adipose-derived stromal cells. Biochem Biophys Res Commun. 2008 Jul 18;372(1):230-5.

94. Gordeladze JO, Noël D, Bony C, Apparailly F, Louis-Plence P, Jorgensen C. Transient down-regulation of cbfa1/Runx2 by RNA interference in murine C3H10T1/2 mesenchymal stromal cells delays in vitro and in vivo osteogenesis, but does not overtly affect chondrogenesis. Exp Cell Res. 2008 Apr 15;314(7):1495-506.

95. Kempf H, Ionescu A, Udager AM, Lassar AB. Prochondrogenic signals induce a competence for Runx2 to activate hypertrophic chondrocyte gene expression. Dev Dyn. 2007 Jul;236(7):1954-62.

96. Jin EJ, Choi YA, Kyun Park E, Bang OS, Kang SS. MMP-2 functions as a negative regulator of chondrogenic cell condensation via down-regulation of the FAK-integrin beta1 interaction. Dev Biol. 2007 Aug 15;308(2):474-84.

97. Wu W, Mwale F, Tchetina E, Kojima T, Yasuda T, Poole AR. Cartilage matrix resorption in skeletogenesis. Novartis Found Symp. 2001;232:158-66; discussion 166-70.

98. Stickens D, Behonick DJ, Ortega N, Heyer B, Hartenstein B, Yu Y, Fosang AJ, Schorpp-Kistner M, Angel P, Werb Z. Altered endochondral bone development in matrix metalloproteinase 13-deficient mice. Development. 2004 Dec;131(23):5883-95.

99. Weston AD, Rosen V, Chandraratna RA, Underhill TM. Regulation of skeletal progenitor differentiation by the BMP and retinoid signaling pathways. J Cell Biol. 2000 Feb 21;148(4):679-90.

100. Koziel L, Wuelling M, Schneider S, Vortkamp A. Gli3 acts as a repressor downstream of Ihh in regulating two distinct steps of chondrocyte differentiation. Development. 2005 Dec;132(23):5249-60.

101. Vortkamp A, Lee K, Lanske B, Segre GV, Kronenberg HM, Tabin CJ. Regulation of rate of cartilage differentiation by Indian hedgehog and PTH-related protein. Science. 1996 Aug 2;273(5275):579.

102. Kanzler B, Kuschert SJ, Liu YH, Mallo M. Hoxa-2 restricts the chondrogenic domain and inhibits bone formation during development of the branchial area. Development. 1998 Jul;125(14):2587-97.

103. Massip L, Ectors F, Deprez P, Maleki M, Behets C, Lengelé B, Delahaut P, Picard J, Rezsöhazy R. Expression of Hoxa2 in cells entering chondrogenesis impairs overall cartilage development. Differentiation. 2007 Mar;75(3):256-67.

104. Yueh YG, Gardner DP, Kappen C. Evidence for regulation of cartilage differentiation by the homeobox gene Hoxc-8. Proc Natl Acad Sci U S A. 1998 Aug 18;95(17):9956-61.

105. Attur MG, Dave MN, Stuchin S, Kowalski AJ, Steiner G, Abramson SB, Denhardt DT, Amin AR. Osteopontin: an intrinsic inhibitor of inflammation in cartilage. Arthritis Rheum. 2001 Mar;44(3):578-84.

106. Xu X, Weinstein M, Li C, Naski M, Cohen RI, Ornitz DM, Leder P, Deng C. Fibroblast growth factor receptor 2 (FGFR2)-mediated reciprocal regulation loop between FGF8 and FGF10 is essential for limb induction. Development. 1998 Feb;125(4):753-65.

107. Nonaka K, Shum L, Takahashi I, Takahashi K, Ikura T, Dashner R, Nuckolls GH, Slavkin HC. Convergence of the BMP and EGF signaling pathways on Smad1 in the regulation of chondrogenesis. Int J Dev Biol. 1999 Nov;43(8):795-807.

108. Pan Q, Yu Y, Chen Q, Li C, Wu H, Wan Y, Ma J, Sun F. Sox9, a key transcription factor of bone morphogenetic protein-2-induced chondrogenesis,

is activated through BMP pathway and a CCAAT box in the proximal promoter. J Cell Physiol. 2008 Oct;217(1):228-41.

109. Hatakeyama Y, Nguyen J, Wang X, Nuckolls GH, Shum L. Smad signaling in mesenchymal and chondroprogenitor cells. J Bone Joint Surg Am. 2003;85-A Suppl 3:13-8.

110. Yoon YM, Oh CD, Kim DY, Lee YS, Park JW, Huh TL, Kang SS, Chun JS. Epidermal growth factor negatively regulates chondrogenesis of mesenchymal cells by modulating the protein kinase C-alpha, Erk-1, and p38 MAPK signaling pathways. J Biol Chem. 2000 Apr 21;275(16):12353-9.

111. Neumann K, Endres M, Ringe J, Flath B, Manz R, Häupl T, Sittinger M, Kaps C. BMP7 promotes adipogenic but not osteo-/chondrogenic differentiation of adult human bone marrow-derived stem cells in high-density micro-mass culture. J Cell Biochem. 2007 Oct 15;102(3):626-37.

112. Hoffmann A, Czichos S, Kaps C, Bächner D, Mayer H, Kurkalli BG, Zilberman Y, Turgeman G, Pelled G, Gross G, Gazit D. The T-box transcription factor Brachyury mediates cartilage development in mesenchymal stem cell line C3H10T1/2. J Cell Sci. 2002 Feb 15;115(Pt 4):769-81.

113. Xu XL, Lou J, Tang T, Ng KW, Zhang J, Yu C, Dai K. Evaluation of different scaffolds for BMP-2 genetic orthopedic tissue engineering. J Biomed Mater Res B Appl Biomater. 2005 Nov;75(2):289-303.

114 Mehlhorn AT, Niemeyer P, Kaschte K, Muller L, Finkenzeller G, Hartl D, Sudkamp NP, Schmal H. Differential effects of BMP-2 and TGF-beta1 on chondrogenic differentiation of adipose derived stem cells. Cell Prolif. 2007 Dec;40(6):809-23.

115. Sharma B, Williams CG, Khan M, Manson P, Elisseeff JH. In vivo chondrogenesis of mesenchymal stem cells in a photopolymerized hydrogel. Plast Reconstr Surg. 2007 Jan;119(1):112-20.

116. Yun K, Moon HT. Inducing chondrogenic differentiation in injectable hydrogels embedded with rabbit chondrocytes and growth factor for neocartilage formation. J Biosci Bioeng. 2008 Feb;105(2):122-6.

117. Jin EJ, Lee SY, Jung JC, Bang OS, Kang SS. TGF-beta3 inhibits chondrogenesis of cultured chick leg bud mesenchymal cells via downregulation of connexin 43 and integrin beta4. J Cell Physiol. 2008 Feb;214(2):345-53.

118. Origuchi N, Ishidou Y, Nagamine T, Onishi T, Matsunaga S, Yoshida H, Sakou T. The spatial and temporal immunolocalization of TGF-beta 1 and

bone morphogenetic protein-2/-4 in phallic bone formation in inbred Sprague Dawley male rats. In Vivo. 1998 Sep-Oct;12(5):473-80.

119. Tuan RS. Cellular signaling in developmental chondrogenesis: N-cadherin, Wnts, and BMP-2. J Bone Joint Surg Am. 2003;85-A Suppl 2:137-41.

120. Hadjiargyrou M, Lombardo F, Zhao S, Ahrens W, Joo J, Ahn H, Jurman M, White DW, Rubin CT. Transcriptional profiling of bone regeneration. Insight into the molecular complexity of wound repair. J Biol Chem. 2002 Aug 16;277(33):30177-82.

121. Lombardo F, Komatsu D, Hadjiargyrou M. Molecular cloning and characterization of Mustn1, a novel nuclear protein expressed during skeletal development and regeneration. FASEB J. 2004 Jan;18(1):52-61.

122. Gerstenfeld LC, Cullinane DM, Barnes GL, Graves DT, Einhorn TA. Fracture healing as a post-natal developmental process: molecular, spatial, and temporal aspects of its regulation. J Cell Biochem. 2003 Apr 1;88(5):873-84.

123. Gersch R, Lombardo F, McGovern S, and Hadjiargyrou M. Re-activation of Hox gene expression during bone regeneration. J. Orthop. Res. 23: 882-890.

124. Hadjiargyrou M, Ahrens W, Rubin CT. Temporal expression of the chondrogenic and angiogenic growth factor CYR61 during fracture repair. J Bone Miner Res. 2000 Jun;15(6):1014-23.

125. Shimizu H, Yokoyama S, Asahara H. Growth and differentiation of the developing limb bud from the perspective of chondrogenesis. Dev Growth Differ. 2007 Aug;49(6):449-54.

126. Montero JA, Hurlé JM. Deconstructing digit chondrogenesis. Bioessays. 2007 Aug;29(8):725-37.

127. Zhong N, Gersch RP, Hadjiargyrou M. Wnt Signaling activation during bone regeneration and the role of Dishevelled in chondrocyte proliferation and differentiation. Bone 39 (2006) 5-16.

128. Bronner-Fraser, M. and Stern, C. 1991. Effects of mesodermal tissues on avian neural crest cell migration. Dev. Biol. 143; 213-217.

129. Johnston, M. C., Sulik, K. K., Webster, W. S. and Jarvis, B. L. 1985. Isotretinoin embryopathy in a mouse model: Cranial neural crest involvement. Teratology 31:26A

130. Larsen, W. J. 1993. Human Embryology. Churchil Livingstone, New York.

131. Gilbert, S. F. 1997. Developmental Biology. Fifth Edition. Sinauer Associates, Inc. Sunderland, Massachuesetts.

132. Davis, A.P., Witte, D.P., Hsieh-Li, H.M., Potter, S. and Capecchi, M. R. 1995. Absence of radius and ulna in mice lacking *hoax-11* and *hoxd-11*. Nature 375-791-795.

Chapter 2

1. Alappat S, Zhang ZY, Chen YP. Msx homeobox gene family and craniofacial development. Cell Res. 2003 Dec;13(6):429-42.

2. Barrow JR, Stadler HS, Capecchi MR. Roles of Hoxa1 and Hoxa2 in patterning the early hindbrain of the mouse. Development. 2000 Mar;127(5):933-44.

3. Blin-Wakkach C, Lezot F, Ghoul-Mazgar S et al. Endogenous Msx1 antisense transcript: in vivo and in vitro evidences, structure, and potential involvement in skeleton development in mammals. Proc Natl Acad Sci U S A. 2001 Jun 19;98(13):7336-41. Epub 2001 Jun 05.

4. Bonnarens F and Einhorn T.A. Production of a standard closed fracture in laboratory animal bone. J. Orthop. Res. 2 (1984), pp. 97–101.

5. de la Cruz CC, Der-Avakian A, Spyropoulos DD et al. Targeted disruption of Hoxd9 and Hoxd10 alters locomotor behavior, vertebral identity, and peripheral nervous system development. Dev Biol. 1999 Dec 15;216(2):595-610.

6. Dodig M, Kronenberg MS, Bedalov A et al. Identification of a TAAT-containing motif required for high level expression of the COL1A1 promoter in differentiated osteoblasts of transgenic mice. J Biol Chem. 1996 Jul 5;271(27):16422-9.

7. Ferguson C, Alpern E, Miclau T, Helms JA. Does adult fracture repair recapitulate embryonic skeletal formation? Mech Dev. 1999 Sep;87(1-2):57-66.

8. Fromental-Ramain C, Warot X, Lakkaraju S et al. Specific and redundant functions of the paralogous Hoxa-9 and Hoxd-9 genes in forelimb and axial skeleton patterning. Development. 1996 Feb;122(2):461-72.

9. Gendron-Maguire M, Mallo M, Zhang M, Gridley T. Hoxa-2 mutant mice exhibit homeotic transformation of skeletal elements derived from cranial neural crest. Cell. 1993 Dec 31;75(7):1317-31.

10. Gerstenfeld LC, Cullinane DM, Barnes GL, Graves DT, Einhorn TA. Fracture healing as a post-natal developmental process: molecular, spatial, and temporal aspects of its regulation. J Cell Biochem. 2003 Apr 1;88(5):873-84.

11. Hadjiargyrou M, Lombardo F, Zhao S et al. Transcriptional profiling of bone regeneration. Insight into the molecular complexity of wound repair. J Biol Chem. 2002 Aug 16;277(33):30177-82.

12. Hadjiargyrou M, Ahrens W, and Rubin C.T. Temporal expression of the chondrogenic and angiogenic growth factor CYR61 during fracture repair. J. Bone Miner. Res. 15 (2000), pp. 1014–1023.

13. Hadjiargyrou M, Rightmire E.P., Ando T, and Lombardo F.T. The E11 osteoblastic lineage marker is differentially expressed during fracture healing. Bone 29 (2001), pp. 149–154

14. Hadjiargyrou M, Halsey M.F, Ahrens W et al. Cloning of a novel cDNA expressed during the early stages of fracture healing. Biochem. Biophys. Res. Commun. 249 (1998), pp. 879–884.

15. Hall BK, Miyake T. All for one and one for all: condensations and the initiation of skeletal development. Bioessays. 2000 Feb;22(2):138-47.

16. Hill RE, Jones PF, Rees AR et al. A new family of mouse homeo box-containing genes: molecular structure, chromosomal location, and developmental expression of Hox-7.1. Genes Dev. 1989 Jan;3(1):26-37.

17. Hombria JC, Lovegrove B. Beyond homeosis--HOX function in morphogenesis and organogenesis. Differentiation. 2003 Oct;71(8):461-76.

18. Hu Y, Flanagan J, Brennan DP et al. rHox: a homeobox gene expressed in osteoblastic cells. J Cell Biochem. 1995 Dec;59(4):486-97.

19. Hu YS, Zhou H, Kartsogiannis V et al. Expression of rat homeobox gene, rHOX, in developing and adult tissues in mice and regulation of its mRNA expression in osteoblasts by bone morphogenetic protein 2 and parathyroid hormone-related protein. Mol Endocrinol. 1998 Nov;12(11):1721-32.

20. Kanzler B, Kuschert SJ, Liu YH, Mallo M. Hoxa-2 restricts the chondrogenic domain and inhibits bone formation during development of the branchial area. Development. 1998 Jul;125(14):2587-97.

21. Komatsu DE, Hadjiargyrou M. Activation of the transcription factor HIF-1 and its target genes, VEGF, HO-1, iNOS, during fracture repair. Bone. 2004 Apr;34(4):680-8.

22. Li H, Huang CJ, Choo KB. Expression of homeobox genes in cervical cancer. Gynecol Oncol. 2002 Feb;84(2):216-21.

23. Lombardo F, Komatsu D, Hadjiargyrou M. Molecular cloning and characterization of Mustang, a novel nuclear protein expressed during skeletal development and regeneration. FASEB J. 2004 Jan;18(1):52-61.

24. MacKenzie A, Ferguson MW, Sharpe PT. Expression patterns of the homeobox gene, Hox-8, in the mouse embryo suggest a role in specifying tooth initiation and shape. Development. 1992 Jun;115(2):403-20.

25. Martin JF, Bradley A, Olson EN. The paired-like homeo box gene MHox is required for early events of skeletogenesis in multiple lineages. Genes Dev. 1995 May 15;9(10):1237-49.

26. Newberry EP, Boudreaux JM, Towler DA. Stimulus-selective inhibition of rat osteocalcin promoter induction and protein-DNA interactions by the homeodomain repressor Msx2. J Biol Chem. 1997 Nov 21;272(47):29607-13.

27. Orestes-Cardoso S, Nefussi JR, Lezot F et al. Msx1 is a regulator of bone formation during development and postnatal growth: in vivo investigations in a transgenic mouse model. Connect Tissue Res. 2002;43(2-3):153-60.

28. Rijli FM, Mark M, Lakkaraju S et al. A homeotic transformation is generated in the rostral branchial region of the head by disruption of Hoxa-2, which acts as a selector gene. Cell. 1993 Dec 31;75(7):1333-49.

29. Robert B, Sassoon D, Jacq B et al. Hox-7, a mouse homeobox gene with a novel pattern of expression during embryogenesis. EMBO J. 1989 Jan;8(1):91-100.

30. Ryoo HM, Hoffmann HM, Beumer T et al. Stage-specific expression of Dlx-5 during osteoblast differentiation: involvement in regulation of osteocalcin gene expression. Mol Endocrinol. 1997 Oct;11(11):1681-94.

31. Satokata I, Ma L, Ohshima H et al. Msx2 deficiency in mice causes pleiotropic defects in bone growth and ectodermal organ formation. Nat Genet. 2000 Apr;24(4):391-5.

32. Selleri L, Depew MJ, Jacobs Y et al. Requirement for Pbx1 in skeletal patterning and programming chondrocyte proliferation and differentiation. Development. 2001 Sep;128(18):3543-57.

33. Vortkamp A, Pathi S, Peretti GM et al. Recapitulation of signals regulating embryonic bone formation during postnatal growth and in fracture repair. Mech Dev. 1998 Feb;71(1-2):65-76.

34. Yaoita H, Orimo H, Shirai Y, Shimada T. Expression of bone morphogenetic proteins and rat distal-less homolog genes following rat femoral fracture. J Bone Miner Metab. 2000;18(2):63-70.

35. Zakany J, Kmita M, Duboule D. A dual role for Hox genes in limb anterior-posterior asymmetry. Science. 2004 Jun 11;304(5677):1669-72.

Chapter 3

1. Akiyamaa H, Kamitanic T, Yanga X, Kandyila R, Bridgewaterd LC, Fellouse M, Mori-Akiyamaa Y, de Crombrugghe B. The transcription factor Sox9 is degraded by the ubiquitin–proteasome system and stabilized by a mutation in a ubiquitin-target site. 2005 Matrix Biology 23, 499–505.

2. Bellows CG, Sodek J, Yao KL, Aubin JE. Phenotypic differences in subclones and long-term cultures of clonally derived rat bone cell lines. J Cell Biochem. 1986;31(2):153-69.

3. Bi W, Deng JM, Zhang Z, Behringer RR, de Crombrugghe B. *Sox9* is required for cartilage formation. Nature Genetics. 1999. Vol 22, 85-89.

4. Eyre D. Collagens and Cartilage Matrix Homeostasis. 2004 Clinical Orthopaedics and Related Research. Vol. 427 pp S118-S122.

5. Ferguson C, Alpern E, Miclau T, Helms JA. Does adult fracture repair recapitulate embryonic skeletal formation? Mech Dev. 1999 Sep;87(1-2):57-66.

6. Gersch RP, Lombardo F, McGovern SC, Hadjiargyrou M. Reactivation of Hox gene expression during bone regeneration. J Orthop Res. 2005 Jul;23(4):882-90.

7. Gerstenfeld LC, Cullinane DM, Barnes GL, Graves DT, Einhorn TA. Fracture healing as a post-natal developmental process: molecular, spatial, and temporal aspects of its regulation. J Cell Biochem. 2003 Apr 1;88(5):873-84.

8. Hadjiargyrou M, Lombardo F, Zhao S et al. Transcriptional profiling of bone regeneration. Insight into the molecular complexity of wound repair. J Biol Chem. 2002 Aug 16;277(33):30177-82.

9. Harrington EK, Lunsford LE, Svoboda KKH. Chondrocyte Terminal Differentiation, Apoptosis, and Type X Collagen Expression Are Downregulated by Parathyroid Hormone. 2004 THE ANATOMICAL RECORD PART A 281A:1286–1295.

10. Hsieh J-C, Lee L, Zhang L, Wefer S, Brown K, DeRossi C, Wines M, Rosenquist T, Holdener BC. Mesd Encodes an LRP5/6 Chaperone Essential for Specification of Mouse Embryonic Polarity. 2003 Cell, Vol. 112, 355–367.

11. Ikeda T, Kamekura S, Mabuchi A, Kou I, Seki S, Takato T, Nakamura K, Kawaguchi H, Ikegawa S, Chung U. The Combination of SOX5, SOX6, and SOX9 (the SOX Trio) Provides Signals Sufficient for Induction of Permanent Cartilage. 2004 ARTHRITIS & RHEUMATISM. Vol. 50, No. 11 pp 3561–3573

12. Johns D, Athanasiou K. Design characteristics for temporomandibular joint disc tissue engineering: learning from tendon and articular cartilage. 2007 Proceedings of the Institution of Mechanical Engineers. Part H, Journal of engineering in medicine. Vol. 221 No. 5 pp 509-26.

13. Kim J-H, Do H-J, Yang H-M, Oh J-H, Choi S-J, Kim D-K, Kwang-Yul Cha K-Y, Chung H-M. Overexpression of SOX9 in mouse embryonic stem cells directs the immediate chondrogenic commitment. 2005 EXPERIMENTAL and MOLECULAR MEDICINE, Vol. 37, No. 4, 261-268.

14. Liu C, Hadjiargyrou M. Identification and characterization of the Mustang promoter: regulation by AP-1 during myogenic differentiation. Bone. 2006 Oct;39(4):815-24.

15. Lombardo F, Komatsu D, Hadjiargyrou M. Molecular cloning and characterization of Mustang, a novel nuclear protein expressed during skeletal development and regeneration. FASEB J. 2004 Jan;18(1):52-61.

16. Rabie ABM, She TT, Harley VR. Forward Mandibular Positioning Up-regulates SOX9 and Type II Collagen Expression in the Glenoid Fossa. 2003 *J Dent Res* 82(9):725-730.

17. Scott J, Dorling J. Differential staining of acid glycosaminoglycans (mucopolysaccharides) by alcian blue in salt solutions. 1965 Histochemistry and Cell Biology. Oct 1;5(3):221-33.

18. Sen M, Cheng Y, Goldring MB, Lotz MK, Carson DA. WISP3-Dependent Regulation of Type II Collagen and Aggrecan Production in Chondrocytes. 2004 ARTHRITIS & RHEUMATISM, Vol. 50, No. 2, pp 488–497

19. Shen G, Rabie AB, Zhao Z, Kaluarachchi K. Forward deviation of the mandibular condyle enhances endochondral ossification of condylar cartilage indicated by increased expression of type X collagen. 2006 Archives of Oral Biology, Vol. 51 315-324.

20. Tchetina EV, Kobayashi M, Yasuda T, Meijers T, Pidoux I, Poole AR. Chondrocyte hypertrophy can be induced by a cryptic sequence of type II collagen and is accompanied by the induction of MMP-13 and collagenase activity: Implications for development and arthritis. 2007 Matrix Biology Vol. 26, 247–258

21. Uchihashi T, Kimata M, Tachikawa K, Koshimizu T, Okada T, Ihara-Watanabe M, Sakai N, Kogo M, Ozono K, Michigami T. Involvement of nuclear factor I transcription/replication factor in the early stage of chondrocytic differentiation. 2007 Bone Vol. 41, 1025–1035

22. Vortkamp A, Pathi S, Peretti GM et al. Recapitulation of signals regulating embryonic bone formation during postnatal growth and in fracture repair. Mech Dev. 1998 Feb;71(1-2):65-76.

23. Wagner EF. Functions of AP1 (Fos/Jun) in bone development. Ann Rheum Dis. 2002 Nov;61 Suppl 2:ii40-2.

Chapter 4

1. Lombardo F, Komatsu D, Hadjiargyrou M. Molecular cloning and characterization of Mustang, a novel nuclear protein expressed during skeletal development and regeneration. FASEB J. 2004 Jan;18(1):52-61.

2. Svensson ME, Haas A. Evolutionary innovation in the vertebrate jaw: A derived morphology in anuran tadpoles and its possible developmental origin. Bioessays. 2005 May;27(5):526-32.

3. Su MW, Suzuki HR, Bieker JJ, Solursh M, Ramirez F. Expression of two nonallelic type II procollagen genes during *Xenopus* laevis embryogenesis is characterized by stage-specific production of alternatively spliced transcripts. J Cell Biol. 1991 Oct;115(2):565-75.

4. Seufert DW, Hanken J, Klymkowsky MW. Type II collagen distribution during cranial development in *Xenopus laevis*. Anat Embryol (Berl). 1994 Jan;189(1):81-9.

5. Bieker JJ, Yazdani-Buicky M. Distribution of type II collagen mRNA in *Xenopus* embryos visualized by whole-mount in situ hybridization J Histochem Cytochem. 1992 Aug;40(8):1117-20.

6. O'Donnell M, Hong CS, Huang X, Delnicki RJ, Saint-Jeannet JP. Functional analysis of Sox8 during neural crest development in *Xenopus*. Development. 2006 Oct;133(19):3817-26.

7. Spokony RF, Aoki Y, Saint-Germain N, Magner-Fink E, Saint-Jeannet JP. The transcription factor Sox9 is required for cranial neural crest development in *Xenopus*. Development. 2002 Jan;129(2):421-32.

8. Schuff M, Rössner A, Wacker SA, Donow C, Gessert S, Knöchel W. FoxN3 is required for craniofacial and eye development of *Xenopus* laevis. Dev Dyn. 2007 Jan;236(1):226-39.

9. Ferguson C, Alpern E, Miclau T, Helms JA. Does adult fracture repair recapitulate embryonic skeletal formation? Mech Dev. 1999 Sep;87(1-2):57-66.

10. Gerstenfeld LC, Cullinane DM, Barnes GL, Graves DT, Einhorn TA. Fracture healing as a post-natal developmental process: molecular, spatial, and temporal aspects of its regulation. J Cell Biochem. 2003 Apr 1;88(5):873-84.

11. Hadjiargyrou M, Lombardo F, Zhao S et al. Transcriptional profiling of bone regeneration. Insight into the molecular complexity of wound repair. J Biol Chem. 2002 Aug 16;277(33):30177-82.

12. Vortkamp A, Pathi S, Peretti GM et al. Recapitulation of signals regulating embryonic bone formation during postnatal growth and in fracture repair. Mech Dev. 1998 Feb;71(1-2):65-76.

13. Frank, D and Harland, R. Transient expression of XMyoD in non-soitic mesoderm of *Xenopus* gastrulae. Development. 1991 113: 1387-1393.

14. Nicolas N, Gallien C-L, Chanoine C. Expression of Myogenic Regulatory Factors During Muscle Development of *Xenopus*: Myogenin mRNA Accumulation Is Limited Strictly to Secondary Myogenesis. Dev. Dyn. 1998 213: 309-321

15. Harland RM. In situ hybridization: an improved whole-mount method for *Xenopus* embryos. Methods Cell Biol. 1991;36:685-95.

16. Nieuwkoop PD, Faber J. 1967. Normal table of *Xenopus laevis* (Daudin), 2nd ed. Amsterdam: Elsevier/North Holland

17. Alexandrova EM, Thomsen GH. Smurf1 regulates neural patterning and folding in *Xenopus* embryos by antagonizing the BMP/Smad1 pathway. Dev Biol. 2006 Nov 15;299(2):398-410.

18. Yabe S, Tazumi S, Yokoyama J, Uchiyama H. Xtbx6r, a novel T-box gene expressed in the paraxial mesoderm, has anterior neural-inducing activity. Int J Dev Biol. 2006;50(8):681-9.

19. Kerney R, Gross JB, Hanken J. Runx2 is essential for larval hyobranchial cartilage formation in *Xenopus laevis*. Dev Dyn. 2007 Jun;236(6):1650-62.

20. Schuff M, Rössner A, Wacker SA, Donow C, Gessert S, Knöchel W. FoxN3 is required for craniofacial and eye development of *Xenopus* laevis. Dev Dyn. 2007 Jan;236(1):226-2):723-32.

21. Tramier M, Zahid M, Mevel JC, Masse MJ, Coppey-Moisan M. Sensitivity of CFP/YFP and GFP/mCherry pairs to donor photobleaching on FRET determination by fluorescence lifetime imaging microscopy in living cells. Microsc Res Tech. 2006 Nov;69(11):933-9.

Chapter 5

1. Akiyama H, Lyons JP, Mori-Akiyama Y, Yang X, Zhang R, Zhang Z, Deng JM, Taketo MM, Nakamura T, Behringer RR, McCrea PD, de Crombrugghe B. Interactions between Sox9 and beta-catenin control chondrocyte differentiation. Genes Dev. 2004 May 1;18(9):1072-87.

2. Amarilio R, Viukov SV, Sharir A, Eshkar-Oren I, Johnson RS, Zelzer E. HIF1alpha regulation of Sox9 is necessary to maintain differentiation of hypoxic prechondrogenic cells during early skeletogenesis. Development. 2007 Nov;134(21):3917-28.

3. Alappat S, Zhang ZY, Chen YP. Msx homeobox gene family and craniofacial development. Cell Res. 2003 Dec;13(6):429-42.

4. Ferguson C, Alpern E, Miclau T, Helms JA. Does adult fracture repair recapitulate embryonic skeletal formation? Mech Dev. 1999 Sep;87(1-2):57-66.

5. Fromental-Ramain C, Warot X, Lakkaraju S et al. Specific and redundant functions of the paralogous Hoxa-9 and Hoxd-9 genes in forelimb and axial skeleton patterning. Development. 1996 Feb;122(2):461-72.

6. Hadjiargyrou M, Lombardo F, Zhao S, Ahrens W, Joo J, Ahn H, Jurman M, White DW, Rubin CT. Transcriptional profiling of bone regeneration. Insight into the molecular complexity of wound repair. J Biol Chem. 2002 Aug 16;277(33):30177-82.

7. Gerstenfeld LC, Cullinane DM, Barnes GL, Graves DT, Einhorn TA. Fracture healing as a post-natal developmental process: molecular, spatial, and temporal aspects of its regulation. J Cell Biochem. 2003 Apr 1;88(5):873-84.

8. Hu Y, Flanagan J, Brennan DP et al. rHox: a homeobox gene expressed in osteoblastic cells. J Cell Biochem. 1995 Dec;59(4):486-97.

9. Hu YS, Zhou H, Kartsogiannis V et al. Expression of rat homeobox gene, rHOX, in developing and adult tissues in mice and regulation of its mRNA expression in osteoblasts by bone morphogenetic protein 2 and parathyroid hormone-related protein. Mol Endocrinol. 1998 Nov;12(11):1721-32.

10. Kanzler B, Kuschert SJ, Liu YH, Mallo M. Hoxa-2 restricts the chondrogenic domain and inhibits bone formation during development of the branchial area. Development. 1998 Jul;125(14):2587-97.

11. Kronenberg HM. PTHrP and skeletal development. Ann N Y Acad Sci. 2006 Apr;1068:1-13.

12. Liu C, Hadjiargyrou M, Identification and characterization of the Mustang promoter: Regulation by AP-1 duirng myogenic differentiation. Bone. 2006 39:815-824.

13. Lombardo F, Komatsu D, Hadjiargyrou M. Molecular cloning and characterization of Mustang, a novel nuclear protein expressed during skeletal development and regeneration. FASEB J. 2004 Jan;18(1):52-61.

14. Malladi P, Xu Y, Chiou M, Giaccia AJ, Longaker MT. Hypoxia inducible factor-1alpha deficiency affects chondrogenesis of adipose-derived adult stromal cells. Tissue Eng. 2007 Jun;13(6):1159-71.

15. Martin JF, Bradley A, Olson EN. The paired-like homeo box gene MHox is required for early events of skeletogenesis in multiple lineages. Genes Dev. 1995 May 15;9(10):1237-49.

16. Murakami S, Lefebvre V, de Crombrugghe B. Potent inhibition of the master chondrogenic factor Sox9 gene by interleukin-1 and tumor necrosis factor-alpha. J Biol Chem. 2000 Feb 4;275(5):3687-92.

17. Satokata I, Ma L, Ohshima H et al. Msx2 deficiency in mice causes pleiotropic defects in bone growth and ectodermal organ formation. Nat Genet. 2000 Apr;24(4):391-5.

18. Seghatoleslami MR, Tuan RS. Cell density dependent regulation of AP-1 activity is important for chondrogenic differentiation of C3H10T1/2 mesenchymal cells. J Cell Biochem. 2002;84(2):237-48.

19. Papachristou D, Pirttiniemi P, Kantomaa T, Agnantis N, Basdra EK. Fos- and Jun-related transcription factors are involved in the signal transduction

pathway of mechanical loading in condylar chondrocytes. Eur J Orthod. 2006 Feb;28(1):20-6.

20. Pan Q, Yu Y, Chen Q, Li C, Wu H, Wan Y, Ma J, Sun F. Sox9, a key transcription factor of bone morphogenetic protein-2-induced chondrogenesis, is activated through BMP pathway and a CCAAT box in the proximal promoter. J Cell Physiol. 2008 Oct;217(1):228-41.

21. Vortkamp A, Pathi S, Peretti GM et al. Recapitulation of signals regulating embryonic bone formation during postnatal growth and in fracture repair. Mech Dev. 1998 Feb;71(1-2):65-76.

22. Yu K, Ornitz DM. FGF signaling regulates mesenchymal differentiation and skeletal patterning along the limb bud proximodistal axis. Development. 2008 Feb;135(3):483-91.

23. Zhou J, Meng J, Guo S, Gao B, Ma G, Zhu X, Hu J, Xiao Y, Lin C, Wang H, Ding L, Feng G, Guo X, He L. IHH and FGF8 coregulate elongation of digit primordia. Biochem Biophys Res Commun. 2007 Nov 23;363(3):513-8.